

**METHOD DEVELOPMENT FOR ELEMENTS DETERMINATION
IN HIGH SALT MEDIUM USING AAS AND AES
AFTER MATRIX REMOVAL**

KAMOLCHANOK KOTAKANOK

**A THESIS SUBMITTED IN PARTIAL FULFILLMENT
OF THE REQUIREMENTS FOR
THE DEGREE OF MASTER OF SCIENCE
(APPLIED ANALYTICAL AND INORGANIC CHEMISTRY)
FACULTY OF GRADUATE STUDIES
MAHIDOL UNIVERSITY
2008**

COPYRIGHT OF MAHIDOL UNIVERSITY

Thesis
Entitled

**METHOD DEVELOPMENT FOR ELEMENTS DETERMINATION
IN HIGH SALT MEDIUM USING AAS AND AES
AFTER MATRIX REMOVAL**

.....
Miss. Kamolchanok Kotakanok
Candidate

.....
Asst.Prof. Atitaya Siripinyanond,
Ph.D.(Analytical Chemistry)
Major-Advisor

.....
Prof. Juwadee Shiowatana,
Ph.D.(Analytical Chemistry)
Co-Advisor

.....
Prof. Banchong Mahaisavariya,
M.D.
Dean
Faculty of Graduate Studies

.....
Asst.Prof. Duangjai Nacapricha,
Ph.D.(Analytical Chemistry)
Chair
Master of Science Programme in Applied
Analytical and Inorganic Chemistry
Faculty of Science

Thesis
Entitled

**METHOD DEVELOPMENT FOR ELEMENTS DETERMINATION
IN HIGH SALT MEDIUM USING AAS AND AES
AFTER MATRIX REMOVAL**

was submitted to the Faculty of Graduate Studies, Mahidol University
for the degree of Master of Science
(Applied Analytical and Inorganic Chemistry)
on
31 October, 2008

.....
Miss. Kamolchanok Kotakanok
Candidate

.....
Asst.Prof. Chatvalee Kalambaheti,
Ph.D.(Analytical Chemistry)
Chair

.....
Asst.Prof. Atitaya Siripinyanond,
Ph.D.(Analytical Chemistry)
Member

.....
Lect. Waret Veerasai,
Dr.rer.nat. (Physical Inorganic Chemistry)
Member

.....
Prof. Juwadee Shiowatana,
Ph.D.(Analytical Chemistry)
Member

.....
Prof. Banchong Mahaisavariya,
M.D.
Dean
Faculty of Graduate Studies
Mahidol University

.....
Prof. Skorn Mongkolsuk,
Ph.D. (Biological Science)
Dean
Faculty of Science
Mahidol University

ACKNOWLEDGEMENTS

I would like to express my deep gratitude to all those who gave me the possibility to complete my Master of Science degree. I am deeply grateful to my supervisor, Asst. Prof. Atitaya Siripinyanond, and my co-advisor, Prof. Juwadee Shiowatana, for valuable guidance, encouragement, and extensive support throughout my graduate study. I am sincerely impressed for their kindness. Sincere appreciation is extended to the thesis examination committee members, Asst.Prof. Chatvalee Kalambaheti and Dr. Waret Veerasai for their valuable guidance, comments, suggestion and kindness.

I also appreciate the financial support and scholarship provided by the Center of Excellence for Innovation in Chemistry: Postgraduate Education and Research Program in Chemistry (PERCH-CIC) and also the teaching assistant scholarship from Faculty of Science, Mahidol University. I am also thankful to all staff members of the Department of Chemistry, Mahidol University for their kindness and assistance, especially Mr. Kasemsun Darasoon who constructed special glasswares for my research.

Special thankful words go to all my teachers in my life, all members in AAICP program, especially PSAC group, my friends, juniors and seniors for all support, friendly environment, and wonderful friendship.

Finally, I would like to thank my family for their support, a lot of love, care, and understanding given from the old time till now.

Kamolchanok Kotakanok

METHOD DEVELOPMENT FOR ELEMENTS DETERMINATION IN HIGH SALT MEDIUM USING AAS AND AES AFTER MATRIX REMOVAL**KAMOLCHANOK KOTAKANOK 4836445 SCAI/M****M.Sc. (APPLIED ANALYTICAL AND INORGANIC CHEMISTRY)****THESIS ADVISORS: ATITAYA SIRIPINYANOND, Ph.D. (ANALYTICAL CHEMISTRY), JUWADEE SHIOWATANA, Ph.D. (ANALYTICAL CHEMISTRY)****ABSTRACT**

A hollow fiber flow filtration (HF-FF) system in the opposed flow mode was applied to perform simultaneous matrix removal and analyte preconcentration in high salt medium based on complexation-ultrafiltration before GFAAS, CVAAS, and ICP-OES detection. Poly (ethylene imine), PEI, was used as a polymeric complexing agent to chelate analyte elements (As, Se, Cd, Hg, Pb, Cu, and Zn) but not matrix elements (Na, K, Ca and Mg). With poly (sulfone) membrane (pore size = 30,000 Da), the analyte-PEI complexes, which were larger than the membrane pore size, were concentrated, whereas free matrix ions were removed by filtering off through membrane. HF-FF system could reduce interference from the high salt matrix with the preconcentration factors in the range of 3-5 times for Cd, Pb, Cu, and Zn.

To increase the sample transport efficiency in ICP-OES, vapor generation sample introduction was employed. A lab-made cyclonic spray chamber (LMSC) was developed and tested for its sample introduction efficiency. It can be employed in solution nebulization as a spray chamber and in vapor generation as a gas liquid separator. The elements in the gaseous forms were generated inside the chamber and then introduced into the plasma by argon carrier gas. The optimum concentrations of reductant (NaBH₄) and acid carrier (HCl) were 1% m/v and 5% v/v, respectively. Plasma power of 1,350 W and nebulizer gas flow rate of 0.65 L min⁻¹ were found to be compromised for solution nebulization and vapor generation. With vapor generation, the sensitivity improvement factors were in the range of ~30-70 times in the presence of matrix elements and ~20-45 times in the absence of matrix elements. Furthermore, percent difference from slopes of calibration curves between with and without matrix elements was < 5% suggesting no effect from matrix elements for determination of As, Se and Hg by vapor generation ICP-OES.

KEY WORDS: HOLLOW FIBER FLOW FILTRATION/ VAPOR GENERATION/ MODIFIED CYCLONIC SPRAY CHAMBER/ AAS/ AES/ MATRIX EFFECT

107 pp.

การพัฒนาวิธีการวิเคราะห์ปริมาณธาตุในตัวอย่างที่มีเกลือปริมาณสูงโดยใช้เทคนิค อะตอมมิกแอบซอร์พชัน และ อะตอมมิกอิมิตชัน สเปกโทรเมตรี หลังผ่านการขจัดสารรบกวน

(METHOD DEVELOPMENT FOR ELEMENTS DETERMINATION IN HIGH SALT MEDIUM USING AAS AND AES AFTER MATRIX REMOVAL)

กมลชนก โคตกนก 4836445 SCAI/M

วท.ม. (เคมีวิเคราะห์และเคมีอนินทรีย์ประยุกต์)

คณะกรรมการควบคุมวิทยานิพนธ์; อติทยา ศิริภิญโญานนท์, Ph.D. (Analytical Chemistry),
ยุวดี เชี่ยววัฒนา, Ph.D. (Analytical Chemistry)

บทคัดย่อ

งานวิจัยนี้ใช้หน่วยกรองแบบไหลด้วยเยื่อเลือกผ่านชนิดทอกลมกลวง ด้วยวิธี opposed flow ซึ่งอาศัยหลักการของการเกิดสารเชิงซ้อนและแยกขนาดด้วยการกรองโดยอาศัยการไหล เพื่อกำจัดสารรบกวนและทำให้สารที่ต้องการวิเคราะห์เข้มข้นขึ้นในตัวอย่างที่มีเกลือปริมาณสูง ก่อนการตรวจวัดด้วย GFAAS CVAAS และ ICP-OES โดยใช้ poly (ethylene imine) หรือ PEI ซึ่งทำให้เกิดสารเชิงซ้อนกับธาตุที่ต้องการวิเคราะห์ (As Se Cd Hg Pb Cu และ Zn) แต่ไม่เกิดสารเชิงซ้อนกับธาตุรบกวน (Na K Ca และ Mg) เมื่อใช้เยื่อเลือกผ่าน poly(sulfone) (ขนาดรูพรุน = 30,000 ดาลตัน) พบว่าสารเชิงซ้อนของ PEI กับธาตุที่ต้องการวิเคราะห์ ซึ่งมีขนาดใหญ่กว่าขนาดรูพรุนของเยื่อเลือกผ่าน จะอยู่ในทอกลวงและถูกทำให้เข้มข้นขึ้น ขณะที่สารรบกวนซึ่งไม่เกิดสารเชิงซ้อนกับ PEI จะถูกกำจัดออกทางรูพรุนของเยื่อเลือกผ่าน หน่วยกรองนี้สามารถลดการรบกวนจากสารรบกวนเกลือปริมาณสูงได้ และทำให้ค่าความไวในการตรวจวัดเพิ่มขึ้น 2-3 เท่า สำหรับธาตุ Cd Pb Cu และ Zn

เพื่อเพิ่มประสิทธิภาพการนำสารเข้าตรวจวัดใน ICP-OES จึงทำให้ธาตุที่ต้องการวิเคราะห์กลายเป็นไอก่อนตรวจวัด โดยพัฒนาและทดสอบประสิทธิภาพของ lab-made cyclonic spray chamber (LMSC) ซึ่งทำหน้าที่เป็น spray chamber เมื่อนำสารเข้าตรวจวัดในรูปสารละลาย และทำหน้าที่เป็นเครื่องมือในการแยกสารละลายกับไอออกจากกัน เมื่อนำสารเข้าตรวจวัดในรูปไอ ธาตุที่ต้องการวิเคราะห์ถูกทำให้กลายเป็นไอภายใน LMSC และถูกพาเข้าสู่พลาสมาด้วยแก๊สอาร์กอน ค่าความเข้มข้นที่เหมาะสมของตัวรีดิวซ์ (NaBH_4) และ กรดตัวพา (HCl) คือ 1% m/v และ 5% v/v ตามลำดับ plasma power 1,350 W และอัตราการไหลของ nebulizer gas 0.65 L min^{-1} คือค่าที่เหมาะสมสำหรับการตรวจวัดในรูปสารละลายและไอ จากการตรวจวัดในรูปไอทำให้ค่าความไวในการตรวจวัดเพิ่มขึ้น ~30-70 เท่าเมื่อมีสารรบกวนและ ~20-45 เท่าเมื่อไม่มีสารรบกวน นอกจากนี้ค่าความชันของกราฟมาตรฐานของธาตุ As Se และ Hg ขณะที่มีและไม่มีสารรบกวน มีค่าเปอร์เซ็นต์ความแตกต่างน้อยกว่า 5 เปอร์เซ็นต์ แสดงให้เห็นว่าไม่มีผลกระทบจากสารรบกวนเมื่อตรวจวัดในรูปของไอใน ICP-OES

CONTENTS

	Page
ACKNOWLEDGEMENTS	iii
ABSTRACT (IN ENGLISH)	iv
ABSTRACT (IN THAI)	v
LIST OF TABLES	xiii
LIST OF FIGURES	xvi
LIST OF ABBREVIATIONS	xx
THE RELEVANCY OF THE RESEARCH WORK TO THAILAND	xxiii
 CHAPTER	
I INTRODUCTION	1
II OBJECTIVE	4
III LITERATURE REVIEWS	5
3.1 Matrix Effects in Atomic Spectrometric Detection	5
3.1.1 Matrix Effects in Graphite Furnace Atomic Absorption Spectrometric Detection	5
3.1.2 Matrix Effects in Cold Vapor Atomic Absorption Spectrometric Detection	5
3.1.3 Matrix Effects in Inductively Coupled Plasma Optical Emission Spectrometric Detection.....	7
3.1.3.1 Proposed Mechanisms Explaining the Matrix Effects in ICP-OES Detection.	8
3.2 Matrix Removal Methods.....	9
3.2.1 Matrix Modification in Graphite Furnace Atomic Absorption Spectrometric Detection.....	9
3.2.2 Matrix Removal for Cold Vapor Atomic Absorption Spectrometric Detection.....	12

CONTENTS (CONTS.)

CHAPTER	Page	
3.2.3	Matrix Removal for Inductively Coupled Plasma Optical Emission Spectrometric Detection.....	13
3.2.4	Complexation-Ultrafiltration for Matrix Removal.....	15
3.3	Sample Introduction for ICP-OES.....	18
3.3.1	Chemical Vapor Generation.....	18
3.3.2	Modified Cyclonic Spray Chamber as A Spray Chamber for Solution Nebulization and as A Gas Liquid Separator for Vapor Generation.....	21
IV	MATERIALS AND METHODS.....	25
4.1	Instrumentation.....	25
4.1.1	Graphite Furnace Atomic Absorption Spectrometer (GFAAS).....	25
4.1.2	Cold Vapor Atomic Absorption Spectrometer (CVAAS).....	26
4.1.3	Inductively Coupled Plasma-Optical Emission Spectrometer (ICP-OES).....	26
4.2	Equipment.....	27
4.2.1	Hollow Fiber Flow Filtration Unit.....	27
4.2.2	Lab-Made Cyclonic Spray Chamber (LMSC).....	29
4.2.3	Peristaltic Pump.....	30
4.2.4	pH Meter.....	30
4.2.5	Analytical Balance.....	30
4.3	Chemical Reagents.....	30
4.4	Preparation of Reagent and Standard Solutions.....	32
4.4.1	Reagents used in HF-FF Experiment.....	32

CONTENTS (CONTS.)

CHAPTER	Page
4.4.1.1	Polymeric Complexing Agent..... 32
4.4.1.2	Borate Buffer..... 32
4.4.2	Reagents used in GFAAS Experiment..... 32
4.4.2.1	Mercury Standard Solution..... 32
4.4.2.2	Palladium Modifier Solution..... 32
4.4.3	Reagents used in CVAAS Experiment..... 33
4.4.3.1	Mercury Standard Solution..... 33
4.4.3.2	Hydrochloric Acid Solution (7% v/v HCl)..... 33
4.4.3.3	Sodium Hydroxide Solution (0.05% m/v NaOH)..... 33
4.4.3.4	Sodium Tetrahydroborate(III) (0.2% v/v NaBH ₄)..... 33
4.4.4	Reagents used in ICP-OES Experiment 33
4.4.4.1	Hydrochloric Acid Solution (5% v/v HCl)..... 33
4.4.4.2	Sodium Hydroxide Solution (0.4% m/v NaOH)..... 34
4.4.4.3	Sodium Tetrahydroborate(III) (1% v/v NaBH ₄)..... 34
4.4.4.4	Mixed Standard Solution..... 34
4.5	Operating Procedures..... 34
4.5.1	Hollow Fiber Flow Filtration System (HF-FF System)..... 34
4.5.2	GFAAS Determination of Mercury..... 35
4.5.2.1	GFAAS: Parameters Optimization for Mercury Determination..... 35

CONTENTS (CONTS.)

CHAPTER		Page
	4.5.2.2 Mercury Detection by GFAAS: Effect of High Salt Medium.....	36
	4.5.2.3 Matrix Removal and Analyte Preconcentration with HF-FF System for Mercury Determination by GFAAS.....	37
4.5.3	CVAAS Determination of Mercury	37
	4.5.3.1 CVAAS: Parameters Optimization for Mercury Determination.....	37
	4.5.3.1a Effect of Acid Carrier (HCl) and Reductant (NaBH ₄) Flow Rates.....	37
	4.5.3.1b Effect of Carrier Gas (Argon Gas) Flow Rate....	38
	4.5.3.1c Effect of NaBH ₄ Concentration.....	38
	4.5.3.1d Effect of HCl Concentration.....	38
	4.5.3.2 Mercury Determination by CVAAS with HF-FF System: Effect of pH	38
4.5.4	ICP-OES Determination of Trace Element.....	39
	4.5.4.1 Sample Introduction Methods.....	39
	4.5.4.1.1 Conventional Solution Nebulization.....	39
	4.5.4.1.2 Conventional Solution Nebulization with HF-FF System.....	40

CONTENTS (CONTS.)

CHAPTER	Page
4.5.4.1.3	Vapor Generation Method 42
4.5.4.2	The Efficiency of Lab-Made Cyclonic Spray Chamber..... 43
4.5.4.3	ICP-OES: Parameters Optimization for Trace Element Determination..... 43
4.5.4.3a	Parameters Optimization in Vapor Generation..... 43
4.5.4.3b	Optimization of Nebulizer Gas Flow Rate and Plasma Power..... 44
4.5.4.4	Preconcentration and Sensitivity Improvement Factors in The Presence and Absence of Matrices..... 44
4.5.4.4a	Preconcentration Factor with HF-FF System..... 47
4.5.4.4b	Sensitivity Improvement Factor with Vapor Generation Method..... 47
V	RESULTS AND DISCUSSION..... 48
5.1	GFAAS Determination of Mercury..... 48
5.1.1	GFAAS: Parameters Optimization for Mercury Determination..... 49
5.1.2	Mercury Determination by GFAAS..... 50
5.1.2.1	Effect of High Salt Medium..... 50
5.1.3	Mercury Determination by GFAAS with HF-FF System..... 51
5.1.3.1	Matrix Removal and Analyte Preconcentration..... 51

CONTENTS (CONTS.)

CHAPTER	Page	
5.1.3.2	Effect of PEI on Signal and Peak Shape of Mercury.....	52
5.1.3.3	Preconcentration Factor Obtained From Using HF-FF System.....	55
5.1.4	Summary: Mercury Determination by GFAAS Without and with HF-FF System.....	57
5.2	CVAAS Determination of Mercury.....	58
5.2.1	CVAAS: Parameters Optimization for Mercury Determination.....	58
5.2.2	Mercury Determination by CVAAS.....	63
5.2.2.1	Effect of pH.....	63
5.2.3	Mercury Determination by CVAAS with HF-FF System.....	63
5.2.3.1	Preconcentration Factor Obtained from Using HF-FF System.....	64
5.2.4	Summary: Mercury Determination by CVAAS Without and with HF-FF System.....	65
5.3	ICP-OES Determination of Trace Elements.....	66
5.3.1	The Lab-Made Cyclonic Spray Chamber (LMSC).....	66
5.3.1.1	The Efficiency of Lab-Made Cyclonic Spray Chamber for Solution Nebulization.....	67
5.3.2	Parameters Optimization for Trace Element Determination by ICP-OES.....	70
5.3.2.1	Parameters Optimization in Conventional Solution Nebulization...	70

CONTENTS (CONTS.)

CHAPTER	Page	
5.3.2.2	Parameters Optimization in Vapor Generation.....	70
5.3.2.3	Optimization of Nebulizer Gas Flow Rate and Plasma Power Conditions...	73
5.3.3	Preconcentration and Sensitivity Improvement Factors in The Presence and Absence of Matrices.....	77
5.3.3.1	Conventional Solution Nebulization...	78
5.3.3.2	Conventional Solution Nebulization with HF-FF.....	79
5.3.3.3	Vapor Generation Method.....	83
5.3.4	Summary: Trace Element Analysis by ICP-OES Detection Using Conventional Solution Nebulization with or Without HF-FF, and Vapor Generation Sample Introduction.....	86
VI	CONCLUSION.....	89
	REFERENCES.....	91
	APPENDIX.....	104
	BIOGRAPHY.....	107

LIST OF TABLES

Table	Page
3.1 Possible interferences on CVAAS determination of mercury [38].....	6
3.2 Mechanisms for analyte excitation [33].....	9
4.1 Furnace operating condition for mercury determination.....	25
4.2 Parameters and operating condition for mercury detection by CVAAS.....	26
4.3 ICP-OES operating conditions.....	27
4.4 HF-FF operating conditions.....	28
4.5 List of chemicals.....	31
5.1 Peak area absorbance of mercury at various ashing and atomization temperatures for mercury determination (5 mg L ⁻¹ mercury in DI water with 15 µL of 400 mg L ⁻¹ PEI buffered at pH 8.92 and 5 µL of 1000 mg L ⁻¹ palladium as chemical modifier).....	49
5.2 Furnace operating conditions for mercury determination.....	50
5.3 The operating conditions of HF-FF system for GFAAS detection.....	52
5.4 The peak area and preconcentration factor obtained for the test solution as shown in Figure 5.1 with or without HF-FF system. (With HF-FF system, a 2-mL volume of test solution containing 5 mg L ⁻¹ of mercury was introduced into the HF-FF unit.).....	56
5.5 The optimum conditions of CVAAS for mercury detection.....	62
5.6 The preconcentration factor obtained for 200 µg L ⁻¹ mercury in DI water with 200 mg L ⁻¹ PEI, using HF-FF system, sample volume 2 mL, focusing time 15 min.....	65

LIST OF TABLES (CONTS.)

Table	Page	
5.7	The optimum conditions of hydride generation and ICP-OES detection.....	77
5.8	Calibration functions obtained for various elements by conventional solution nebulization without HF-FF.....	78
5.9	Limit of detection obtained for various elements by conventional solution nebulization without HF-FF.....	79
5.10	Calibration functions obtained for various elements by conventional solution nebulization with HF-FF (good correlation coefficient, $r^2 > 0.9xxx$).....	81
5.11	Calibration functions obtained for various elements by conventional solution nebulization with HF-FF (poor correlation coefficients, $r^2 < 0.9xxx$).....	81
5.12	Preconcentration factors obtained for various analyte elements by conventional solution nebulization with HF-FF.....	82
5.13	Limit of detection obtained for various elements by conventional solution nebulization with HF-FF.....	82
5.14	Calibration functions obtained for various elements by vapor generation method.....	84
5.15	Sensitivity improvement factors obtained for various analyte elements by vapor generation method.....	85
5.16	Percent difference of slope between with and without matrices obtained for various analyte elements by vapor generation method.....	85
5.17	Limit of detection obtained for various elements by vapor generation method.....	86
5.18	Limit of detection (LOD, $\mu\text{g L}^{-1}$) of vapor generation method compared to conventional solution nebulization without HF-FF..	87

LIST OF TABLES (CONTS.)

Table		Page
5.19	Limit of detection ($\mu\text{g L}^{-1}$) of conventional solution nebulization with HF-FF compared to without HF-FF.....	88

LIST OF FIGURES

Figure		Page
3.1	Influence of NaCl concentration on the shape of the absorbance-time curve. (3 ng mL ⁻¹ mercury in 5% v/v HCl and 1% v/v stabilization solution (0.5% m/v K ₂ Cr ₂ O ₇) ; SnCl ₂ as a reducing agent). NaCl concentrations (% m/v) are given on the curves [42].....	7
3.2	(a) Idealized structure of the polymeric complex poly-(ethylenimine) with copper(II) ions [77], (b) general structure of polymer-metal amine type complexes [76].....	16
3.3	Stages of hydride generation with AES detection. Abbreviations: X, Y, Z, hydride-forming elements; A, matrix element; RS, reaction-separation system; ES, excitation source; DU, detection unit [83].....	20
3.4	CVG systems based on use of spray chambers and nebulizers: (a) Refs. [86-87, 90], (b) Ref. [91], and (c) Refs. [92, 93-94]. A, acid solution; C, carrier gas flow; M, makeup gas flow; P, linking with plasma torch; R, reducing agent solution; S, acidified sample solution; W, waste solution.....	23
4.1	A laboratory made hollow fiber channel.....	28
4.2	Schematic diagram of LMSC for sample introduction system in ICP-OES. Dimension is displayed in centimeter unit. a = nebulizer, b = acidified sample for vapor generation, c = reducing agent for vapor generation, d = transport to ICP, and e = waste.....	29
4.3	HF-FF system matrix removal and sample preconcentration a) sample loading and focusing step b) elution step.....	36

LIST OF FIGURES (CONTS.)

Figure		Page
4.4	Schematic diagram of LMSC set-up for conventional solution nebulization.....	40
4.5	Schematic diagram of HF-FF sample introduction method for trace element detection by ICP-OES. a = sample loading and focusing step, b = elution step.....	41
4.6	Schematic diagram of vapor generation for trace element determination by ICP-OES.....	42
4.7	Schematic diagram showing operating procedure of sample introduction for ICP-OES detection.....	45
4.8	Schematic diagram of conventional solution nebulization with and without HF-FF and vapor generation methods for trace element determination by ICP-OES.....	46
5.1	Peak area absorbance of mercury at various ashing and atomization temperatures for mercury determination (5 mg L ⁻¹ mercury in DI water with 15 µL of 400 mg L ⁻¹ PEI buffered at pH 8.92 and 5 µL of 1000 mg L ⁻¹ palladium as chemical modifier).....	51
5.2	Absorption peak profiles of 5 mg L ⁻¹ mercury in 10% seawater and all other conditions are as in Figure 5.1: (a) without HF-FF system; (b) with HF-FF system.....	53
5.3	Absorption peak profiles of 5 mg L ⁻¹ mercury in DI water and all other conditions are as in Figure 5.1: (a) without HF-FF system; (b) with HF-FF system.....	54
5.4	Absorption peak profiles of background without HF-FF system: (a) 5 mg L ⁻¹ mercury in DI water with 400 mg L ⁻¹ PEI; (b) 5 mg L ⁻¹ mercury in DI water without 400 mg L ⁻¹ PEI. All other conditions are as in Figure 5.1.....	55

LIST OF FIGURES (CONTS.)

Figure		Page
5.5	Effect of carrier (5% v/v HCl) and reductant (0.2% m/v NaBH ₄ in 0.05% m/v NaOH) flow rates on absorbance signal of 200 µg L ⁻¹ mercury in DI water: sample volume 500 µL, Ar gas flow rate 100 mL min ⁻¹ , (—◆—) peak area, (--■--) peak height.....	59
5.6	Effect of Ar gas flow rate on measured absorbance of mercury, carrier and reductant flow rate 3.4 mL min ⁻¹ . All other conditions are as in Figure 5.5. (—◆—) peak area, (--■--) peak height.....	60
5.7	Effect of NaBH ₄ concentration on measured absorbance of mercury: carrier and reductant flow rate 3.4 mL min ⁻¹ , sample volume 200 µL. All other conditions are as in Figure 5.5. (—◆—) peak area, (--■--) peak height.....	61
5.8	Effect of HCl concentration on measured absorbance of mercury: 0.2% m/v NaBH ₄ . All other conditions are as in Figure 5.7. (—◆—) peak area, (--■--) peak height.....	62
5.9	Effect of pH on the absorption signal of mercury, (—◆—) peak area, (--■--) peak height. All other conditions are as in Table 5.5.....	63
5.10	Effect of pH on the complex formation of mercury with PEI as observed from absorption signal, (—◆—) peak area, (--■--) peak height. All other conditions are as in Table 5.5.....	64
5.11	The lab-made cyclonic spray chamber (LMSC) for two sample introduction methods a) conventional solution nebulization method; b) vapor generation method: S _{Neb} = sample nebulization line; S _{VG} = sample vapor generation line; Ar = argon nebulizer gas; R = reduction solution (NaBH ₄); C = cap; and D = drain.....	68

LIST OF FIGURES (CONTS.)

Figure		Page
5.12	Calibration curves of cadmium (a), mercury (b) and lead (c) obtained with conventional solution nebulization using three chambers with plasma power of 1200 W, nebulizer flow rate of 0.7 L min ⁻¹ ; (--■--) MLSC, (—▲—) LMSC and (—◆—) CCSC.....	69
5.13	Sensitivity of selenium (a), cadmium (b), arsenic (c), and mercury (d) at each % HCl in vapor generation method. (Plasma power of 1200 W, nebulizer gas flow rate of 0.7 L min ⁻¹ and 0.2% NaBH ₄).....	72
5.14	Sensitivity of selenium (a), arsenic (b) and mercury (c) at each % NaBH ₄ in vapor generation method. (Plasma power of 1200 W, nebulizer gas flow rate of 0.7 L min ⁻¹ and 5% HCl).....	73
5.15	Effect of nebulizer argon gas flow rate on emission intensity of selenium (a) and mercury (b) in vapor generation method; selenium (c) and mercury (d) in conventional solution nebulization method; Plasma power, 1350 W.....	75
5.16	Effect of plasma power on emission intensity of selenium (a), mercury (b) and arsenic (c) in vapor generation method; selenium (d), mercury (e) and arsenic (f) in conventional solution nebulization method; nebulizer argon gas flow rate, 0.65 L min ⁻¹	76

LIST OF ABBREVIATIONS

ICP	Inductively coupled plasma
AES	Atomic emission spectrometry
ICP-OES	Inductively coupled plasma optical emission spectrometry
MIP-OES	Microwave induced plasma optical emission spectrometry
GFAAS	Graphite furnace atomic absorption spectrometry
CVAAS	Cold vapor atomic absorption spectrometry
CMA	Concomitant metals analyzer
CVG	Chemical vapor generation
EIEs	Easily ionized elements
IP	Ionization potential
HF-FF	Hollow fiber flow filtration
FIFFF	Flow field-flow fractionation
MWCO	Molecular weight cut-off
Da	Dalton
RF	Radio frequency
MHz	Mega Hertz
W	Watt
min	Minute
s	Second
%	Percent
wt %	Percent by weight
% m/v	Mass per Volume Percent
% v/v	Volume by Volume Percent
cm	Centimeter
mm	Millimeter
nm	Nanometer
i.d.	Inner diameter

LIST OF ABBREVIATIONS (CONTS.)

o.d.	Outer diameter
mL	Milliliter
μL	Microliter
g	Gram
mg L^{-1}	Milligram per liter
$\mu\text{g L}^{-1}$	Microgram per liter
ng mL^{-1}	Nanogram per liter
mol L^{-1}	Mole per liter
L min^{-1}	Liter per minute
mL min^{-1}	Milliliter per minute
cm^3	Cubic centimeters
$^{\circ}\text{C}$	Degree of celsius
rpm	Rotations per minute
MSIS	Multimode sample introduction system
LMSC	Lab-made cyclonic spray chamber
MLSC	Modified licthe spray chamber
CCSC	Commercial cyclonic spray chamber
Neb	Conventional pneumatic nebulization
VG	Vapor generation
S_{Neb}	Nebulizer sample line
S_{VG}	Vapor generator line
PEI	Poly (ethylene imine)
DI	Deionized water
APDC	1-pyrrolidinecarbodithioic acid
MDTC	Morpholine dithiocarbamate
DTC	Dithiocarbamate
LOD	Limit of detection
RSD	Relative standard deviation

LIST OF ABBREVIATIONS (CONTS.)

r^2	Coefficient of determination
r	Correlation coefficient
<i>et al.</i>	Et alia (Latin), and others
<i>etc.</i>	Et cetera (Latin), and the rest or and so on
<i>e.g.</i>	Exempli gratia (Latin), for example
<i>i.e.</i>	Id est (Latin), that is

THE RELEVANCY OF THE RESEARCH WORK TO THAILAND

As water quality problems become more serious, water quality monitoring becomes a more important component of national efforts. The study of trace elements in environmental is becoming increasingly important for pollution monitoring. These trace elements, especially heavy metal elements, are originated primarily from industrialized regions. GFAAS, CVAAS, and ICP-OES are widely used for trace elements determination in various samples, including natural water, food and beverages, industrial samples, and environmental samples. However, matrix interference is the main factor causing the determination to be inaccurate. The conventional methods for matrix removal are time consuming and expensive.

A lab-made hollow fiber flow filtration (HF-FF) system in the opposed flow method was applied to perform simultaneous matrix removal and analyte preconcentration based on complexation-ultrafiltration. This system is low cost and simple to operate. HF-FF was used for elements determination in high salt medium. It is an alternative system for matrix removal and analyte preconcentration.

In addition, the most common sample introduction method for ICP-OES is pneumatic nebulization of solution. Although, it is simple and offers good stability, sample introduction is inefficient. Therefore, effort has been made to couple alternative sample introduction system to ICP-OES to eliminate this drawback. Vapor generation is one of the sample introduction techniques to improve the sensitivity of volatile vapors when they are introduced into the plasma as vapor. Moreover, it can separate analyte from problematic matrix species which cause spectral and non-spectral interferences. A lab-made cyclonic spray chamber (LMSC) was developed for efficient sample introduction. It can be employed in solution nebulization as a spray chamber and in vapor generation as a gas liquid separator. LMSC is simple and inexpensive to construct since it is made of glass.

CHAPTER I

INTRODUCTION

At the present time, the study of trace elements in seawater is becoming increasingly important for monitoring environmental pollution. These elements, especially heavy metals, are originated primarily from industrialized regions. The level of Ag, As, Cd, Cr, Cu, Hg, Ni, Pb, and Zn in seawater has been restricted by European Directive [1] to store mollusks.

In atomic spectrometric detection techniques such as atomic absorption spectrometry (flame, graphite furnace, and cold vapor), atomic emission spectrometry (flame and plasma) as well as inductively coupled plasma mass spectrometry, the determination of trace metals in seawater remains a challenge. This is due to the very high salinity of the sample matrix elements (in particular sodium chloride, which can cause a variety of spectral and non-spectral interferences), and the very low concentrations of some trace metals [2-3]. Thus, pre-treatment steps, such as matrix removal and analyte preconcentration are required for the determination of trace metals in high salt sample. Many methods can be used for sample pre-treatment including solid-phase extraction [1, 4, 5], cloud point extraction [6], liquid-liquid microextraction [2], electrodeposition [7-8], and chromatographic separation [9]. However, these techniques have some drawbacks, e.g., risk of contamination; and time consuming. An alternative approach for preconcentration and matrix removal based on complexation-ultrafiltration was then proposed. Poly (ethylene imine) polymer, PEI, was reported to be a complexing agent, which strongly chelated with analyte elements, e.g., Cd, Cu, Pb, Zn, Hg, and etc, but not with the matrix elements (Ca, K, Mg, and Na). The PEI-analyte complexes, which are larger than the membrane pore size (6,000-30,000 Da), are concentrated, whereas free matrix ions are removed by filtering off through membrane. Recently, two interesting studies were reported for matrix

removal before ICP detection using flow field-flow fractionation [11], and a laboratory-made hollow fiber flow filtration (HF-FF) unit [10].

The hollow fiber membrane matrix removal device is easy to construct and inexpensive. In addition, to overcome the spectral and non-spectral interferences in ICP-OES, the use of vapor generation techniques for sample introduction with ICP-OES detection is a method of choice. This sample introduction can reduce the matrix effect, increase sensitivity and lower the limit of detection owing to the improvement of transport efficiency of the analytes from < 5% up to 100% compared with sample introduction in the form of an aerosol by using conventional pneumatic nebulization [12]. Unfortunately, this sample introduction can only be used for determination of volatile hydride-forming elements (the common ones are: As, Bi, Ge, Hg, Pb, Sb, Se, Sn, and Te). With vapor generation technique, gas-liquid separator (GLS) is used to separate volatile elements from solution before transporting into ICP detection [14-15]. Recently, the multimode sample introduction system (MSIS, patent pending), a system that can perform dual-mode sample introduction (nebulization and vapor generation) in a single device for ICP-OES, was reported. These devices were of various shapes and designs depending on the usability [12-13].

In this research, simultaneous sample preconcentration and matrix removal in high salt sample using HF-FF system based on complexation-ultrafiltration before GFAAS, CVAAS, and ICP-OES detection was examined. Matrix removal efficiency and preconcentration factor were investigated.

Moreover, a lab-made cyclonic spray chamber (LMSC) was developed and tested for its sample introduction efficiency. It can be employed in solution nebulization as a spray chamber and vapor generation as a gas liquid separator. LMSC is simple and inexpensive to construct since it is made of glass. Nebulization efficiency of the LMSC compared with modified licthe (MLSC) and commercial cyclonic (CCSC) spray chamber was investigated.

In ICP-OES, several analytes were simultaneously examined for their sensitivities obtained from the use of two different sample introduction methods, including conventional solution nebulization and vapor generation methods. In the conventional solution nebulization method, sample solution is introduced to the plasma as an aerosol by pneumatic nebulization. In vapor generation method, sample is introduced into plasma by argon carrier gas in vapor form. In this experiment, the LMSC can be employed as a spray chamber for solution nebulization or a gas liquid separator for vapor generation. The preconcentration and matrix removal were performed by conventional solution nebulization with HF-FF. For HF-FF system, parameters affecting complex formation, which are pH and PEI concentration, were investigated. In addition, focusing time and focusing point affecting matrix removal and analytical preconcentration efficiency were examined. In vapor generation method, the sensitivity improvement factor was determined. The concentration of reductant (NaBH_4) and acid carrier (HCl) was evaluated. Moreover, nebulizer gas flow rate and plasma power were investigated and optimized.

CHAPTER II

OBJECTIVE

The purposes of this study are:

1. To test the performance of hollow fiber flow filtration (HF-FF) system for matrix removal and analyte preconcentration using an opposed flow method before detection by GFAAS, CVAAS, and ICP-OES.
2. To increase the sample transport efficiency in ICP-OES using vapor generation sample introduction.

Details of the study include:

1. Application of HF-FF system for matrix removal and analyte preconcentration before GFAAS, CVAAS, and ICP-OES detection.
2. Evaluation of sensitivity improvement factors obtained from vapor generation ICP-OES as compared to those from conventional solution nebulization.

CHAPTER III

LITERATURE REVIEWS

3.1 Matrix Effects in Atomic Spectrometric Detection

3.1.1 Matrix Effects in Graphite Furnace Atomic Absorption Spectrometric Detection

Graphite furnace atomic absorption spectrometry (GFAAS) is widely used for trace metal determinations in a variety of environmental samples. However, the direct determination of trace element in high salinity matrix by GFAAS is difficult because the matrix components cause spectral (high background absorption) and non-spectral interferences [34-36, 43-52]. The molecular absorption produced by NaCl in the ultraviolet range or the light scattering by sodium chloride particles results in spectral interferences, whereas chemical interferences are mainly caused by the formation of volatile halides, or by occlusion of the analyte in the chloride matrix [34-36]. The interference effect of MgCl₂ matrix has been found more severe than that of NaCl matrix as reported by several authors [35-36]. To overcome interferences, different pre-concentration and separation procedures have been used.

3.1.2 Matrix Effects in Cold Vapor Atomic Absorption Spectrometric Detection

Because of the high toxicity of mercury and its compound, the determination of this element in environmental sample is still important. Cold vapor atomic absorption spectrometry (CVAAS) is one of the most popular techniques for determining mercury in various samples owing to its high sensitivity, rather free from interferences, low operating costs, fast and readily applicable to liquid sample [37]. Nevertheless, matrix components in sample often has an influence on the signal of

mercury determination by CVAAS, as other elements can interfere by either gaseous or solution phase reaction [38-39, 42].

Krata *et al.* [38] reported that interferences of mercury determination in natural water can be separated into three groups, as illustrated in Table 3.1. At concentrations up to 50 mg L⁻¹ of Na, K, Mg, Ca, Ni, Zn, Cd, Se(VI), Sb(V), Sb(III), As(III), and Pb(II), the mercury signal was not affected by the presence of these elements. In contrast the absorption signal of mercury decreased 50% and 40% in the presence of 10 mg L⁻¹ of Cu and Fe, respectively. This study agrees with the results reported by other groups [39-40]. In addition, 5 mg L⁻¹ of Se(IV) causes significant suppression of the mercury signal owing to the reduction of selenium to its elemental form and simultaneous adsorption of Hg on the resulting colloidal selenium [41].

Table 3.1 Possible interferences on CVAAS determination of mercury [38].

Group	Elements
I. Alkali and alkaline earth elements	Na, K, Mg, and Ca
II. Elements, which in the applied conditions, undergo reduction and form amalgams	Ni, Fe, Zn, Cd, and Cu
III. Elements, which in the applied conditions, form volatile hydrides	Se, Sb, As, and Pb

Haase *et al.* [42], working without preconcentration step and using tin(II) chloride as reductant for determining mercury in high concentration of sodium chloride (NaCl) by flow injection-CVAAS, observed that high concentrations of sodium chloride influence the absorption profile of mercury as shown in Figure 3.1. The curves lost their Gaussian shape and developed a double peak character at above 14% m/v of sodium chloride. Besides, at 20% m/v sodium chloride the initial absorbance reduced to approximately 30% of the original signal.

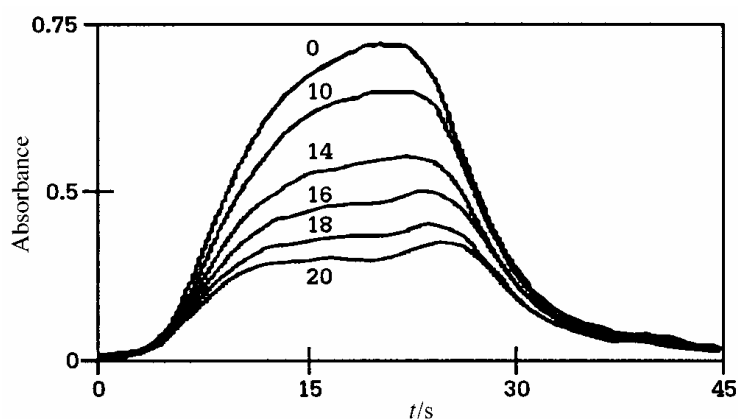


Figure 3.1 Influence of NaCl concentration on the shape of the absorbance-time curve. (3 ng mL⁻¹ mercury in 5% v/v HCl and 1% v/v stabilization solution (0.5% m/v K₂Cr₂O₇) ; SnCl₂ as a reducing agent). NaCl concentrations (% m/v) are given on the curves [42].

3.1.3 Matrix Effects in Inductively Coupled Plasma Optical Emission Spectrometric Detection

The inductively coupled plasma optical emission spectrometry (ICP-OES) is largely employed for simultaneous and multi-elements determination in routine analysis. Nevertheless, the accuracy of this technique is often limited by interferences. Matrix effects in ICP-OES are spectral and non-spectral interferences. Spectral interferences are due to spectral overlap while non-spectral interferences are chemical and easily ionized elements interferences [16].

One type of interferences occasionally encountered in ICP-OES is called easily ionized elements (EIEs) effect. The EIEs are elements with low ionization potentials (IP) that are ionized easily at lower temperatures than the other elements in the periodic table. The common elements of EIEs are Li, Na, K, Ca, and Cs. The presence of EIEs in samples may result either in suppression or enhancement of analyte emission signals for various atom and ion lines [16]. In the presence of EIEs, ionic line is suppressed [18-19]. However, the non-EIEs (at concentrations higher than 0.05 mol L⁻¹) [20-21] and several parameters, such as the plasma power,

argon gas flows, and spatial position of observation point in the ICP also affect on analyte signal intensity [17-18].

The sample containing high concentrations of EIEs and non-EIEs can lead to a change in the characteristics of the aerosol generated by the nebulizer. Further, the transport of the aerosol to the plasma may be different from that in water. The aerosol transport interferences are the characteristics of the aerosols entering the plasma, the total mass of solvent (liquid and vapor) delivered to the plasma and the total mass of analyte transported to the plasma [17-18].

The effect of EIEs on ICP-OES detection is rather complex, and no clear evidence has been reported in previously published work [22-25]. The presence of EIEs into the plasma may cause a modification in electron density and the excitation temperature, as well as a modification in the spatial distribution of atomic and ionic species, and can affect the excitation mechanism of the elements determined [31]. Finally, they can lead to increasing in the total population of analyte excited species, a concomitant increase in the analyte atomic number density and a reduction in the ionic density in the plasma observation zone [26].

3.1.3.1 Proposed Mechanisms Explaining the Matrix Effects in ICP-OES Detection

Various mechanisms were suggested for the explanation of the effect of easily ionized elements (EIEs) on the metal excitation in the plasma, namely, ionization shift, enhanced collisional excitation, vaporization effect, ambipolar diffusion, and others [27-31]. Effect of high salt concentration on the efficiency of nebulization and sample transport to the plasma has been evaluated. Normally, one excitation mechanism is not enough for explaining the results of experiments. The excitation mechanism indicates that various factors essentially affect the overall behavior of the analyte, resulting in the signal measured [31].

Turk *et al.* [32] studied the recombination kinetics between the strontium ions and the electrons in ICP. They reported that the addition of EIEs (K, Li) increased the rate of electron-ion recombination owing to the increase in electron number density. Therefore, the ionization equilibrium would be displaced towards the atomic species and a rise in the atomic emission would be expected together with a collateral drop in ionic emission. The recombination time constant was directly proportional to the ion/atom ratio.

Chan and Hieftje [33] presented a brief review of excitation mechanisms in the ICP. They classified the analyte excitation mechanisms in ICP into four main types, which are summarized in Table 3.2. Although, direct experimental evidence showed that some mechanisms (e.g., charge transfer and ion-electron recombination) were dominant over the others in specific situations, the dominant mechanism was not conclusive and debatable for some classes of energy levels.

Table 3.2 Mechanisms for analyte excitation [33].

Mechanism	Reactions
I. Electron-impact excitation and ionization	$M_p + e^- \rightarrow M_q + e^-$ $M_p + e^- \rightarrow M_p^+ + e^- + e^-$ $M_p^+ + e^- \rightarrow M_q^+ + e^-$
II. Charge transfer	$Ar^+ + M \rightarrow Ar + M^{+*} + \Delta E$
III. Penning ionization	$Ar^* + M \rightarrow Ar + M^+ + e^-$ $Ar^* + M \rightarrow Ar + M^{+*} + e^-$
IV. Ion-electron recombination	$M^+ + e^- \rightarrow M^* + h\nu_{cont} (radiative)$ $M^+ + e^- + e^- \rightarrow M^* + e^-$

In the above reactions, M represents a generic analyte atom and the subscripts p and q pertain to lower and upper energy levels, respectively [33].

3.2 Matrix Removal Methods

3.2.1 Matrix Modification in Graphite Furnace Atomic Absorption Spectrometric Detection

One of the most popular method for reduction of influence occurring from matrix in high salt sample for GFAAS is modification of the sample matrix with a chemical modifier. Several permanent and non-permanent chemical modifiers were applied to minimize the simultaneous background absorption signal. Two ways can be considered: 1) delay the vaporization of element 2) increase the volatility of the element and select a low atomization temperature. The former is employed to eliminate the sodium species and volatile decomposition products, which is a major part of the salts before atomization. The latter is performed to gain a good separation of analyte and the vaporization of sodium species without important losses of analyte [43].

For instance, copper and manganese determination in seawater by GFAAS were affected by a strong background absorption signal and chemical interference from sodium chloride and magnesium chloride. Different chemical modifiers such as organic acid [45-46], various forms of palladium [47-48], sodium hydroxide [49], ammonium nitrate [44] and nitric acid [45, 51] have been used for decreasing these effects. However, the pyrolytic graphite coatings were relatively aggressive when using nitrate-based modifier [53]. Moreover, organic acids also lead to production of carbon residues in atomizer and decomposition products [43].

Cabon [43, 52] added the hydrogen fluoride modifier into seawater sample for removing chloride at the drying step in the determination of cadmium, lead, copper and manganese. This modifier can suppress the chloride interference effects. However, when hydrogen fluoride and seawater are added together into the furnace, calcium and magnesium are still present in atomization step and produce the background absorption signal limiting the sample volume that can be introduced into

the furnace. Consequently, calcium and magnesium need to be eliminated before GFAAS analysis [50].

Wang *et al.* [55] performed preconcentration of 25 mL drinking water containing 2,3-dimercaptopropane-1-sulfonate complexing agent (DMPS, 15 μg) and mercury (5-100 ng) then concentrating on two Sep-Pak C₁₈ cartridges in series by gravitational force before determination by GFAAS. The DMPS chelating agent exhibits a large formation constant ($\log k = 42.2$) with Hg^{2+} [56]. Two cartridges in series were used since the distribution of mercury-DMPS complex on both cartridges was affected by sample volume and flow rate. The larger sample volume and faster flow rate result in fewer portions retained on the first cartridge, and therefore the second cartridge was necessary to be used for collecting the unretained mercury from the first cartridge. The total volume obtained from two C₁₈ cartridges must be used for quantitative analysis.

Colbert *et al.* [54] developed an online preconcentration method for the determination of cadmium in seawater followed by GFAAS using deuterium lamp background correction. The sample was added with soluble ligand, 1-pyrrolidinecarbodithioic acid (APDC) in a continuous flow system to form non-polar metal complex which was adsorbed onto a C₁₈ column. The metal complex was eluted from the column and transported directly into graphite furnace. Although, this automated preconcentration method can reduce matrix elements in samples, the average preconcentration time was 55 s and the running cost was high.

The preconcentration method based on complexation-separation was also reported. The HF-FF unit with opposed flow method reported by Sawatsuk *et al.* [10] was demonstrated to be capable for matrix removal and analyte preconcentration with low cost. The performance test of HF-FF system for matrix removal and preconcentration in high salt sample before determination by GFAAS was investigated in this research.

3.2.2 Matrix Removal for Cold Vapor Atomic Absorption Spectrometric Detection

Various modifications have been introduced to cold vapor atomic absorption spectrometry (CVAAS), aiming to improve the sensitivity, precision, lower interferences, and increase practicality of the methodology. The enrichment process based on the amalgamation of generated mercury vapor on a gold trap is recommended for quantification of low mercury content in environmental samples. [60].

Ombaba [61] developed the method for total mercury determination in biological and environmental samples using high-pressure microwave digestion to reduce the organic and inorganic materials which will bring about some interferences during the analysis and preconcentration by mercury amalgamation followed by CVAAS. They concluded that this method was effective for total mercury determination in these samples.

Costley *et al.* [62] determined mercury in both solid environmental and biological samples using atomic absorption spectrometry with gold amalgamation. The advantages of this technique are due to unnecessary for sample preparation or lengthy derivatization processes. The method can be performed directly on the solid sample in a dedicated automated system. However, some disadvantages are caused by background interferences for samples with high organic content. Moreover, other analytes present in the sample may be concentrated via amalgamation, and hence give rise to background problems.

Although, the gold trap is a simple on-line preconcentration system and does not require the use of reagent and could easily be adopted to the flow-injection technique but some authors reported two drawbacks of this amalgamation technique. First, the efficiency of mercury collection may be weakened by moisture [58] or other gaseous reaction products which damage the surface of the amalgamation medium, necessitating occasional cleaning [57]. Second, during heating of the collector to

release the mercury, a gas flow is used to transport the vapor to the absorption cell, which means that the sensitivity is affected by the gas flow rate. Slight changes in the flow-rate between measurements will also impair the reproducibility [59].

Furthermore, other frequently used methods for preconcentration and matrix removal of mercury from various samples followed by CVAAS are liquid extraction [63], electrochemical CVAAS [64], solid phase extraction [38], and addition of some chemicals in sample to reduce interferences [65]. Conversely, some of these techniques have limitations, such as: solvent wastes, time consuming, and high operating cost. To overcome these limitations, the HF-FF system was used for matrix removal and preconcentration in high salt sample before CVAAS.

3.2.3 Matrix Removal for Inductively Coupled Plasma Optical Emission Spectrometric Detection

Many preconcentration and matrix removal methods for the determination of trace metal in environmental samples followed by ICP-OES have been reported including solid-phase extraction, liquid extraction, complexation-ultrafiltration method, and etc.

Chang *et al.* [70] synthesized a new poly (epoxy-melamine) chelating resin from epoxy resin for the preconcentration and separation of traces of Ru(III), Au(III), V(V) and Ti(IV) ions from sample solutions for further detection by ICP-OES. The chelating resin can be reused 7 times without obvious loss of efficiency. Although, the synthesis of the chelating resin is simple and cheap but this chelating resin is not available in the market.

A conical mini-column packed with activated carbon was applied to carry out preconcentration of cobalt in drinking water comprising a flow injection system prior ICP-OES detection. Trace amounts of cobalt were preconcentrated by sorption on activated carbon and then removed with 20% (v/v) nitric acid. An enrichment factor of 95-fold for 50 mL sample volume was obtained. This method was

reported by Farias *et al.* [71]. The preconcentration systems using activated charcoal may still need the addition of chelating agents to desorb and concentrated nitric acid to the analyte complex from activated carbon, resulting in time-consuming [72].

Rao *et al.* [73] developed an analytical procedure for the preconcentration and separation of trace metal ions in saline matrices using morpholine dithiocarbamate (MDTC) as a chelating agent coated on Amberlite XAD-4. The advantage of MDTC is a strong metal binding property combining with the insolubility of metal complexes resulting in high sorption capacity of the new matrix for preconcentration and determination of metals in saline water. Nonetheless, solid-phase extraction requires desorption step which can cause sample contamination.

Batterham *et al.* [74] performed an off-line dithiocarbamate (DTC) solvent extraction system with ICP-OES for the determination of heavy metals in seawater at ultra-trace levels. DTC was used to form complex with trace metals in seawater. The complexes were extracted into diisobutyl ketone phase and then back-extraction by exchanging with mercury which has a much greater DTC stability constant [75]. The method gave good reproducibility. Unfortunately, the solvent of liquid extraction process that has high vapor pressure may extinguish the plasma while low-vapor-pressure solvents may remain in the sample introduction devices [72].

Sangsawong *et al.* [11] modified flow-field flow fractionation (FIFFF) for matrix removal before ICP-OES detection based on the complexation-ultrafiltration method. Poly(ethylene imine) (PEI) was added in the test solutions to form PEI-analyte complexes. These complexes remained in the channel and were subsequently eluted and detected. The procedure was illustrated to be an efficient approach to remove matrix elements and that can be considered as an alternative way for both routine and research in sample containing high salt concentration.

3.2.4 Complexation-Ultrafiltration for Matrix Removal

Among many separation techniques, membrane separation is an efficient method, avoiding heterogeneous two-phase system. It is comparable to other separation techniques in terms of technical and economical feasibility. The soluble polymer is found to be suitable for the separation and enrichment of metal ions in conjunction with membrane filtration. Ultrafiltration is fast emerging as a new and versatile technique in separation, preconcentration, and purification processes [76-77].

In 1996, Geckeler *et al.* [77] reviewed the concept, factors influencing the separation of analyte, and application of separation method using ultrafiltration in conjunction with soluble polymers. The process is consisted of two steps: (1) complexation of a metal ion by a macroligand; and (2) ultrafiltration of the complex. At complexation step, a water-soluble polymeric binding agent is added to a multicomponent solution so that this agent will form macromolecular compounds with the analyte but not with the sample matrix. The matrix solution is pumped through an ultrafiltration membrane to separate and concentrate analyte from matrix.

The fundamental requirements of the polymer are high affinity toward analyte, inactivity toward matrix, high molecular mass, possibility of regeneration, chemical and mechanical stability, low toxicity, and low cost. Many water soluble polymers were used such as poly(allylamine) (PALA) (for Cu^{2+} , Co^{2+} , and Ni^{2+}), poly(4-vinylpyridine quaternized) (PVPyQ) (for Ag^+ , Hg^{2+}), poly(N-methacryloyl-4-aminosalicylic acid) (PMAAMSA) (for Ca^{2+} and Zn^{2+}), etc. [76]. Nonetheless, poly-(ethylenimine) (PEI) is one of the most commonly used binding agents in complexation-ultrafiltration process [79-80] because it demonstrates a good selectivity toward transition metal ions. PEI was applied to remove heavy metals from industrial wastes and natural waters. It was shown that it could be effectively used even for the selective concentration of microcomponents of seawater where concentrations of alkali and alkaline earth metals were several orders of magnitude higher than the concentrations of the target transition metal ions [77]. Figure 3.2 shows molecules of

PEI chelated with Cu^{2+} in aqueous solutions and the general structure of polymer-metal amine type complexes [76].

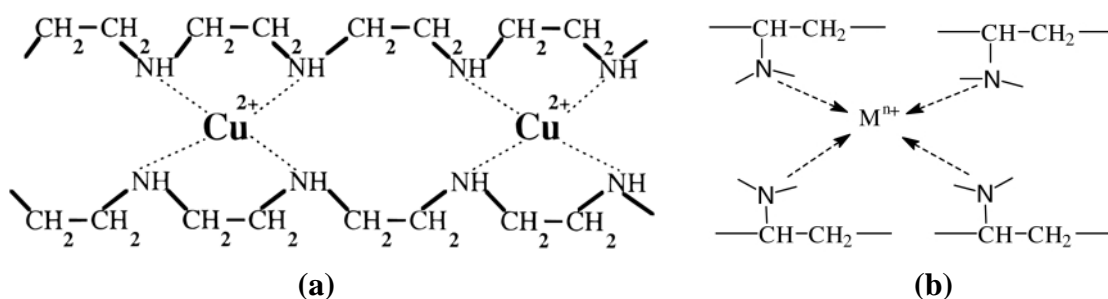


Figure 3.2 (a) Idealized structure of the polymeric complex poly-(ethylenimine) with copper(II) ions [77], (b) general structure of polymer-metal amine type complexes [76].

Al-Ammar *et al.* [78] used PEI to study analyte preconcentration and matrix elimination in the presence of sodium and calcium as matrices, since this polymer forms strong complexes at pH 7-8 with most elements except alkaline and alkaline earth elements. The preconcentration factor of 50-1400 fold was obtained.

The important factor in most cases of polymeric binding is pH value due to the fact that either protons or hydroxyl anions can compete with analyte to be bound to the polymer. In the case of PEI, at low pH electron donating imino groups become positively charged from protonation and thus unable to form chelates with cations. Moreover, when the analyte is present in the feed solution in an anionic form, the presence of hydroxyl anions may affect the binding due to the possible competition [77].

Barron-Zambrano *et al.* [81] studied the effects of pH and chloride ions concentration on the separation of mercury from aqueous solutions using PEI and complexation-ultrafiltration method. In acidic medium the mercury retention strongly depends on pH and chloride ion concentration. To achieve high values of mercury retention rate, PEI solution was filtered with the same membrane to eliminate the low

molecular weight fractions. This filtered PEI solution leads to mercury retention close to 100% for pH higher than 7.

In addition, the precipitation of polymer may also occur when the ionic strength of the solution is high as it reduces the solubility of a polymer [77].

The emerging technology which undergoes a rapid growth during the past few decades are membrane separation processes. Hollow fiber is widely used in industries for many types of samples including food, juice, pharmaceutical, dairy, wine, and drinking water. Since the process occurred in hollow fiber is filtration, it does not create any waste from its operation except the unwanted component in the feed stream. This can help decrease the cost of operation to handle the waste. Hollow fiber has large membrane surface per unit volume and its operation is cost compared to other types of unit operation. However, membrane fouling is considered as a drawback. The hollow fiber membrane made of polymer cannot be used for corrosive substances and at high temperature condition [66-67].

Hollow fiber ultrafiltration membrane is made of high molecular chemical material by special technology. It is an asymmetric semi-permeable membrane presenting hollow capillary tube shape with micro-pore covering tube wall densely. Filtration can be carried out by 2 ways, either "inside-out" or "outside-in".

The flow through method has one flow streams that entered at channel inlet. The flow is separated into two ways which are radial flow (the flow penetrates the membrane pore) and axial flow (the flow exits from the hollow fiber channel outlet). The radial flow field was generated causing small molecules or solvent permeate through membrane whereas large molecules (protein, polysaccharide, and etc.), and colloid particles retained in channel.

Bishop and Mitra [68] demonstrated the feasibility of solvent pervaporation and on-line analyte preconcentration using two types of hollow fiber membrane. These include a microporous composite hydrophobic hollow fiber

membrane and a polar solvent permeable Nafion hollow fiber membrane. Large increase in analyte enrichment factors was obtained using both concentrator modules.

Sawatsuk *et al.* [10] used hollow fiber flow filtration (HF-FF) with focusing method to perform matrix removal and analyte preconcentration before ICP-OES detection. The matrix removal efficiency of their system was nearly 100% with preconcentration factor as high as 7.

3.3 Sample Introduction for ICP-OES

3.3.1 Chemical Vapor Generation

The sample introduction of ICP-OES is an important part. The conventional pneumatic nebulizer suffers from low analyte transport efficiency (< 5%) [102] and matrix effects [103]. Some of these interferences can be eliminated by introduction of the analyte in its gaseous hydride into the plasma [82]. Chemical vapor generation (CVG) is extensively utilized gas-phase sample-introduction technique in the atomic emission spectrometry (AES) for the determination of those analytes that can be readily converted into stable cold vapor or hydride derivatives and transferred into an excitation source.

The convenience of CVG for AES arises from high transport efficiency of the analytes into plasma. The analytes are injected as homogeneous medium that regularly requires much lower power input to achieve a complete atomization compared to traditional liquid-sample introduction (*i.e.* pneumatic nebulization). Other advantages of the CVG are the separation of the elements of interest from the other constituents of the troublesome matrices examined, high enrichment of the analytes along with the possibility for speciation, and effective sample throughput using flow injection and continuous flow devices. These benefits increase the analytical performance of AES detection techniques in terms of improved sensitivities and lower limits of detection (LODs) in conjunction with a very good precision of measurements, as found by comparing the figures of merit obtained when the

pneumatic nebulization sample-introduction technique is used. However, the technique is limited to a small number of elements (i.e. arsenic, antimony, bismuth, germanium, lead, selenium, tellurium, tin, and mercury), which at ambient temperature, can form their covalent hydrides or cold vapor (AsH_3 , SbH_3 , BiH_3 , GeH_4 , PbH_4 , H_2Se , H_2Te , SnH_4 , and Hg , respectively) in the reaction performed in acid media and in the presence of a reducing agent [83]. Within the last ten years, several more elements were added to the list of elements determinable from volatile species. These elements include platinum, cobalt, silver, copper, rhodium, gold, nickel, iridium, titanium, and manganese [85-86].

The CVG process for further detection by AES can be considered as four steps:

- (1) chemical reaction generating the hydrides or cold vapor
- (2) collection and preconcentration of the evolved hydrides or cold vapor (if necessary)
- (3) transport of the gaseous hydrides or cold vapor and other by products of the reaction (hydrogen, carbon dioxide and water vapor) into the excitation source
- (4) atomization of the hydrides or cold vapor, excitation of the analyte atoms and emission of the radiation combined with its detection.

The schematic of process is shown in Figure 3.3.

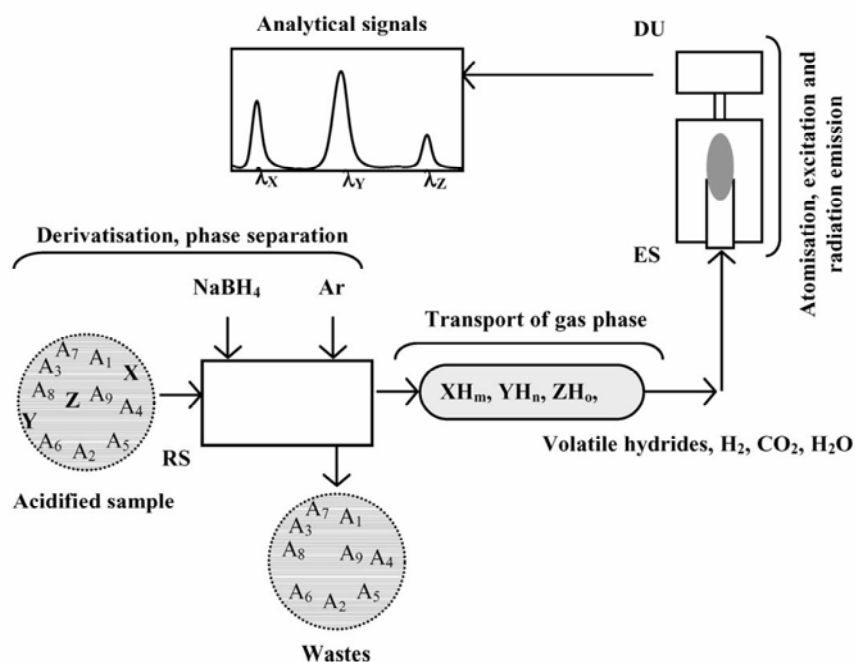
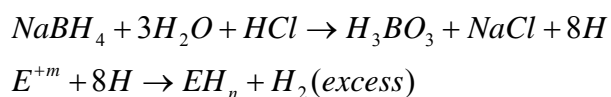


Figure 3.3 Stages of hydride generation with AES detection. Abbreviations: X, Y, Z, hydride-forming elements; A, matrix element; RS, reaction-separation system; ES, excitation source; DU, detection unit [83].

The hydride or cold vapor forming is often performed by mixing the acidified sample solution with the alkaline solution of sodium tetrahydroborate (NaBH₄) and the reaction occurs instantly and extremely rapid. The volatile analyte species formed and the by products of the reaction, corresponding to the excess of H₂, CO₂ and H₂O, are separated in a gas-liquid phase separator. The spent liquid is driven to waste. Reaction-forming hydride EH_n of element E at the oxidation state +m may be described as follows [83]:



The reaction condition depends commonly on the number of hydride or cold vapor forming elements examined, the content of the sample matrix, and the

concentration and flow rate of acid and reductant. To acidify the reaction medium, hydrochloric acid (HCl) was mainly used by adding it to the sample at the appropriate concentration. The optimal concentration of the acid serving as the reaction medium ranged from 0.020 mol L⁻¹ to 10 mol L⁻¹. Also, the NaBH₄ concentration in the reductant solution was also extensive, ranging from 0.25% (m/v) to 10% (m/v). However, NaBH₄ concentration of 1% (m/v) was most common [77].

The first report on the use of hydride generation as a procedure for sample introduction in an ICP is by Thompson *et al.* [84], who performed the simultaneous determination of arsenic, antimony, bismuth, selenium, and tellurium. The best limits of detection were found at higher RF-power and with 5 mol L⁻¹ HCl. The LOD obtained was 500 times lower with respect to pneumatic nebulization. Goulden *et al.* [85] determined arsenic and selenium at RF-power of 1400 W in the ICP–OES. A large diameter torch (5 mm) than usual (2 mm) was used to provide stability of the plasma discharge.

Different kinds of samples with various degrees of complexity were analyzed by hydride generation-AES methods, including waters, food and beverages, biological tissues and fluids, plants and environmental, geological, and metallurgical samples [83].

3.3.2 Modified Cyclonic Spray Chamber as A Spray Chamber for Solution Nebulization and as A Gas Liquid Separator for Vapor Generation

The two most widely employed spray chambers in ICP-OES are the double pass (Scott type) and the cyclonic-type spray chambers. The spray chamber plays a crucial role in the liquid sample introduction system [88]. Recently, an effort has been made to adapt these spray chamber designs to the work in chemical vapor generation (CVG) in conjunction with ICP. Figure 3.4 illustrates some of special design of double pass and cyclonic spray chambers using in vapor introduction into ICP. With the spray chamber in Figure 3.4 (a), the reaction can be performed outside

the chamber in a T-junction then a shear gas facilitates rapid release of the reaction products inside the chamber when introduced through the concentric channels of a modified parallel-path nebulizer [86-87, and 90]. A cross-flow nebulizer of spray chamber in Figure 3.4 (b) was modified by insertion of an additional capillary into the sample-introduction tube. Both the sample and the reducing agent are introduced into the chamber through the concentric channel of this nebulizer [91]. The reaction occurs inside the mixing zone of channel, resulting in a very short residence time of the sample in the reaction zone, rapid introduction of liquid and gases into the spray chamber for phase separation, and reduction of concurrent aerosol formation. The cyclonic spray chambers (Figure 3.4 (c)) were used as the reactor and gas phase separator. The reaction and separation of the species can also be performed inside the chamber [92-94] after delivery of the reagents in separate streams.

In addition, the cyclonic spray chambers normally have lower inner volumes than the double pass type (e.g., 50 cm³ or less compared to 100 cm³). It gives rise to higher ICP-OES sensitivity, lower LODs, and leads to lower matrix effects when either inorganic acids or salts are present, as compared to the double pass ones [89, 95].

The concomitant metals analyzer (CMA) has been commercialized by Jobin Yvon to be operated both in solution nebulization and hydride generation systems [96]. Pohl and Żyrnicki [97] employed CMA without a gas-liquid phase separator for the determination of arsenic, bismuth, selenium, tin using hydride generation and non-hydride forming elements using solution nebulization by the ICP-OES technique. McLaughlin and Brindle [98] reported a multimode sample introduction system (MSIS) in which hydride formation took place at the outlet of the two capillaries, located in a modified cyclonic spray chamber. These capillaries transport the sample and sodium tetrahydroborate solutions to form volatile species. The MSIS system provides convenient means of determining elements, either by nebulization or vapor generation, or simultaneously in the same device.

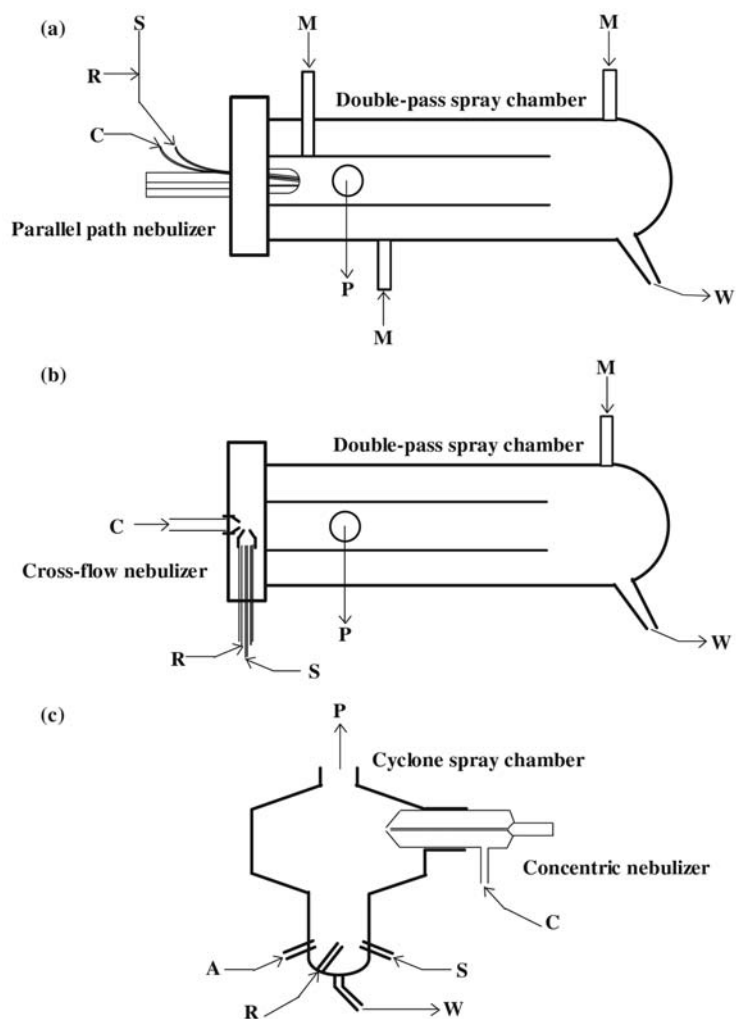


Figure 3.4 CVG systems based on use of spray chambers and nebulizers: (a) Refs. [86-87, 90], (b) Ref. [91], and (c) Refs. [92, 93-94]. A, acid solution; C, carrier gas flow; M, makeup gas flow; P, linking with plasma torch; R, reducing agent solution; S, acidified sample solution; W, waste solution.

Asfaw and Wibetoe [99-100] applied a commercial MSIS for the determination of arsenic, bismuth, antimony, selenium, introduced as the hydride, simultaneously with the other non-hydride forming elements (calcium, cadmium, cobalt, copper, magnesium, nickel, potassium, phosphorus, lead, sulfur, zinc) by ICP-

OES or ICP-MS. Various samples were examined including beer, instant coffee, milk, milk powder, and various certified reference materials.

Matusiewicz and Ślachciński [101] developed a slurry sampling method for the simultaneous determination of hydride and non-hydride forming elements, without total sample digestion, using the commercial MSIS coupled with microwave induced plasma optical emission spectrometry (MIP-OES) from biological and environmental reference materials and real samples. The method requires small amounts of reagents and reduces contamination and losses.

CHAPTER IV

MATERIALS AND METHODS

The system set up, operating condition, chemical reagents and preparation of solutions are described in this chapter.

4.1 Instrumentation

4.1.1 Graphite Furnace Atomic Absorption Spectrometer (GFAAS)

A Perkin Elmer Model AAnalyst 100 with deuterium background corrector was employed for mercury determination. The Perkin Elmer Model AS-72 autosampler was used to introduce solution into graphite tube. The furnace operating condition for mercury measurement is summarized in Table 4.1.

Table 4.1 Furnace operating condition for mercury determination.

Step	Temperature (°C)	Ramp/Hold Time (s)	Argon Flow (mL min ⁻¹)
1. Drying	120	10/20	250
2. Ashing	150	1/15	250
3. Pre-atomization	20	1/15	250
4. Atomization	1200	0/10	0
5. Clean up	2400	1/5	250

4.1.2 Cold Vapor Atomic Absorption Spectrometer (CVAAS)

CVAAS determination of mercury was performed with a Perkin Elmer FIAS 400 with Perkin Elmer 3100 atomic absorption spectrometer. Absorbance of mercury was measured at 253.7 nm with 0.7 nm slit width. The parameters and operating conditions are presented in Table 4.2.

Table 4.2 Parameters and operating condition for mercury detection by CVAAS.

Step	Time (s)	Speed pump (rpm)		Ar Gas Flow (mL min ⁻¹)
		Pump 1	Pump 2	
Prefill	15	70	100	100
1.	10	70	100	100
2.	5	70	100	100
3.*	58	70	100	100
4.	1	0	0	100

*Read step

4.1.3 Inductively Coupled Plasma-Optical Emission Spectrometer (ICP-OES)

The ICP-OES system was a Spectro Ciros^{CCD} (Spectro Analytical Instruments, Kleve, Germany), axial configuration. The Thermo Neslab chiller was used as a cooling system. The ICP-OES operating conditions are shown in Table 4.3.

Table 4.3 ICP-OES operating conditions.

Plasma Conditions	
RF generator frequency/MHz	27.2
RF power/W	1,350
Nebulizer gas flow rate/L min ⁻¹	0.65
Coolant gas flow rate/L min ⁻¹	12.0
Auxiliary gas flow rate/L min ⁻¹	1.0
Measurement Parameter	
Number of replicate	15
Sample Introduction	
Sample uptake rate/mL min ⁻¹ (HF-FF and solution method)	1
Line monitored/ nm	
As	189.042 (I), 193.759 (I)
Se	196.090 (I)
Cd	214.438 (I), 226.502 (I)
Hg	184.950 (I), 194.227 (II)
Pb	217.000 (I), 405.780 (I), 220.351 (II)
Cu	324.754 (I), 224.700 (II)
Zn	213.856 (I), 206.191 (II)

4.2 Equipment

4.2.1 Hollow Fiber Flow Filtration Unit

The hollow fiber membrane was poly(sulfone) with a membrane pore size of 6,000-30,000 Da. The fiber dimension was 31 cm long, 0.8 mm internal diameter, and 1.2 mm outer diameter. The geometrical volume was approximately 150 μ L. The HF-FF unit was constructed in the laboratory with the use of low cost materials. The hollow fiber membrane was inserted into a T-shaped glass tube (3.7

mm i.d., 5.7 mm o.d., and 31 cm long). The ends of membrane inlet and outlet were joined to PTFE tube (poly(tetrafluoroethylene), 1.55 mm od, 5 cm long) and sealed with epoxy glue. At the middle of hollow fiber channel, a three way valve was inserted for controlling the waste drain. The hollow fiber channel is shown in Figure 4.1 and the HF-FF operating conditions are summarized in Table 4.4.

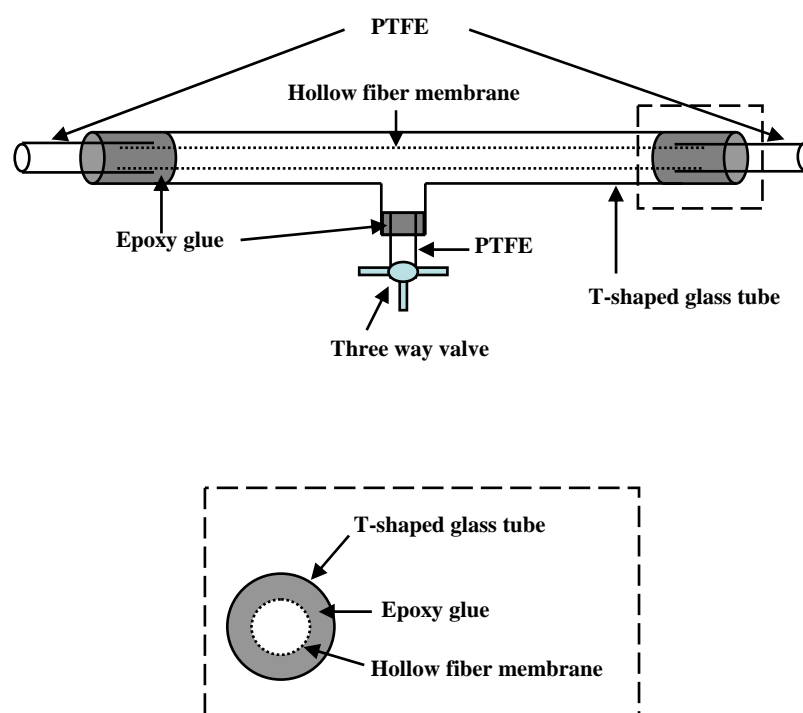


Figure 4.1 A laboratory made hollow fiber channel.

Table 4.4 HF-FF operating conditions.

Carrier liquid	Doubly distilled deionized water
Membrane	30,000 Da MWCO, poly(sulfone)
Channel volume/mL	0.150
Forward flow rate/mL min ⁻¹	1.8
Backward flow rate/mL min ⁻¹	0.2
Elution flow rate/mL min ⁻¹	1.0

4.2.2 Lab-Made Cyclonic Spray Chamber (LMSC)

Lab-made cyclonic spray chamber (LMSC) is simple and inexpensive to construct since it is made of glass. LMSC was made in our laboratory, and its construction was based on a design of commercially cyclonic spray chamber. LMSC consists of a cyclonic spray chamber that has been modified by the addition of two tubes located vertically in the spray chamber. As shown in Figure 4.2, LMSC has five opening lines for (a) nebulizer, (b) acidified sample for vapor generation, (c) reducing agent for vapor generation, (d) transport to ICP, and (e) waste. The approximate volume of LMSC is 42 mL.

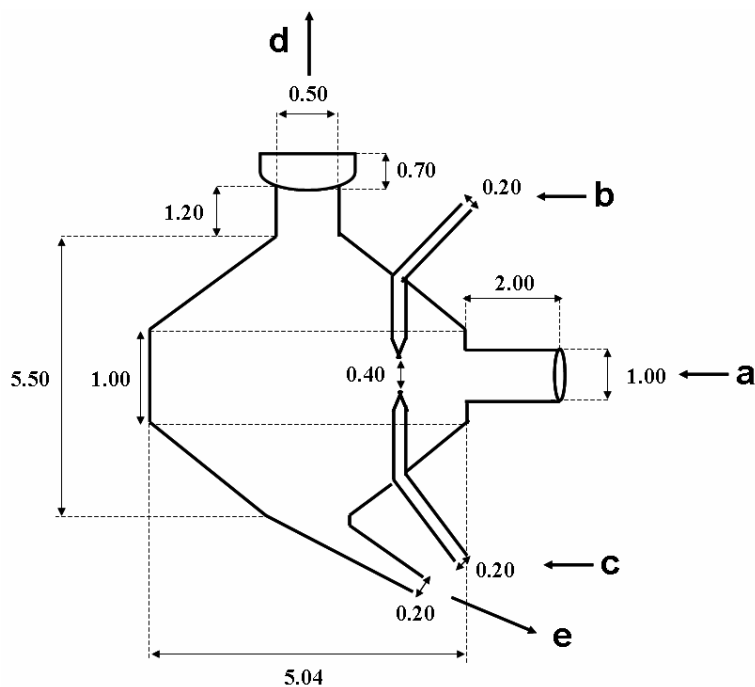


Figure 4.2 Schematic diagram of LMSC for sample introduction system in ICP-OES. Dimension is displayed in centimeter unit. a = nebulizer, b = acidified sample for vapor generation, c = reducing agent for vapor generation, d = transport to ICP, and e = waste.

4.2.3 Peristaltic Pump

For vapor generation sample introduction in ICP-OES experiment, the acidified sample and the reduction solution were continuously pumped to LMSC using a peristaltic pump (Ismatec, Reglo Analog, Glatt brugg, Switzerland) and the drain was sucked from the spray chamber by a separate peristaltic pump.

The same pump was employed to control forward, backward, and elution flows in HF-FF system.

4.2.4 pH Meter

A powerful pH meter (Orion, Model PCM 500, Massachusetts, USA) with a combination glass electrode (i.d. 6 mm) was used for pH measurement. Commercial standard buffers of pH 4.00 ± 0.01 , 7.00 ± 0.01 and 10.00 ± 0.01 from Merck, Germany were used to calibrate the pH meter.

4.2.5 Analytical Balance

A precisa 240A (Zurich, Switzerland) was used for weighing reagents, chemicals, and samples.

4.3 Chemical Reagents

All chemicals used in experiments were of analytical grade which are listed in Table 4.5. Deionized water (Fresh deionized water was prepared daily by water purification system (Barnstead International, Dubuque, IA, USA)) or nitric acid was used to prepare reagent and standard solution.

Table 4.5 List of chemicals.

Chemical reagents	Supplier
Poly(ethylene imine) solution, 50 wt% in water, Mw ~ 750,000 Da	Aldrich, Germany
Boric acid	Merck, Germany
Di-sodium tetraborate	BDH, England
Sodium hydroxide (99%)	Merck, Germany
Nitric acid, (65%)	Merck, Germany
Hydrochloric acid (37%)	Merck, Germany
Mercury (II) sulfate	BDH, England
Sodium selenite (99%)	Sigma, USA
Cadmium nitrate (99%)	Ajax Finechem, Australia
Di-sodium hydrogen arsenate heptahydrate (98.5%)	Fluka chemie GmbH, Germany
Lead nitrate	Merck, Germany
Zinc nitrate hexahydrate (98.5-102%)	Schalan Chemie S.A., Spain
Copper (II) nitrate trihydrate (99.5%)	Merck, Germany
Calcium nitrate tetrahydrate (99-103%)	Merck, Germany
Magnesium nitrate hexahydrate (99-102%)	BDH, England
Sodium nitrate (99%)	Ajax Finechem, Australia
Potassium nitrate	Ajax Finechem, Australia
Palladium nitrate	Merck, Germany
Sodium borohydride ($\geq 96\%$)	Merck, Germany

4.4 Preparation of Reagent and Standard Solutions

4.4.1 Reagents Used in HF-FF Experiment

4.4.1.1 Polymeric Complexing Agent

A 10,000 mg L⁻¹ stock solution of poly(ethylene imine), PEI, was prepared by dissolving approximately 1.0 g of 50 wt.% PEI solution in 50 mL deionized water.

4.4.1.2 Borate Buffer

Borate buffer was prepared to control pH at approximately 8-10 by dissolving 0.3 g of boric acid and 1.2 g of di-sodium tetraborate in 50 mL deionized water.

4.4.2 Reagents Used in GFAAS Experiment

4.4.2.1 Mercury Standard Solution

Mercury standard solution of 5 mg L⁻¹ in DI water or 10% seawater was prepared from 50,000 mg L⁻¹ stock solution. A stock standard solution was prepared from mercury sulfate by dissolving appropriate amount in 2% HNO₃ then preserved in a refrigerator.

4.4.2.2 Palladium Modifier Solution

A 1,000 mg L⁻¹ palladium was prepared from 10,000 mg L⁻¹ stock solution. A stock solution of palladium was prepared from nitrate salt and dissolved in 2% HNO₃ then preserved in a refrigerator.

4.4.3 Reagents Used in CVAAS Experiment

4.4.3.1 Mercury Standard Solution

Mercury standard solution of $200 \mu\text{g L}^{-1}$ in DI water was prepared from $50,000 \text{ mg L}^{-1}$ stock solution and preserved in a refrigerator.

4.4.3.2 Hydrochloric Acid Solution (7% v/v HCl)

An aliquot of 18.9 mL of conc. HCl was made up volume to 100 mL with deionized water to obtain 7% v/v HCl.

4.4.3.3 Sodium Hydroxide Solution (0.05% m/v NaOH)

Solid sodium hydroxide (0.25 g) was dissolved in deionized water and made up volume to 500 mL.

4.4.3.4 Sodium Tetrahydroborate(III) (0.2% v/v NaBH_4)

Sodium tetrahydroborate(III), used as reducing solution, was prepared daily by dissolving NaBH_4 powders in sodium hydroxide solution to decrease its decomposition rate, and was used without filtration. A 0.2 g NaBH_4 was dissolved in 0.05% m/v sodium hydroxide solution and made up volume to 100 mL.

4.4.4 Reagents Used in ICP-OES Experiment

4.4.4.1 Hydrochloric Acid Solution (5% v/v HCl)

An aliquot of 13.5 mL of conc. hydrochloric acid was made up volume to 100 mL with deionized water.

4.4.4.2 Sodium Hydroxide Solution (0.4% m/v NaOH)

Solid sodium hydroxide (4 g) was dissolved in deionized water and made up volume to 1,000 mL.

4.4.4.3 Sodium Tetrahydroborate(III) (1% v/v NaBH₄)

Sodium tetrahydroborate(III) 2.5 g was dissolved in 0.4 % m/v sodium hydroxide solution and made up volume to 250 mL.

4.4.4.4 Mixed Standard Solution

A mixed standard solution containing 100 mg L⁻¹ Cd, Hg, and Pb was prepared in 2% HNO₃ from 50,000 mg L⁻¹ stock solution of each. Cadmium and lead stock solutions were dissolved in deionized water except that mercury was dissolved in 2% HNO₃ and then preserved in a refrigerator. This mixed standard was used in the experiment for investigation of LMSC efficiency.

A mixed standard solution containing 100 mg L⁻¹ Se, Cd, Hg, Pb, As, Cu, and Zn was prepared in 2% HNO₃ from 50,000 mg L⁻¹ stock solution of each except As (25,000 mg L⁻¹). A mixed standard solution containing 12,500 mg L⁻¹ Na, K, Ca and Mg was prepared from 50,000 mg L⁻¹ stock standard of each. All stock standard solutions were dissolved in deionized water except that Hg was dissolved in 2% HNO₃ then preserved in a refrigerator. These mixed standard solutions were used in parameter optimization and preconcentration and sensitivity improvement factors study.

4.5 Operating Procedures

4.5.1 Hollow Fiber Flow Filtration System (HF-FF System)

The opposed flow HF-FF was used. It consists of two steps, which are

sample loading and focusing, and elution, as illustrated in Figure 4.3. Sample was loaded into hollow fiber channel, then two opposing flow streams were applied to focus the sample zone into a narrow band near the membrane outlet (Figure 4.3 a). Solution permeated through the membrane wall by radial flow field, which was generated inside channel. The filtrate was drained through the center outlet of the T-shape glass tube. The focusing time was the summation of sample loading and focusing since these two processes occurred simultaneously. The point, where two flow streams met, is called focusing point. The analyte-PEI complexes, which were introduced, migrated to the focusing point. These complexes were kept inside the hollow fiber channel whereas the unbound matrix elements were filtered off through the membrane, owing to high molecular weight of analyte-PEI complexes (~750,000 Da) as compared with the fiber membrane pore size (~30,000 Da). After suitable focusing time, the analyte-PEI complexes were then eluted by applying only the forward (channel) flow of 1 mL min⁻¹ (Figure 4.3 b). For off-line detection, the fraction collection at each 15 min interval was performed instead of the on-line coupling between HF-FF and detector instrument.

4.5.2 GFAAS Determination of Mercury

4.5.2.1 GFAAS: Parameters Optimization for Mercury Determination

Solution containing 5 mg L⁻¹ mercury in DI water with 15 µL 400 mg L⁻¹ PEI buffered at pH 8.92 and 5 µL of 1000 mg L⁻¹ palladium as chemical modifier was employed for the study of suitable ashing and atomization temperatures. Ashing temperature was varied at a fixed atomization temperature of 1200°C. Then, atomization temperature was varied at a fixed ashing temperature of 150°C. Peak area (sensitivity) and %RSD (reproducibility) were considered to obtain optimum ashing and atomization temperatures. The results are given in Section 5.1.1.

4.5.2.2 Mercury Detection by GFAAS: Effect of High Salt Medium

The standard calibration curves of mercury in 10% seawater and DI water were obtained under the optimized furnace operating conditions, which is shown in Table 4.2 with varying mercury concentration (1, 2, 3, and 4 mg L⁻¹). The 1000 mg L⁻¹ palladium was used as chemical modifier.

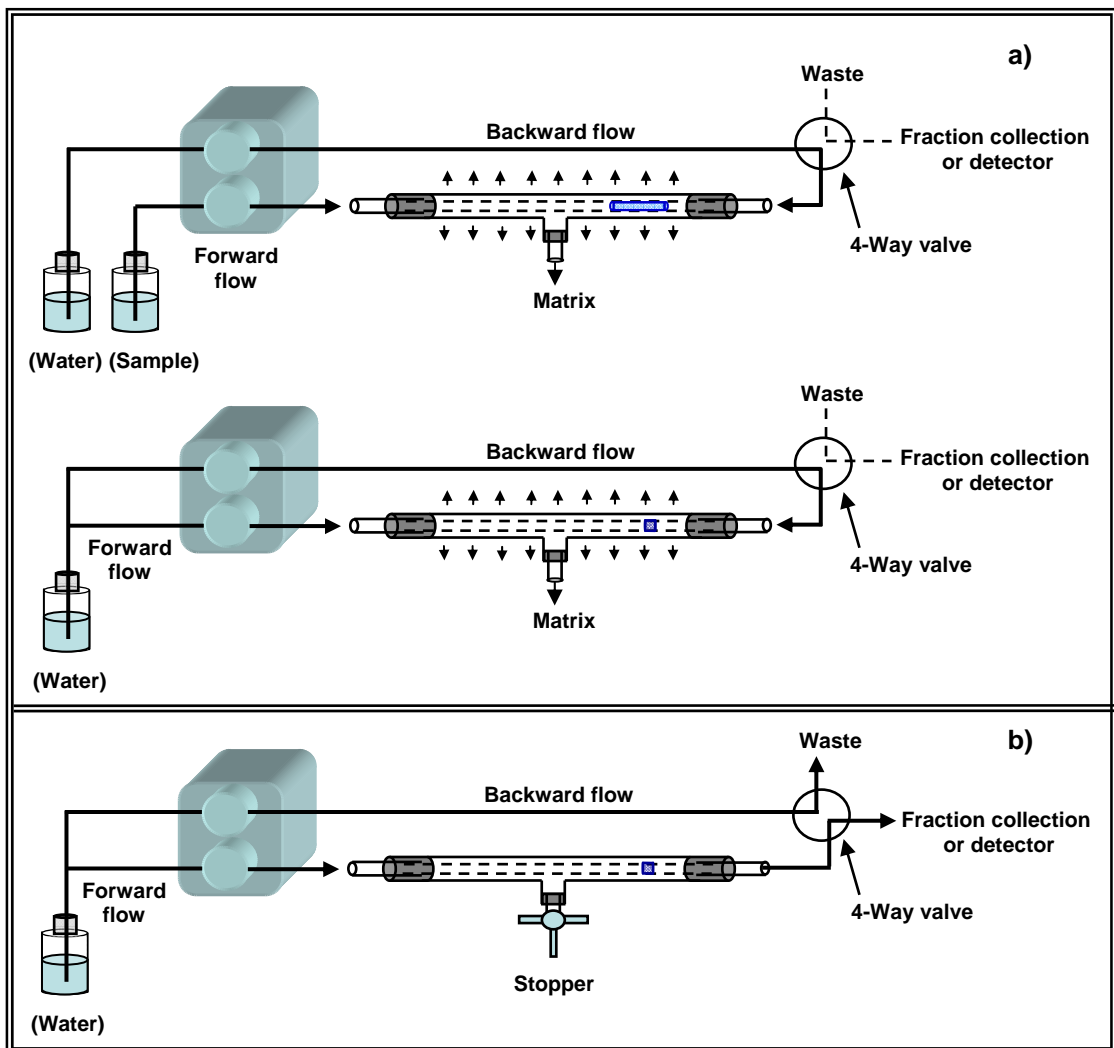


Figure 4.3 HF-FF system matrix removal and sample preconcentration a) sample loading and focusing step b) elution step.

4.5.2.3 Matrix Removal and Analyte Preconcentration with HF-FF System for Mercury Determination by GFAAS

GFAAS was used as a detector to observe the ability of HF-FF system for matrix removal and analyte preconcentration. Test solution was 5 mg L⁻¹ mercury with 400 mg L⁻¹ PEI buffered at pH 8.92 and 5 µL of 1000 mg L⁻¹ palladium as chemical modifier in 10% seawater or DI water. With the optimum conditions of GFAAS and HF-FF system as shown in Table 4.1 and 4.4, a 2 mL-test solution was loaded into channel using focusing time of 15 min and focusing point of 28 cm from channel inlet. An off-line GFAAS detection of mercury after fraction collection was performed instead of the on-line coupling between HF-FF and GFAAS instrument. The preconcentration factors were determined and results are summarized in Section 5.1.3.3.

To study effect of PEI on mercury signal and peak shape, test solution containing 5 mg L⁻¹ mercury in DI water without 400 mg L⁻¹ PEI at pH 8.92 was investigated using GFAAS without HF-FF system.

4.5.3 CVAAS Determination of Mercury

4.5.3.1 CVAAS: Parameters Optimization for Mercury Determination

Experiments regarding optimization studies of mercury determination with CVAAS are described in Sections 4.5.3.1a - 4.5.3.1d.

4.5.3.1a Effect of Acid Carrier (HCl) and Reductant (NaBH₄) Flow Rates

Flow rates of 5% v/v HCl and 0.2% m/v NaBH₄ in 0.05% m/v NaOH were varied between 1.9 and 4.0 mL min⁻¹, by using 200 µg L⁻¹ mercury in DI water, sample volume 500 µL, and argon gas flow rate 100 mL min⁻¹.

4.5.3.1b Effect of Carrier Gas (Argon Gas) Flow Rate

Effect of argon gas flow rate on measured absorbance of mercury was studied by varying the argon gas flow rate between 40 and 200 mL min⁻¹. The carrier (HCl) and reductant (NaBH₄) flow rates were 3.4 mL min⁻¹ and all other conditions are as in Section 4.5.3.1a.

4.5.3.1c Effect of NaBH₄ Concentration

In order to investigate the effect of reductant (NaBH₄) concentration on the sensitivity, NaBH₄ concentration (in 0.05% m/v NaOH) was varied from 0.01 to 1% m/v using a fixed flow rate of 3.4 mL min⁻¹. The absorbance signal for 200 µg L⁻¹ mercury in DI water was monitored using 5% v/v HCl flow rate 3.4 mL min⁻¹, argon gas flow rate 100 mL min⁻¹, and sample volume 200 µL.

4.5.3.1d Effect of HCl Concentration

The influence of HCl concentration on sensitivity was investigated by varying HCl concentration between 1 and 9% v/v. The 0.2% m/v NaBH₄ in 0.05 % m/v NaOH was employed and all other conditions are as in Section 4.5.3.1c.

4.5.3.2 Mercury Determination by CVAAS with HF-FF System: Effect of pH

The test solution, 200 µg L⁻¹ mercury in DI water with 200 mg L⁻¹ PEI, was pH adjusted to the range of 3.8 to 8.9. A 2 mL test solution was loaded into hollow fiber channel to perform simultaneous matrix removal and analyte preconcentration. The process and optimized conditions of HF-FF system were the same as described in Section 4.5.1. The preconcentration factors were determined by comparing the sensitivity obtained from CVAAS detection between with and without HF-FF system.

4.5.4 ICP-OES Determination of Trace Element

4.5.4.1 Sample Introduction Methods

In this experiment, two sample introduction methods for trace element detection by ICP-OES were used. The sample introduction methods include conventional solution nebulization and vapor generation. Conventional solution nebulization was used with or without HF-FF system. Each sample introduction mode is described in the following section.

4.5.4.1.1 Conventional Solution Nebulization

In conventional solution nebulization, LMSC chamber serves as a conventional sample introduction system. The liquid sample was supplied to the nebulizer with sample flow rate of 1 mL min^{-1} . The sample was introduced to the plasma as an aerosol. With conventional solution nebulization, the two inlet lines for introduction of acidified sample and reductant were not used, and hence they were plugged with cap. The instrument set-up is shown in Figure 4.4.

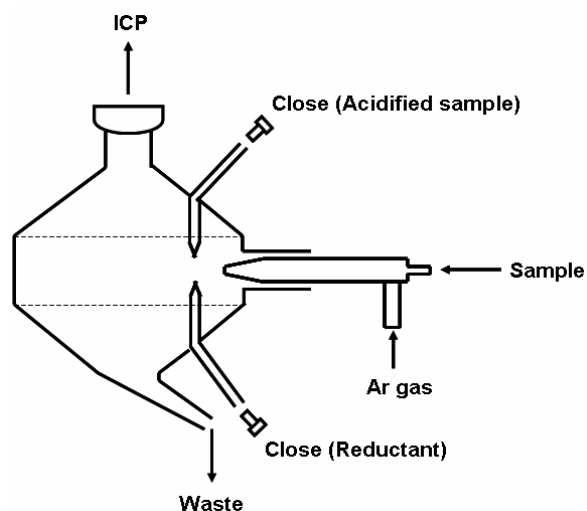


Figure 4.4 Schematic diagram of LMSC set-up for conventional solution nebulization.

4.5.4.1.2 Conventional Solution Nebulization with HF-FF System

Conventional solution nebulization with HF-FF was used for an on-line matrix removal and sample preconcentration using HF-FF system. After matrix removal and sample preconcentration with HF-FF system, the test solution was introduced into plasma with conventional solution nebulization. HF-FF system was explained in Section 4.5.1. The set-up of conventional solution nebulization with HF-FF system is shown in Figure 4.5.

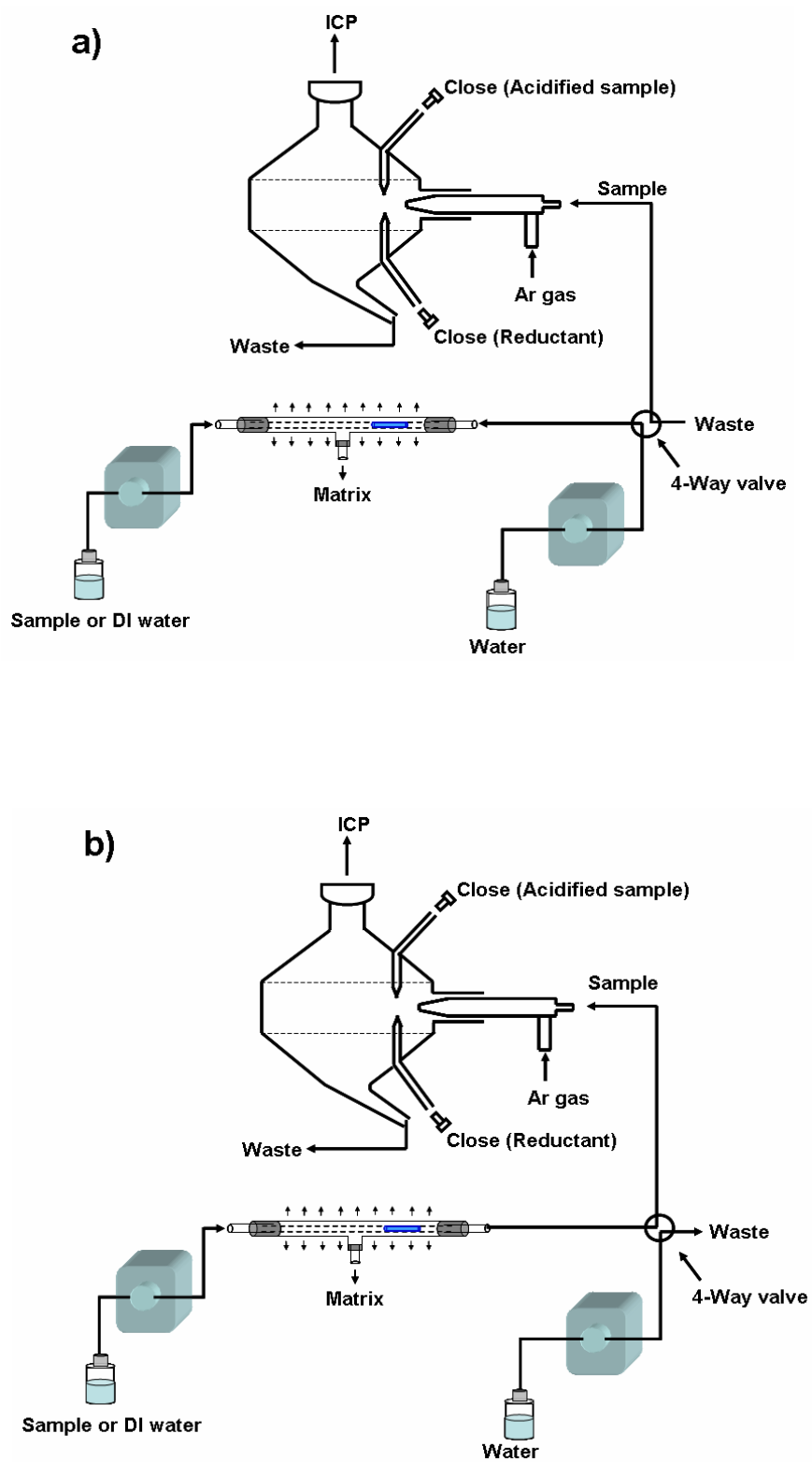


Fig 4.5 Schematic diagram of HF-FF sample introduction method for trace element detection by ICP-OES. a = sample loading and focusing step, b = elution step.

4.5.4.1.3 Vapor Generation Method

With vapor generation, the sample line in conventional solution nebulization was closed. The acidified sample and reductant were introduced through opposing tubes, one of which was located on the top and the other was located at the bottom, using a peristaltic pump. The flow rate of acidified sample, reductant, and waste were 1, 1, and 20 mL min⁻¹, respectively. The solutions were then mixed and reacted in the gap (1-4 mm) between the two inlets inside the spray chamber. The elements in the gaseous forms were introduced into the plasma by argon carrier gas, which was introduced into the system through the nebulizer. The remaining reagents flowed down the outer surface of the lower tube and were pumped to waste at the bottom of the spray chamber. The set-up of vapor generation sample introduction is illustrated in Figure 4.6. Simultaneous matrix removal and sample preconcentration with this method is discussed in Section 5.3.4-5.3.5.

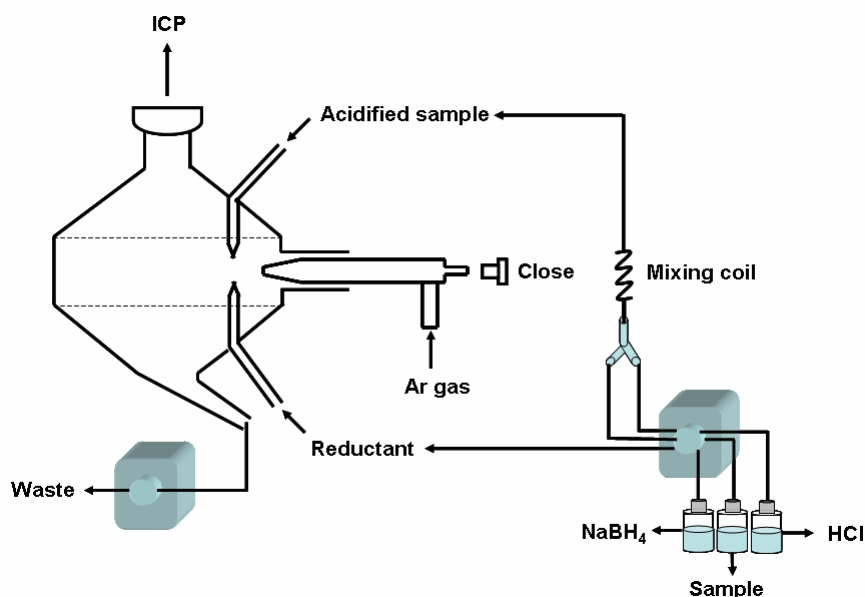


Figure 4.6 Schematic diagram of vapor generation for trace element determination by ICP-OES.

4.5.4.2 The Efficiency of Lab-Made Cyclonic Spray Chamber (LMSC) for Solution Nebulization

The efficiency of LMSC was investigated, compared with modified licthe (MLSC) and commercial cyclonic (CCSC) spray chambers in conventional solution nebulization method. Calibration curves of Cd, Hg and Pb using these three chambers with plasma power of 1200 W, nebulizer flow rate of 0.7 L min⁻¹ were established. The mixed standard solution was prepared in 2% HNO₃ in the range of 0.5, 1, 2, 5, and 10 mg L⁻¹.

4.5.4.3 ICP-OES: Parameters Optimization for Trace Element Determination

Experiments regarding optimization studies of trace element determination with ICP-OES are described in Sections 4.5.4.3a and b

4.5.4.3a Parameters Optimization in Vapor Generation

In vapor generation method, the rate of volatile vapor generation greatly depends on the concentration of NaBH₄ and acidity. Therefore, the concentrations of reductant (NaBH₄) and acid carrier (HCl) were evaluated. The test solution containing As, Se, Cd, Hg, Pb, Cu, Zn and using Bi as an internal standard in 2% v/v nitric acid were monitored for their emission intensities to construct calibration curve. The calibration was performed for standard solutions 10, 20, 50, 150, and 250 µg L⁻¹. Plasma power and nebulizer flow rate were 1200 W and 0.7 L min⁻¹, respectively. The hydrochloric acid (HCl) concentration was varied from 0.1 to 7% in turn with 1% m/v NaBH₄ in 0.4% m/v NaOH. With a compromised value of HCl acid concentration, NaBH₄ concentration was varied from 0.2 to 1% m/v in 0.4% m/v NaOH in turn with 5% HCl with the same condition.

4.5.4.3b Optimization of Nebulizer Gas Flow Rate and Plasma Power

The same test solution as in Section 4.5.4.3a with concentration of $500 \mu\text{g L}^{-1}$ was used to assess the influence of nebulizer gas flow rate and plasma power. Nebulizer gas flow rate were examined at $0.4 - 1.0 \text{ L min}^{-1}$ using plasma power of 1,350 W. The adjustment of the ICP-OES plasma power was investigated in the range of 1100 - 1400 W at 0.65 L min^{-1} nebulizer argon gas flow rate.

4.5.4.4 Preconcentration and Sensitivity Improvement Factors in The Presence and Absence of Matrices

The conventional solution nebulization with and without HF-FF, and vapor generation sample introduction methods were used for quantitative determination of As, Se, Cd, Hg, Pb, Cu, and Zn in the presence and absence of matrices (Na, K, Ca, and Mg). To reduce analysis time, HF-FF was operated in parallel with either solution nebulization or vapor generation, as illustrated in Figures 4.7 and 4.8. A test solution was subjected to HF-FF for sample loading and focusing (25 min), while the other test solutions were subjected to ICP-OES determination of trace elements with either solution nebulization or vapor generation (12 min for each replicate including the washout time). Once the loading and focusing with HF-FF was finished (after 25 min), solution nebulization or vapor generation was discontinued. At the same time, elution of preconcentrated analytes from the hollow fiber channel was carried out with subsequent ICP-OES detection.

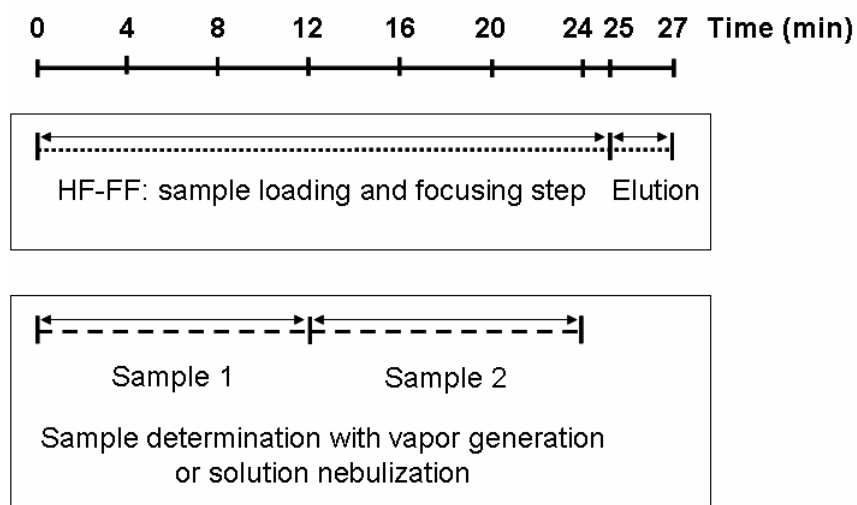
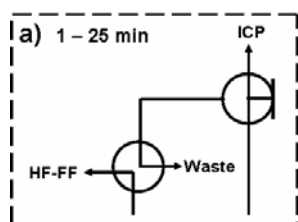
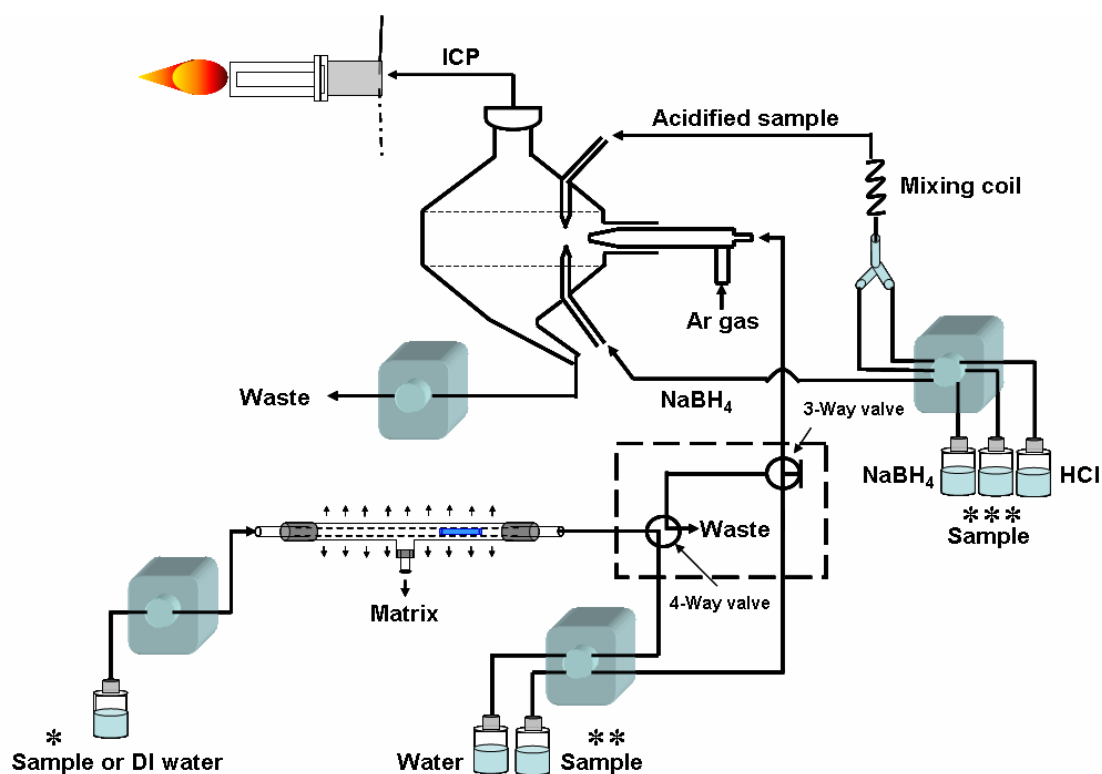
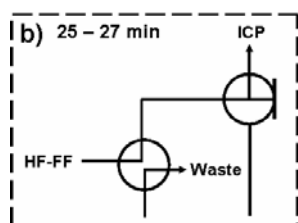


Figure 4.7 Schematic diagram showing operating procedure of sample introduction for ICP-OES detection.

The preconcentration factor obtained from conventional solution nebulization with HF-FF and sensitivity improvement factor from vapor generation methods were examined using conventional solution nebulization without HF-FF as a reference method. The set-up of conventional solution nebulization with or without HF-FF, and vapor generation method is illustrated in Figure 4.8.



- a) 1. HF-FF : sample loading and focusing step
2. ICP-OES determination of trace elements using either vapor generation or solution nebulization



- b) 1. The sample loading and focusing was finished.
2. The preconcentrated analytes from hollow fiber channel were eluted with subsequent ICP-OES detection.

* = Sample for HF-FF system: analyte elements containing PEI buffered at pH ~ 9

** = Sample for solution nebulization: analyte elements in 2% HNO₃

*** = Sample for vapor generation: analyte elements in 2% HNO₃

Figure 4.8 Schematic diagram of conventional solution nebulization with and without HF-FF and vapor generation methods for trace element determination by ICP-OES.

Experiments regarding preconcentration and sensitivity improvement factors study in the presence and absence of matrices using conventional solution nebulization with HF-FF and vapor generation method before ICP-OES detection are described in Sections 4.5.4.4a and b

4.5.4.4a Preconcentration Factor with HF-FF System

Under the optimized conditions, the calibration curves of analyte elements were examined. A 2 mL test solutions containing PEI of 200 mg L⁻¹ buffered at pH 9 with borate buffer, analyte elements 10, 20, 50 150, and 200 µg L⁻¹ of each, with and without matrix elements (Na, K, Ca and Mg) 2,000 mg L⁻¹ of each, were loaded into the hollow fiber channel. The focusing time and focusing point were 25 min and 28 cm from the channel inlet, respectively. The preconcentration factors were determined for Cd, Pb, Cu, and Zn.

4.5.4.4b Sensitivity Improvement Factor with Vapor Generation Method

With the optimized condition, the calibration curves of analyte elements were investigated. The analyte elements of 10, 20, 50 150, and 200 µg L⁻¹ with and without matrix elements (Na, K, Ca and Mg) 2,000 mg L⁻¹ of each were introduced into LMSC chamber and reacted with NaBH₄. Then volatile elements were swept into plasma by argon carrier gas. The sensitivity improvement factors were determined for As, Se, Cd, and Hg.

CHAPTER V

RESULTS AND DISCUSSION

In this study, the performance of hollow fiber flow filtration (HF-FF) system for matrix removal and analyte preconcentration using an opposed flow method before detection by GFAAS, CVAAS, and ICP-OES was examined. The optimum conditions of HF-FF system for each detection method such as parameters affecting complex formation (pH, PEI concentration), and parameters affecting matrix removal efficiency and analytical preconcentration (focusing time, focusing point) are reported in this section. In addition, vapor generation sample introduction was applied to perform matrix removal before ICP-OES detection.

5.1 GFAAS Determination of Mercury

Graphite furnace atomic absorption spectrometry (GFAAS) has been widely used for trace metal determination in various types of environmental samples [43] and it has been the primary tool for determination of metals dissolved in seawater. Direct analysis of seawater by GFAAS is limited not only because of the low concentration of many trace metals, but also the high salt matrix of seawater may cause interferences [113]. The serious matrix effects arising from seawater salts often cause the determination more difficult, as the background absorption signal may increase the baseline noise and cause spectral interference [104]. To overcome these problems, many investigators have employed preconcentration step such as organic extraction or ion exchange prior to analysis [114]. In addition, previous research about matrix removal and analyte preconcentration of seawater sample before ICP detection using a hollow fiber flow filtration unit (HF-FF) was reported [10]. However, simultaneous sample preconcentration and matrix removal with hollow fiber membrane before GFAAS detection of mercury in seawater has never been reported.

5.1.1 GFAAS: Parameters Optimization for Mercury Determination

The operating parameters of GFAAS such as ashing and atomization temperatures were optimized. The optimum ashing and atomization temperatures were found to be 150 and 1200°C, respectively considering from a large peak area (sensitivity) and relatively low %RSD (reproducibility). The absorbance peak area and %RSD are given in Table 5.1.

Table 5.1 Peak area absorbance of mercury at various ashing and atomization temperatures for mercury determination (5 mg L⁻¹ mercury in DI water with 15 µL of 400 mg L⁻¹ PEI buffered at pH 8.92 and 5 µL of 1000 mg L⁻¹ palladium as chemical modifier).

Parameters	Ashing Temperature (°C) (At Atomization Temp. = 1200°C)					Atomization Temperature (°C) (At Ashing Temp. = 150°C)			
	120	150	170	200	250	1200	1300	1400	1500
Peak area	0.948	0.889	0.765	0.614	0.508	0.889	0.806	0.747	0.693
%RSD	2.4	1.6	2.4	2.9	14.2	1.6	2.0	19.5	21.0

The optimum temperature program for measurement of mercury is shown in Table 5.2.

Table 5.2 Furnace operating conditions for mercury determination.

Step	Temperature (°C)	Ramp/Hold Time (s)	Argon Flow (mL min ⁻¹)
1. Drying	120	10/30	250
2. Ashing	150	1/15	250
3. Pre-atomization	20	1/15	250
4. Atomization	1200	0/10	0
5. Clean up	2400	1/5	250

5.1.2 Mercury Determination by GFAAS

5.1.2.1 Effect of High Salt Medium

The standard calibration curves of mercury in 10% seawater and DI water were examined, as illustrated in Figure 5.1. The results showed that in 10% seawater the sensitivity of standard calibration curve and absorbance peak area of mercury were higher as compared to in DI water. The coefficient of determinations of the calibration curve for mercury in 10% seawater and DI water were 0.9288 and 0.9985, respectively. The sensitivity of mercury determination increased 2 times in 10% seawater medium compared with DI water, suggesting that seawater matrix cause signal enhancement in mercury determination by GFAAS. Therefore, this matrix effect should be eliminated.

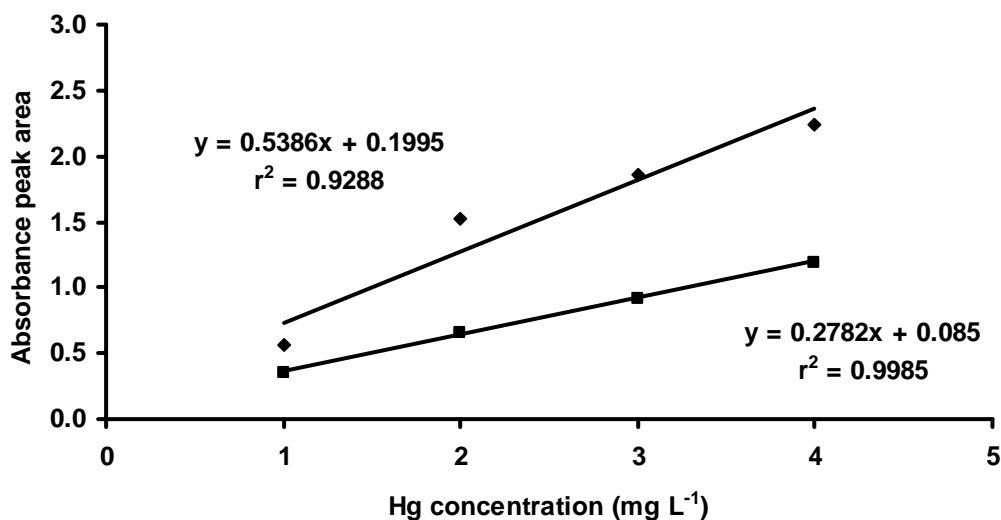


Figure 5.1 Calibration curve of mercury in DI water (■) or 10% seawater (◆): with 15 μL of 400 mg L^{-1} PEI buffered at pH 8.92 and 5 μL of 1000 mg L^{-1} palladium as chemical modifier.

5.1.3 Mercury Determination by GFAAS with HF-FF System

5.1.3.1 Matrix Removal and Analyte Preconcentration

In HF-FF system for GFAAS detection, the optimum experimental condition of HF-FF was the same as that reported by Sawatsuk *et al.* [10] except that the focusing time was changed from 25 to 15 min. The focusing time of 15 min was enough to perform matrix removal and analyte preconcentration by HF-FF system before GFAAS detection to shorten the analysis time and therefore to increase sample throughput. With GFAAS detection, off-line analysis after fraction collection was performed. The operating conditions of HF-FF system prior to GFAAS are shown in Table 5.3.

Table 5.3 The operating conditions of HF-FF system for GFAAS detection.

Parameters	Optimum conditions
Sample volume (mL)	2
Parameter affecting complex formation	
- pH	~ 8 - 9
- PEI concentration (mg L ⁻¹)	200
Parameter affecting matrix removal and analytical preconcentration efficiency	
- Focusing time (min)	15
- Focusing point (cm from channel inlet)	28

With the optimum conditions of GFAAS and HF-FF as shown in Table 5.1-5.3, GFAAS was used as a detector to observe the ability of hollow fiber (Hf) membrane for matrix removal. Test solution was 5 mg L⁻¹ mercury with 400 mg L⁻¹ PEI in 10% seawater at pH ~8-9. In Figure 5.2a (without HF-FF), the background absorption peak of sodium chloride appeared at 8 min whereas this peak was not found in Figure 5.2b (with HF-FF matrix removal). This indicates that sodium chloride was removed by filtering off the membrane during HF-FF matrix removal process. Nonetheless Figure 5.2b shows that the background absorption peak at 2 min appeared. The cause of background peak at 2 min will be discussed in the following section.

5.1.3.2 Effect of PEI on Signal and Peak Shape of Mercury

As shown in Figure 5.2b, the background peak at 2 min might be contributed from PEI. In order to confirm this assumption, 5 mg L⁻¹ mercury with 400 mg L⁻¹ PEI in DI water at the same pH value was used as test solution and its absorption peak profiles are displayed in Figure 5.2b. It is apparent that background absorption at 2 min was observed for both with and without HF-FF in Figure 5.3.

With HF-FF system, the obtained peak signal of PEI background at 2 min was higher than that without HF-FF system for mercury in DI water at pH ~8-9 as a test solution, as illustrated in Figure 5.3. This is caused by preconcentration process that exhibited an effect on peak signal of background and analyte so the background peak at 2 min in with HF-FF (Figure 5.3b) was higher than the background peak at 2 min without HF-FF (Figure 5.3 a).

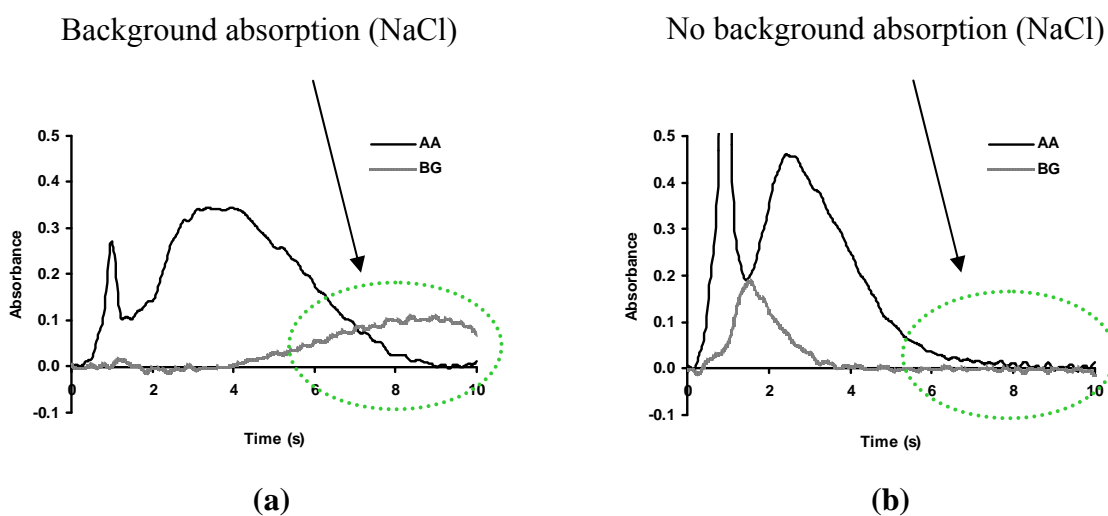


Figure 5.2 Absorption peak profiles of 5 mg L^{-1} mercury in 10% seawater and all other conditions are as in Figure 5.1: (a) without HF-FF system; (b) with HF-FF system.

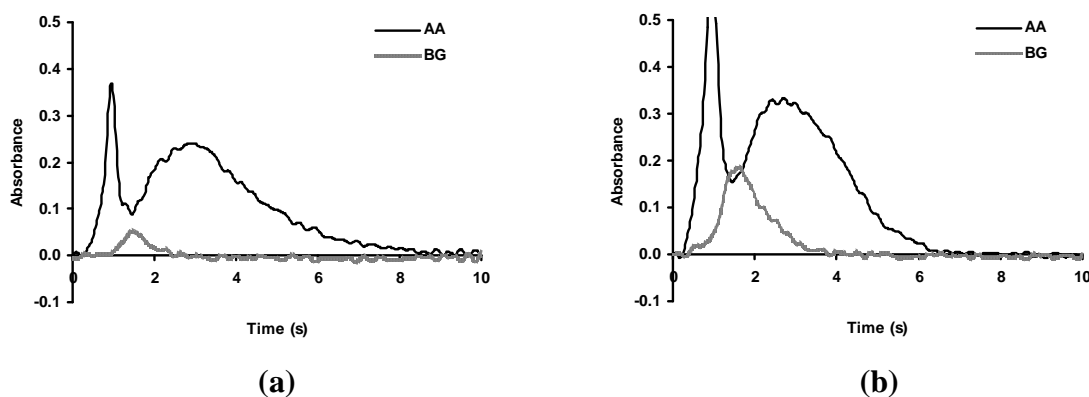


Figure 5.3 Absorption peak profiles of 5 mg L^{-1} mercury in DI water and all other conditions are as in Figure 5.1: (a) without HF-FF system; (b) with HF-FF system.

Figure 5.4 (a) shows that double peak was always observed for absorption of atomic mercury in the test solution containing PEI. This might be due to the difference in volatilization of mercury. The analyte peak at 1.5 min showed a small peak area but high peak height, whereas analyte peak at 3.5 min was broader, resulting in larger peak area as compared to the analyte peak at 1.5 min. The peak at 1.5 min might be assigned to mercury-PEI complex. The second peak at 3.5 min might be contributed from mercury in a more stable form, *i.e.*, mercury stabilized by palladium modifier. Mercury can be stabilized in the furnace at higher temperatures with the usage of palladium which is known to form intermetallic compounds with mercury [105]. Moreover, without HF-FF system, the test solution containing 5 mg L^{-1} mercury without 400 mg L^{-1} PEI buffered at pH 8.92 in DI water medium was investigated. The $1,000 \text{ mg L}^{-1}$ palladium was used as chemical modifier for verifying the cause of double peak. The results illustrated in Figure 5.4 (b) displayed a single peak at 4 min and no background absorption peak of PEI at ~ 2 min.

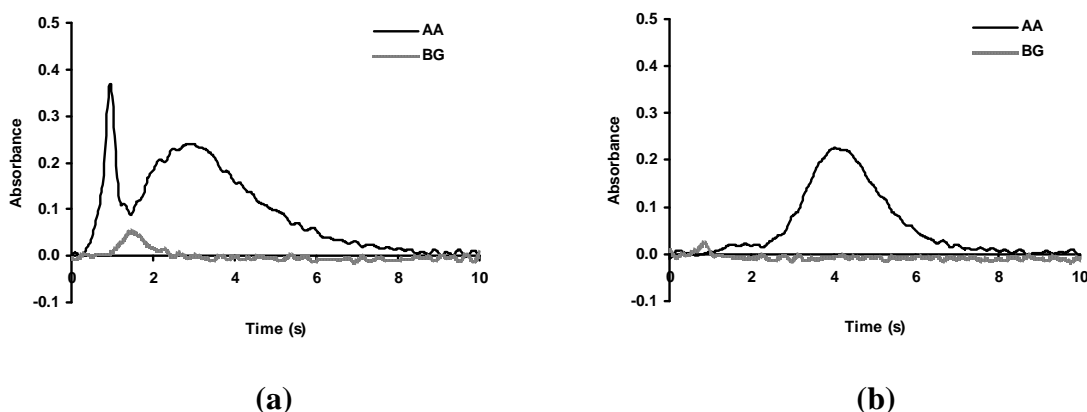


Figure 5.4 Absorption peak profiles of background without HF-FF system: (a) 5 mg L^{-1} mercury in DI water with 400 mg L^{-1} PEI; (b) 5 mg L^{-1} mercury in DI water without 400 mg L^{-1} PEI. All other conditions are as in Figure 5.1.

5.1.3.3 Preconcentration Factor Obtained From Using HF-FF System

The preconcentration factor gained for mercury was calculated from the ratio of the peak area obtained from with HF-FF and that without HF-FF. The preconcentration factors for mercury in 10% seawater and in DI water were 0.99 and 1.28, respectively (sample loading volume of 2 mL, elution volume of 1 mL), as summarized in Table 5.4. Relatively low preconcentration factors were obtained in both media owing to weak interaction between mercury and PEI causing less mercury-PEI complexes retained in hollow fiber channel. The unbound mercury was lost through the membrane together with matrix elements, whereas the mercury-PEI complexes were kept inside the hollow fiber channel owing to their high molecular weight (750,000 Da) as compared with the fiber membrane pore size (30,000 Da).

Table 5.4 The peak area and preconcentration factor obtained for the test solution as shown in Figure 5.1 with or without HF-FF system. (With HF-FF system, a 2-mL volume of test solution containing 5 mg L⁻¹ of mercury was introduced into the HF-FF unit.)

Conditions	Peak area		Preconcentration factor
	with HF-FF	without HF-FF	
Hg in 10% seawater	1.521	1.530	0.99
Hg in DI water	1.171	0.917	1.28

Without HF-FF, absorbance peak area of 10% seawater was higher than that in DI water because of enhancement effect from seawater matrix (see Figure 5.1 and 5.2). In DI water absorbance peak area obtained (see Section 5.1.2.1 and Figure 5.3) with HF-FF was higher than that obtained without HF-FF owing to preconcentration process from HF-FF. Considering the results from HF-FF, absorbance peak area of mercury in 10% seawater was higher than that in DI water (see Figures 5.2b and 5.3b). This might be resulted from charge repulsion between uncomplexed analyte ions and matrix elements in seawater. This effect caused less amount of uncomplexed analyte ions penetrated through the membrane pore. Therefore, the amount of analyte retained in hollow fiber channel was higher in 10% seawater. However, in 10% seawater medium absorbance peak area obtained from with HF-FF was accidentally equal to that without HF-FF (see Figure 5.2). This might be due to the combined effects of preconcentration process from HF-FF, causing absorbance of mercury to be higher than in DI water and enhancement effect from seawater matrix without HF-FF, leading to higher absorbance of mercury than that in DI water.

5.1.4 Summary: Mercury Determination by GFAAS Without and with HF-FF System

In case of mercury determination by GFAAS without HF-FF system, sodium chloride in seawater causes an enhancement effect to the mercury signal. However, the coefficient of determination of the calibration curve for mercury in 10% seawater (0.9288) was not as good as that obtained from DI water (0.9985).

In the determination of mercury by GFAAS with HF-FF system, interference from sodium chloride was removed by filtering off the membrane during HF-FF matrix removal process. The HF-FF system can be used to prevent the introduction of high sodium chloride concentration into furnace, which could affect on signal and peak shape of mercury. However, when PEI is used as a complexing agent for removal of sodium chloride interference by HF-FF, its background absorption peak appeared. In addition, PEI led to the double peak on mercury absorption profile. Although the preconcentration factor obtained from the proposed method was only ~ 1.0-1.3 times, it appeared that HF-FF system could be used as a matrix removal method for the determination of mercury in seawater.

5.2 CVAAS Determination of Mercury

Cold vapor atomic absorption spectrometry (CVAAS) is one of the most popular techniques for determining mercury in a wide variety of samples. But on account of extremely low concentration of mercury in water samples (ng L^{-1}) and the high salinity of seawater, a separation and preconcentration step is required [106]. Therefore, HF-FF system for preconcentration and separation of traces of mercury in seawater samples based on CVAAS was developed.

5.2.1 CVAAS: Parameters Optimization for Mercury Determination

The chemical and physical variables of the manifold were optimized to achieve the best analytical performance by investigating each variable in turn with all other variables constant. These parameters included carrier (HCl) and reductant (NaBH_4) flow rates, HCl and NaBH_4 concentrations, and argon flow rate. Optimization was performed using a $200 \mu\text{g L}^{-1}$ mercury standard with peak area and peak height measurements.

The effect of carrier (HCl) and reductant (NaBH_4) flow rates on the absorbance peak area and peak height of mercury is shown in Figure 5.5. The flow rate of the carrier (HCl) and reductant (NaBH_4) are recognized to affect the mixing dynamics of the reagents. The HCl and NaBH_4 stream flow rates were varied between 1.9 and 4.0 mL min^{-1} . The signal increased as the flow rate was increased up to 3.4 mL min^{-1} considering from peak area. As the flow rate was increased above 3.4 mL min^{-1} , the signal decreased. It could be due to incomplete reaction when flow rate was increased. Considering the peak height, the absorbance signal raised when the flow rate was increased from 1.9 up to 4.0 mL min^{-1} . Therefore, the compromised condition was 3.4 mL min^{-1} .

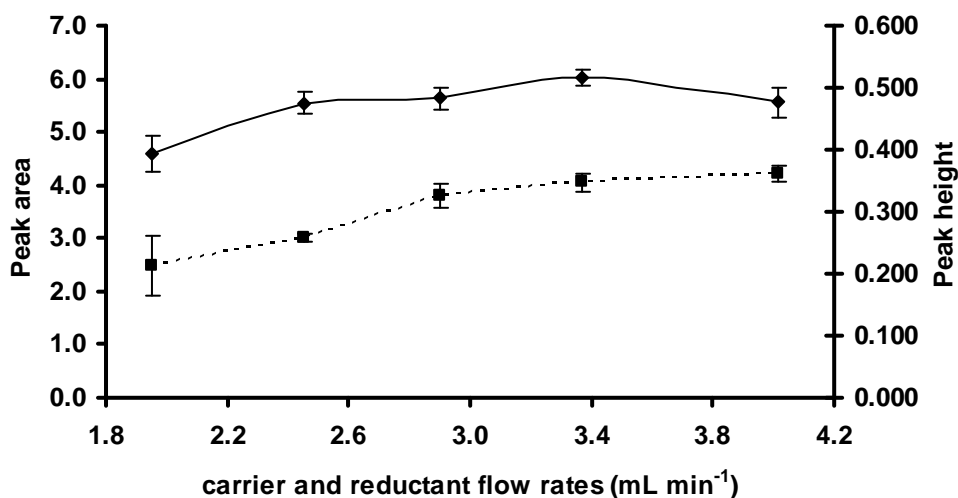


Figure 5.5 Effect of carrier (5% v/v HCl) and reductant (0.2% m/v NaBH₄ in 0.05% m/v NaOH) flow rates on absorbance signal of 200 $\mu\text{g L}^{-1}$ mercury in DI water: sample volume 500 μL , Ar gas flow rate 100 mL min^{-1} , (—◆—) peak area, (---■---) peak height.

The argon gas drives volatile mercury species from the gas liquid separator and carries it to the light path. The effect of the argon flow rate on peak area and peak height can be seen in Figure 5.6. Argon flow rates were varied between 40 and 200 mL min^{-1} . Peak area and peak height increased with gas flow rate and reached maximum at 50 mL min^{-1} . Increasing carrier gas flow rate from 40 to 50 mL min^{-1} , peak area and peak height were increased as a result of the increased amount of volatile mercury entering the light path. Moreover, at faster carrier gas flow rate, the separation of the volatile mercury from the reaction solution was more efficient. At argon gas flow rate of faster than 50 mL min^{-1} , the increase in gas flow rate caused peak area and peak height to decrease. The decreasing peak area and peak height with increasing flow rate from 50 to 200 mL min^{-1} may be caused by the dilution of volatile mercury by carrier gas and the short residence time of mercury in the light path. However, at gas flow rate of 50 mL min^{-1} , reproducibility was poor as seen from high %RSD. Therefore, the optimum gas flow rate was found to be 100 mL min^{-1} . This flow rate provided an optimal signal with relatively good precision.

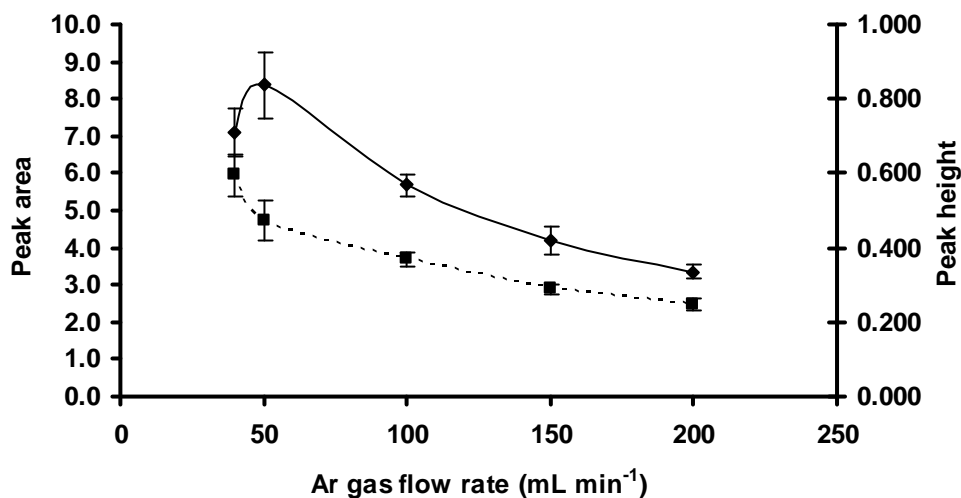


Figure 5.6 Effect of Ar gas flow rate on measured absorbance of mercury, carrier and reductant flow rate 3.4 mL min⁻¹. All other conditions are as in Figure 5.5. (—◆—) peak area, (--■--) peak height.

A sodium tetrahydroborate(III) (NaBH₄) solution was chosen as the reductant because of its ability to reduce both inorganic and organic forms of mercury [115]. In order to investigate the effect of reductant (NaBH₄) concentration on the sensitivity, the NaBH₄ was varied from 0.01 to 1% m/v and the absorbance signal of 200 µg L⁻¹ mercury in DI water was monitored (Figure 5.7). The peak area and peak height absorbance increased when NaBH₄ concentration was increased from 0.01 to 0.2% due to the increase in volatile mercury generation. With NaBH₄ concentration of higher than 0.2%, a plateau with a slight decrease in absorbance peak area at 1% was observed. This decrease is due to the dilution of the volatiles mercury by the molecular hydrogen by-product of the chemical reaction. Moreover, a large amount of NaBH₄ results in vigorous evolution of hydrogen and water vapor, leading to an inefficient gas-liquid phase separation [112]. The 0.2% m/v NaBH₄ was found to be a good compromise between high absorbance and reductant consumption. Hence, 0.2% m/v NaBH₄ was selected as a suitable amount of reductant.

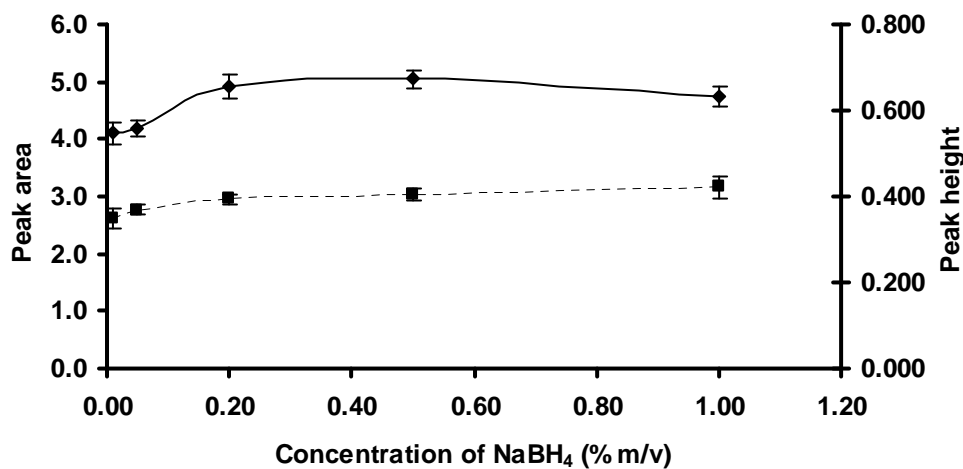


Figure 5.7 Effect of NaBH₄ concentration on measured absorbance of mercury: carrier and reductant flow rate 3.4 mL min⁻¹, sample volume 200 μL. All other conditions are as in Figure 5.5. (—◆—) peak area, (--■--) peak height.

The efficient chemical condition for cold vapor generation reaction in a particular system would be obtained by evaluation of the actual concentration of acid available for the reaction. The hydrochloric acid (HCl) concentration was varied between 1 and 9% v/v. The results shown in Figure 5.9 failed to yield a notable trend and found that 5% v/v HCl provided the highest absorbance signal but the standard deviation at this concentration was poor. Consequently, a concentration of 7% v/v was used for subsequent experiments as the standard deviation was better than any of the other tested concentrations. Investigation of HCl concentrations between 1 and 5% v/v was thought to be unlikely to produce improvements in peak height.

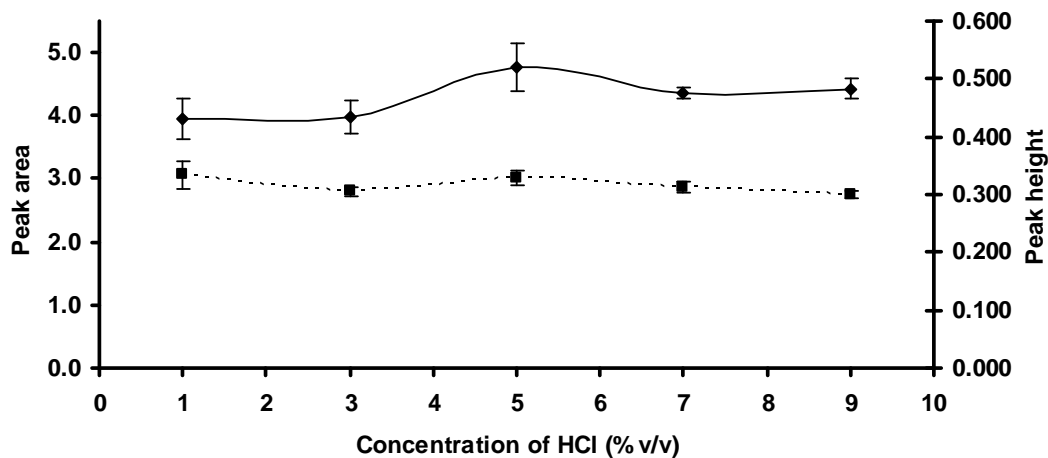


Figure 5.8 Effect of HCl concentration on measured absorbance of mercury: 0.2% m/v NaBH₄. All other conditions are as in Figure 5.7. (—◆—) peak area, (--■--) peak height.

The selected conditions that provided optimum peak area and peak height with acceptable precision are summarized in Table 5.5.

Table 5.5 The optimum conditions of CVAAS for mercury detection.

Parameters	The optimum conditions
- Ar gas flow rate (mL min ⁻¹)	100
- Carrier (HCl) and reductant (NaBH ₄) flow rates (mL min ⁻¹)	3.4
- Concentration of NaBH ₄ (% m/v) in 0.05 % (m/v) NaOH	0.2
- Concentration of HCl (% v/v)	7

5.2.2 Mercury Determination by CVAAS

5.2.2.1 Effect of pH

The effect of pH was studied between 3.8 to 8.9 using $200 \mu\text{g L}^{-1}$ mercury in DI water with 200 mg L^{-1} PEI, as shown in Figure 5.9. Within the pH range studied, pH of mercury solution did not show significant effect on signal of mercury. This might be due to the sufficient concentration of HCl and NaBH₄ for mercury vapor generation.

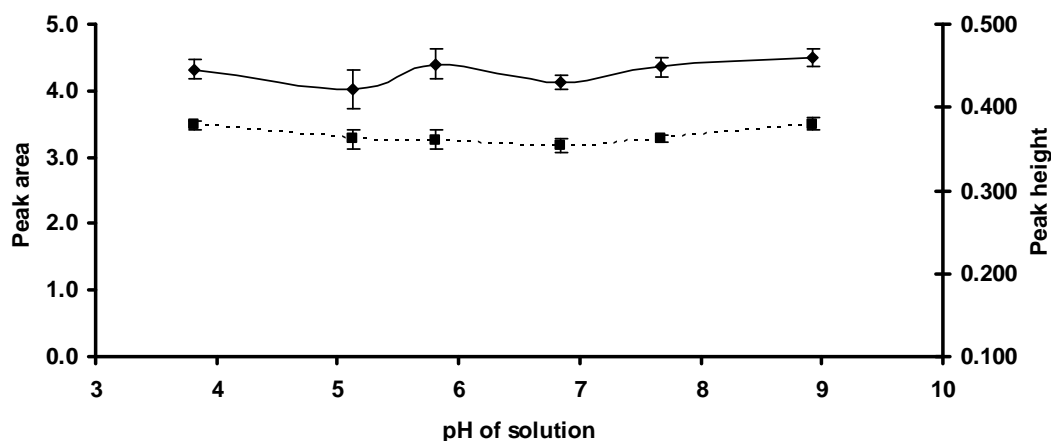


Figure 5.9 Effect of pH on the absorption signal of mercury, (—◆—) peak area, (--■--) peak height. All other conditions are as in Table 5.5.

5.2.3 Mercury Determination by CVAAS with HF-FF System

The optimum conditions of HF-FF system for CVAAS detection were the same as shown in Table 5.3 except the parameters affecting complex formation. Effect of pH on complex formation between PEI and mercury was investigated using HF-FF system. The test solution, $200 \mu\text{g L}^{-1}$ mercury in DI water with 200 mg L^{-1} PEI, was pH adjusted to be in the range of 3.8 to 8.9. The result is shown in Figure 5.10. In acidic solution ($\text{pH} < 6$), most of N atoms of the amino groups in the macromolecular chains of PEI are in protonation state [116]. The protonation degree of N atoms of

amino groups decreases with the decrease of acidity, and the coordination ability of N atoms of amino groups towards metal ions strengthens, thus the complex formation between mercury and PEI increases with the rising of pH value. However, the results at pH 5.8-8.9 cannot be explained with the protonation degree of N atoms of amino groups as the opposite trend was observed. The mercury absorbance decreased when pH increased from 5.8 to 8.9. A pH > 6, the hydrolytic action of Hg^{2+} occurs, and thus the ability of mercury to form complex with PEI decreases [117]. Therefore, the optimum pH value is 6.

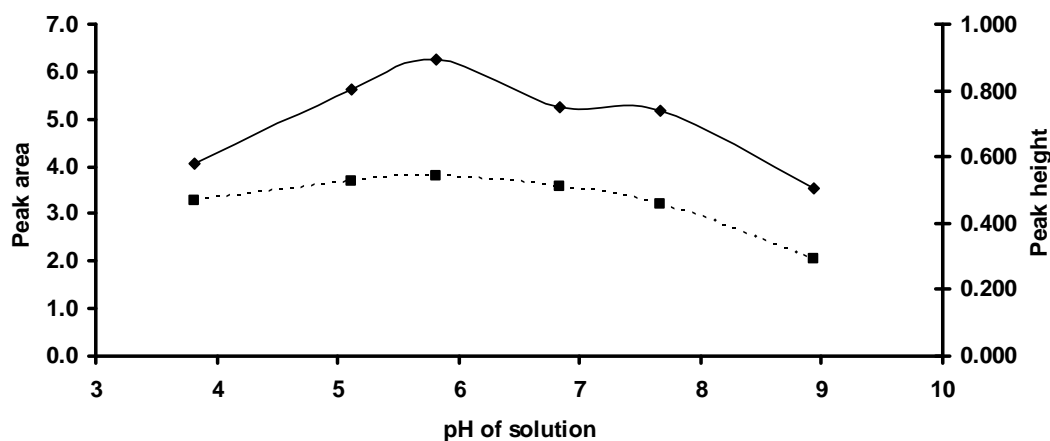


Figure 5.10 Effect of pH on the complex formation of mercury with PEI as observed from absorption signal, (—◆—) peak area, (--■--) peak height. All other conditions are as in Table 5.5.

5.2.3.1 Preconcentration Factor Obtained from Using HF-FF System

At each pH, the preconcentration factors of mercury in DI water was calculated from the ratio of the peak area or peak height obtained from with and without HF-FF system as shown in Table 5.6. The preconcentration factor of ~ 1.5 times was obtained.

Table 5.6 The preconcentration factor obtained for 200 $\mu\text{g L}^{-1}$ mercury in DI water with 200 mg L^{-1} PEI, using HF-FF system, sample volume 2 mL, focusing time 15 min.

pH of solution	Ratio of peak area (With HF-FF / Without HF-FF)	Ratio of peak height (With HF-FF / Without HF-FF)
5.12	1.40	1.46
5.81	1.43	1.50
6.84	1.27	1.44
7.67	1.19	1.27

5.2.4 Summary: Mercury Determination by CVAAS Without and with HF-FF System

The optimized conditions were obtained for determination of mercury by CVAAS with prior HF-FF. The mercury-PEI complexes were loaded into hollow fiber channel for simultaneous matrix removal and analytical preconcentration to obtain higher sensitivity. This system shows preconcentration factor in range ~ 1.2 - 1.5 which was not sufficient to improve the sensitivity. In this case, HF-FF may not be necessary. With CVAAS, the separation of analyte in gaseous form from the matrix was possible. Nevertheless, HF-FF system is simple and inexpensive, thus it is expected that the developed procedure be applied for the determination of mercury in natural waters, especially seawater. In addition, the preconcentration factor can be improved by increasing sample volume with the expense of longer focusing time and thus longer analysis time.

5.3 ICP-OES Determination of Trace Elements

In this section, two sample introduction methods for ICP-OES determination of trace elements are discussed. These include conventional solution nebulization and vapor generation methods. Simultaneous matrix removal and/or analyte preconcentration were performed before ICP-OES detection using HF-FF system or vapor generation. The conventional solution nebulization method without HF-FF was used as a standard method for comparison purpose. In this experiment, a lab-made cyclonic spray chamber (LMSC) was developed for sample introduction. It can be employed in solution nebulization as a spray chamber and in vapor generation as a gas liquid separator.

5.3.1 The Lab-Made Cyclonic Spray Chamber (LMSC)

The lab-made cyclonic spray chamber (LMSC) can be used for the introduction of samples in two different methods, *i.e.*, conventional solution nebulization (Neb) and vapor generation (VG). LMSC is simple and inexpensive to construct. As shown in Figure 5.11, LMSC consists of a cyclonic spray chamber that has been modified by addition of two tubes located vertically in the spray chamber. The regular cyclonic spray chamber has three opening lines, *i.e.*, for insertion of the nebulizer; for introduction of aerosols to the ICP; and for waste drain. The home made LMSC has five opening lines. Two new lines were used to introduce acidified sample and reductant when operated in vapor generation method.

In conventional solution nebulization, the spray chamber serves as a sample introduction system as for the regular cyclonic spray chamber by keeping the new lines closed by cap (see Figure 5.11 a). The sample solution passes through the nebulizer sample line (S_{Neb}) only and is introduced to the plasma as an aerosol. When utilizing the vapor generation (Figure 5.11 b), the nebulizer sample line is closed and the acidified sample or standard passes through the vapor generator line (S_{VG}) and reacts with the reduction solution (R) in the chamber. The formed vapors are

transported to the ICP by the nebulizer gas (Ar). In the vapor generation method the spray chamber serves as a gas-liquid separator.

Before use, the efficiency of LMSC in conventional solution nebulization method was investigated in comparison with modified licthe (MLSC) and commercial cyclonic (CCSC) spray chambers. The results are described in the following section.

5.3.1.1 The Efficiency of Lab-Made Cyclonic Spray Chamber for Solution Nebulization

For the comparison of the LMSC sample introduction with MLSC and CCSC, calibration curves of cadmium, mercury and lead were established. The results presented in Figure 5.12 show the sensitivity of calibration curves from the three chambers to decrease in the following order: MLSC > LMSC > CCSC. The coefficient of determinations (r^2) of all calibration curves were 0.999x - 1. Differences in sensitivity obtained from the three chambers might be due to different geometry of the chambers and the position of a nebulizer in the chambers.

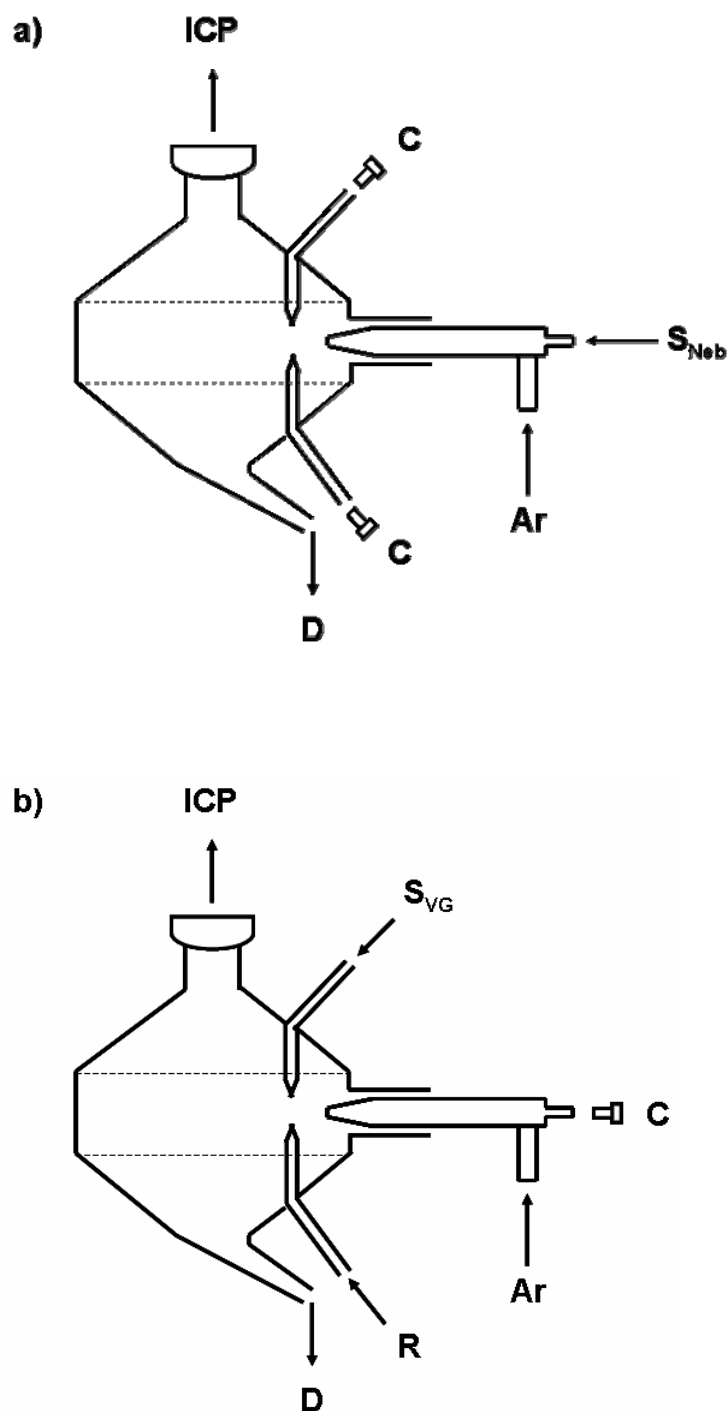
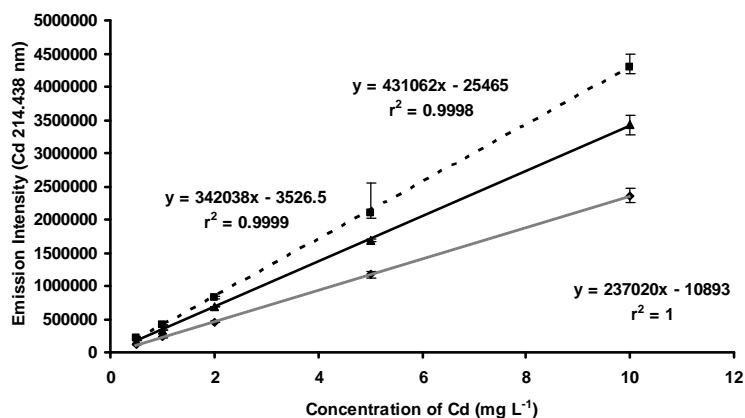
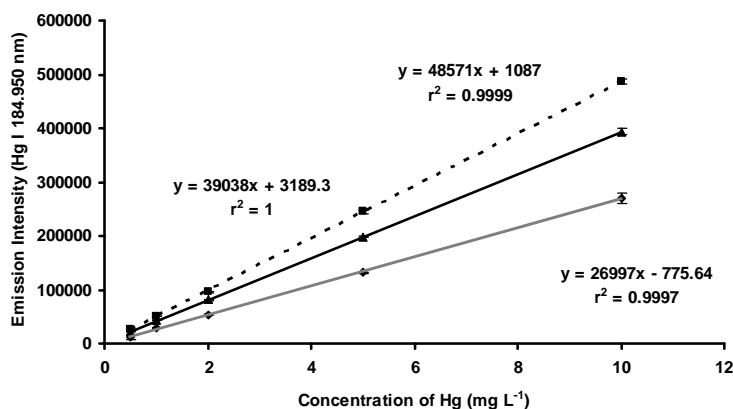


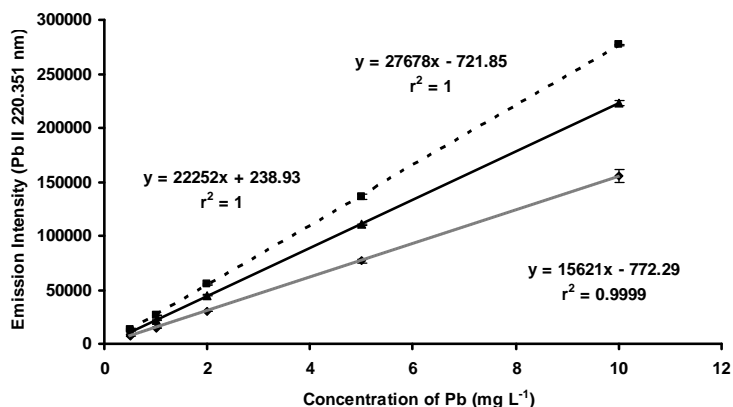
Figure 5.11 The lab-made cyclonic spray chamber (LMSC) for two sample introduction methods a) conventional solution nebulization method; b) vapor generation method: S_{Neb} = sample nebulization line; S_{VG} = sample vapor generation line; Ar = argon nebulizer gas; R = reduction solution ($NaBH_4$); C = cap; and D = drain.



(a)



(b)



(c)

Figure 5.12 Calibration curves of cadmium (a), mercury (b) and lead (c) obtained with conventional solution nebulization using three chambers with plasma power of 1200 W, nebulizer flow rate of 0.7 L min⁻¹; (---■---) MLSC, (—▲—) LMSC and (—◆—) CCSC.

5.3.2 Parameters Optimization for Trace Element Determination by ICP-OES

Simultaneous determinations of several analytes by online conventional solution nebulization with HF-FF and vapor generation methods with ICP-OES were performed and compared with conventional solution nebulization method without HF-FF (standard method). With the conventional solution nebulization, the sample solution was introduced to the plasma as an aerosol by pneumatic nebulizer. In the vapor generation method, the rate of generation of volatile vapors greatly depends on the concentration of reductant (NaBH_4) and acidity. Besides, the effect of NaBH_4 dissolved in 0.4% (m/v) NaOH and carrier liquid (HCl) to generate the vapor was evaluated, whereas sample, reductant, and carrier liquid flow rates were set at 1, 2, and 1 mL min^{-1} , respectively. By manually operated in combined conventional solution nebulization and vapor generation methods, the effect of nebulizer flow rate and plasma power on sensitivity was investigated.

5.3.2.1 Parameters Optimization in Conventional Solution Nebulization

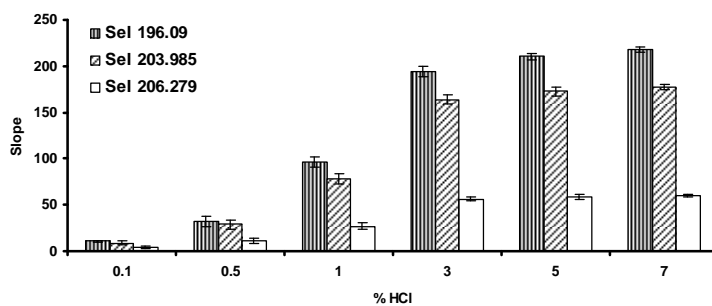
With conventional solution nebulization the influence of nebulizer gas flow rate and plasma power on sensitivity were investigated. The results are discussed in Section 5.3.2.3. Moreover, the optimum condition of all parameters for HF-FF system was the same as that reported by Sawatsuk *et al.* [10].

5.3.2.2 Parameters Optimization in Vapor Generation

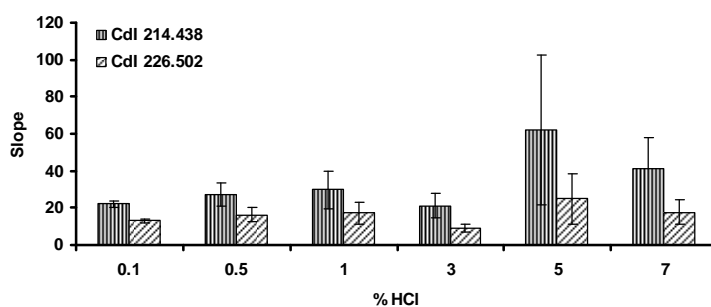
With vapor generation, effects of nebulizer gas flow rate, plasma power, and concentrations of HCl and NaBH_4 were examined. The rate of volatile vapor generation greatly depends on the concentration of NaBH_4 and acidity. The hydrochloric acid (HCl) concentration was varied from 0.1 to 7% in turn with 1% m/v NaBH_4 in 0.4% m/v NaOH. The emission intensity of standard solution containing arsenic, selenium, cadmium, mercury, lead, copper, and zinc using bismuth

as an internal standard in 2% v/v nitric acid were monitored to make calibration curves. The results of selenium, cadmium, arsenic and mercury are illustrated in Figure 5.13. In the first group, the sensitivity of two pilot elements (selenium and cadmium) increased at increase in HCl from 0.1 - 7%. The second group is arsenic and mercury of which the sensitivity increased with increasing HCl from 0.1-1%, and the sensitivity slightly decreased with further increase of %HCl (above 1%). Therefore, in this study a compromised value of 5% HCl was chosen.

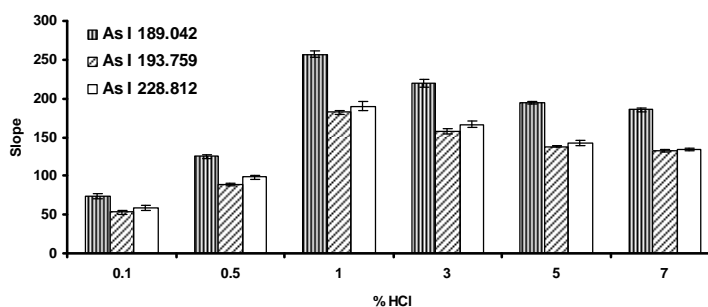
The effect of sodium tetrahydroborate(III) (NaBH_4) concentration was examined by varying NaBH_4 from 0.2 to 1% m/v in 0.4% m/v NaOH with 5% HCl and the same standard solution in varying %HCl. As shown in Figure 5.14, the sensitivity increased when NaBH_4 was increased from 0.2 to 1%, therefore 1% NaBH_4 was adopted as optimal value. In addition at % NaBH_4 of higher than 1%, the plasma was not stable and finally it was off. This may have been due to the hydrolysis of NaBH_4 generating more hydrogen gas and moisture by product at higher concentrations of NaBH_4 , which perturbed the plasma.



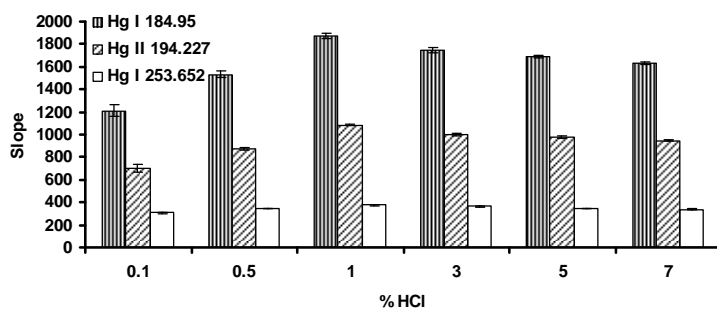
(a)



(b)



(c)



(d)

Figure 5.13 Sensitivity of selenium (a), cadmium (b), arsenic (c), and mercury (d) at each % HCl in vapor generation method. (Plasma power of 1200 W, nebulizer gas flow rate of 0.7 L min^{-1} and $0.2\% \text{ NaBH}_4$)

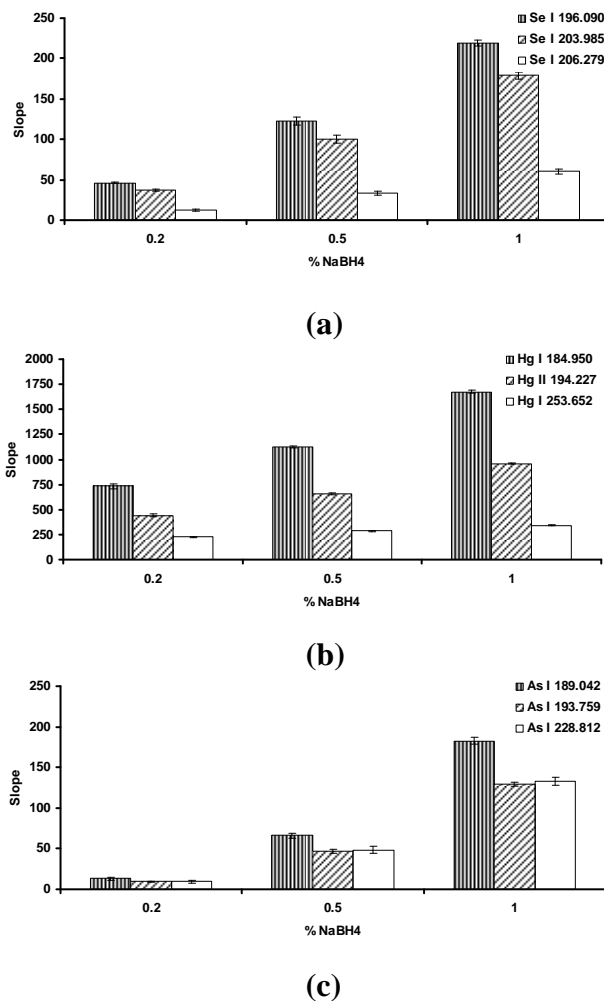


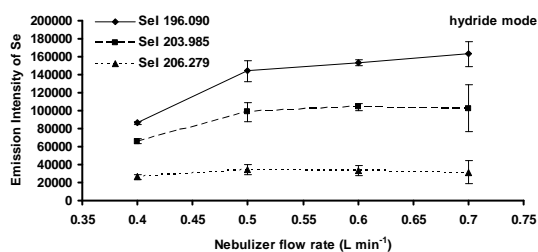
Figure 5.14 Sensitivity of selenium (a), arsenic (b) and mercury (c) at each % NaBH₄ in vapor generation method. (Plasma power of 1200 W, nebulizer gas flow rate of 0.7 L min⁻¹ and 5% HCl)

5.3.2.3 Optimization of Nebulizer Gas Flow Rate and Plasma Power Conditions

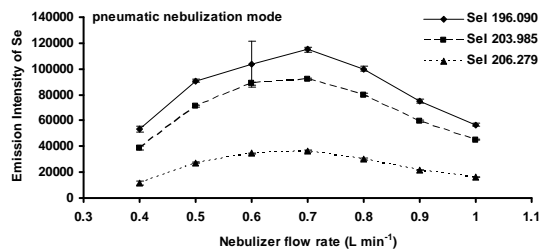
To assess the influence of nebulizer gas flow rate for conventional solution nebulization and carrier gas flow rate for vapor generation method, measurements were made at 0.4 – 1.0 L min⁻¹ using the same test solution in varying % HCl. The results of selenium and mercury on both methods are presented in Figure 5.15. In vapor generation method, the concentration of NaBH₄ and HCl were

set to 1% m/v NaBH₄ in 0.4% m/v NaOH and 5% HCl. The emission intensity of selenium and mercury in vapor generation (Figures 5.15 (a) and (b)) was higher when nebulizer gas flow rate was increased from 0.4 to 0.7 L min⁻¹. Furthermore, nebulizer gas flow rate of faster than 0.7 L min⁻¹ caused plasma go off because of the large amounts of hydrogen, carbon dioxide and water vapor being introduced into the plasma discharge. These products of the chemical reaction may cause instability or even extinguish the plasma [107]. In conventional solution nebulization method, the emission intensity of both elements (Figure 5.15 (c) and (d)) shows the same trend as that in vapor generation. At nebulizer gas flow rates of 0.4 – 0.7 L min⁻¹, the intensity increased with increasing in nebulizer gas flow rate and reached maximum at 0.7 L min⁻¹, as a result of increase in the amount of analyte entering the plasma. In contrast, the intensity continually decreased with increasing nebulizer gas flow rate from 0.7 to 1.0 L min⁻¹ because the residence time of analyte in plasma was shorter. Therefore, the compromised condition for both methods is 0.65 L min⁻¹.

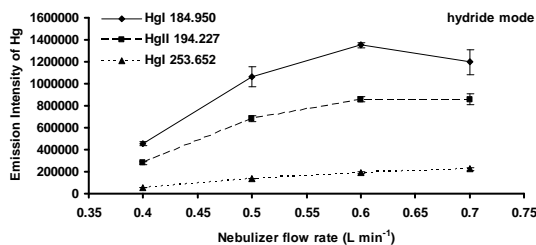
The adjustment of the ICP-OES plasma power of conventional solution nebulization and vapor generation method was investigated. To achieve the best emission intensity of analyte elements, the same standard solution in varying % HCl was used. It was studied in the range of 1100 - 1400 W. This effect is shown in Figure 5.16. In vapor generation, power of 1350 W provided highest intensity. Plasma power of higher than 1350 W did not only produce a strong heating of the plasma source and environment but also the response of light elements decreased (see selenium and arsenic in Figure 5.16 (a) and (b)). The intensity of mercury (Figure 5.16 (c)) increased with plasma power raising from 1200 - 1400 W. At power of less than 1200 W, plasma was extinguished. In conventional solution nebulization, the results indicate that the intensity of selenium, arsenic and mercury (Figure 5.16 (d), (e) and (f), respectively) increased with plasma power raising from 1100 - 1400 W. The optimum value for both methods is 1350 W.



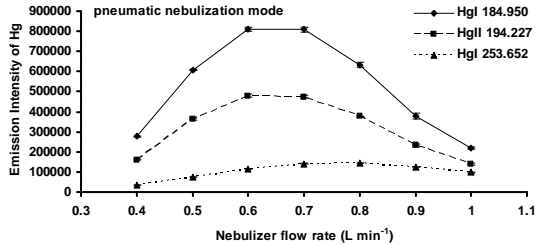
(a)



(c)

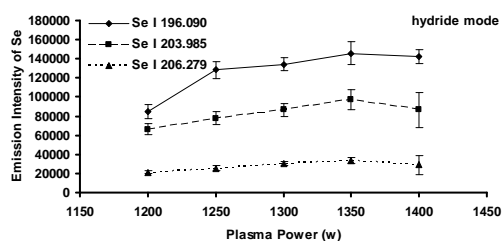


(b)

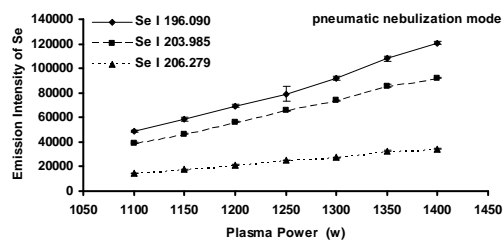


(d)

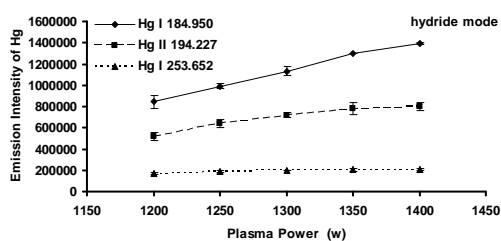
Figure 5.15 Effect of nebulizer argon gas flow rate on emission intensity of selenium (a) and mercury (b) in vapor generation method; selenium (c) and mercury (d) in conventional solution nebulization method; Plasma power, 1350 W.



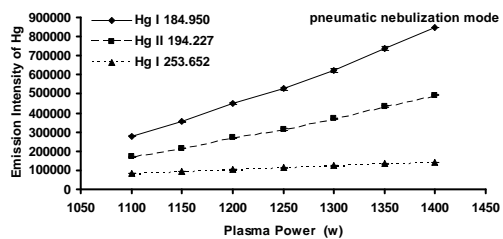
(a)



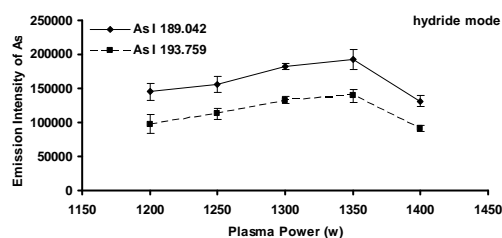
(d)



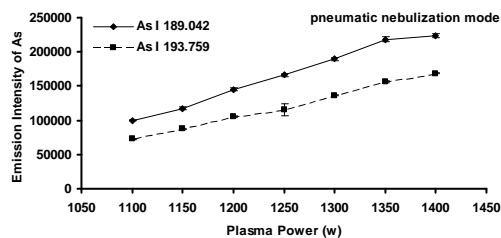
(b)



(e)



(c)



(f)

Figure 5.16 Effect of plasma power on emission intensity of selenium (a), mercury (b) and arsenic (c) in vapor generation method; selenium (d), mercury (e) and arsenic (f) in conventional solution nebulization method; nebulizer argon gas flow rate, 0.65 L min^{-1} .

The optimum conditions with acceptable precision are summarized in Table 5.7.

Table 5.7 The optimum conditions of vapor generation and ICP-OES detection.

Parameters	The optimum conditions
- Concentration of HCl (% v/v)	5
- Concentration of NaBH ₄ (% m/v) in 0.4 % (m/v) NaOH	1
- Nebulizer gas flow rate (L min ⁻¹)	0.65
- Plasma power (W)	1,350

5.3.3 Preconcentration and Sensitivity Improvement Factors in The Presence and Absence of Matrices

The conventional solution nebulization with HF-FF and vapor generation method before ICP-OES detection were used for quantitative determination of As, Se, Cd, Hg, Pb, Cu, and Zn in the presence and absence of matrices (Na, K, Ca, and Mg). To reduce analysis time, test solution was loaded into HF-FF system to perform matrix removal and analyte preconcentration. The HF-FF operation consists of two steps, which are sample loading and focusing, and elution. The sample loading and focusing step takes 25 min. Therefore, during this step, other analyte elements were determined with conventional solution nebulization without HF-FF or vapor generation method, as described in Section 4.5.4.4. Then the preconcentration factor obtained from HF-FF and sensitivity improvement factor of vapor generation were examined. The preconcentration factor was defined as the ratio of the slope (sensitivity) between two calibration curves. For example, the preconcentration factor of HF-FF system was calculated from slope of calibration curve with HF-FF divided by the slope of calibration curve without HF-FF as standard method. The sensitivity improvement factor of vapor generation method was calculated in the same way.

5.3.3.1 Conventional Solution Nebulization

Calibration functions of various elements obtained for conventional solution nebulization without HF-FF are shown in Table 5.8. In the presence of matrix elements, slopes for As, Se, Cd, Hg, Pb, Cu, and Zn were smaller than without matrices resulting from effect of EIEs. The EIEs can affect plasma thermal properties by changing electron density in the plasma which caused signal suppression. With conventional solution nebulization without HF-FF, the emission intensity with matrices was smaller than without matrices.

Table 5.8 Calibration functions obtained for various elements by conventional solution nebulization without HF-FF.

Analytes	Slope and r^2 in the presence of matrix elements		Slope and r^2 in the absence of matrix elements	
	Slope	r^2	Slope	r^2
As I 189.042	14	0.9965	20	0.9973
As I 193.759	8	0.9873	15	0.999
Se I 196.090	6	0.9603	12	0.9952
Cd I 214.438	437	1	619	1
Cd I 226.502	348	1	493	0.9999
Hg I 184.950	56	0.9291	72	0.9896
Hg II 194.227	34	0.9341	48	0.9919
Pb I 217.000	4	0.9849	5	0.9651
Pb I 405.780	6	0.9175	8	0.9918
Pb II 220.351	25	0.9984	37	0.9993
Cu I 324.754	131	0.9994	160	0.9998
Cu II 224.700	70	0.9984	109	0.9974
Zn I 213.856	273	0.9998	350	0.9992
Zn II 206.191	243	0.9998	350	0.9992

The detection limits for As, Se, Hg, Pb, Cu, and Zn were investigated. The detection limit (3σ) was obtained by blank determination, $n=5$. The results are summarized in Table 5.9.

Table 5.9 Limit of detection obtained for various elements by conventional solution nebulization without HF-FF.

Analytes	LOD ($\mu\text{g L}^{-1}$) in the presence of matrix elements	LOD ($\mu\text{g L}^{-1}$) in the absence of matrix elements
As I 189.042	38.0	19.4
As I 193.759	82.7	39.7
Se I 196.090	128	37.6
Hg I 184.950	3.12	6.85
Hg II 194.227	16.9	10.6
Pb I 217.000	163	144
Pb I 405.780	218	27.4
Pb II 220.351	14.4	9.38
Cu I 324.754	6.70	6.64
Cu II 224.700	9.12	8.32
Zn I 213.856	2.18	1.69
Zn II 206.191	1.80	2.09

5.3.3.2 Conventional Solution Nebulization with HF-FF

Under the optimized conditions of HF-FF system, as shown in Table 5.3, the calibration of As, Se, Cd, Hg, Pb, Cu, and Zn were determined. Calibration was constructed for elements concentrations in range of 10, 20, 50, 150, and 200 $\mu\text{g L}^{-1}$. The test solutions containing analyte elements, 200 mg L^{-1} PEI buffered at pH \sim 9, with and without matrices (Na, K, Ca and Mg, 2,000 mg L^{-1} of each) were loaded into HF-FF unit. The slopes and coefficient of determinations (r^2) of the calibration curves are shown in Tables 5.10 ($r^2 > 0.9xxx$) and 5.11 ($r^2 < 0.9xxx$). In the presence of matrices, the coefficient of determination (r^2) of Cd, Pb, Cu, and Zn was $> 0.9xxx$ whereas that of As, Se, and Hg was very poor. The poor sensitivity may be caused by the fact that As, Se, and Hg form only weak complex with PEI. However, in the absence of matrices, the coefficient of determination (r^2) of Hg was $> 0.9xxx$ while Pb I 405.78 was 0.7210. The Pb I 405.78 may be affected with high background emission from Ar emission line at 404.442 or 404.597 nm.

The preconcentration factors are summarized in Table 5.12. For all cases, the slope and preconcentration factors obtained in the presence of matrices solution were higher than those without matrices. This is due to the different amount of uncomplexed analyte ions filtering off through the fiber membrane between with and without matrices. Without matrices, the uncomplexed analyte ions passed through the fiber membrane pore. With matrix ions, charge repulsion between uncomplexed analyte ions and matrix ions occurred, causing less amount of uncomplexed analyte ions penetrated through the membrane pore. Then, more uncomplexed analyte ions retained in the hollow fiber channel. Therefore, the amount of analyte retained (analyte-PEI complexes and uncomplexed analyte ions) was higher in the presence of matrices.

Moreover, plots showing relationship between emission intensities obtained from conventional solution nebulization (standard method) and those with HF-FF were constructed as summarized in Appendix A. The slope obtained for this plot indicated the preconcentration factor obtained. The correlation coefficients (r) were very close to 1, implying that the two sets of results were not different. These results are summarized in Tables A-1 and A-2 as given in Appendix A.

In addition, the preconcentration factors obtained for analytes when considering from their ionic lines were greater than atomic lines. This ion-signal enhancement might be due to charge transfer ion process, resulting from charge exchange between C^+ ions present in PEI and analytes atom. Charge-exchange reactions are efficient when the excited state of the product ion is close in energy to that of the initial reactant ion [109].



Table 5.10 Calibration functions obtained for various elements by conventional solution nebulization with HF-FF (good coefficient of determination, $r^2 > 0.9xxx$).

Analytes	Slope and r^2 in the presence of matrix elements		Slope and r^2 in the absence of matrix elements	
	Slope	r^2	Slope	r^2
Cd I 214.438	2028	0.9998	1114	0.9992
Cd I 226.502	1663	0.9999	9000	0.9974
Pb I 217.000	12	0.9595	4	0.9833
Pb II 220.351	91	0.9981	31	0.9846
Cu I 324.754	536	0.9984	241	0.9997
Cu II 224.700	329	0.9976	173	0.9983
Zn I 213.856	1081	0.9984	514	0.9973
Zn II 206.191	1070	0.9989	504	0.9980

Table 5.11 Calibration functions obtained for various elements by conventional solution nebulization with HF-FF (poor coefficient of determination, $r^2 < 0.9xxx$).

Analytes	Slope and r^2 in the presence of matrix elements		Slope and r^2 in the absence of matrix elements	
	Slope	r^2	Slope	r^2
As I 189.042	1	0.1304	9	0.3928
As I 193.759	0	0.0170	5	0.4441
Se I 196.090	-1	0.0261	2	0.4418
Hg I 184.950	185	0.5745	197	0.9534
Hg II 194.227	119	0.5831	121	0.9361
Pb I 405.780	21	0.9422	8	0.7210

Table 5.12 Preconcentration factors obtained for various analyte elements by conventional solution nebulization with HF-FF.

Analytes	Preconcentration factor in the presence of matrix elements	Preconcentration factor in the absence of matrix elements
Cd I 214.438	4.6	1.8
Cd I 226.502	4.8	1.8
Pb I 217.000	3.1	0.7
Pb II 220.351	3.6	0.9
Cu I 324.754	4.1	1.5
Cu II 224.700	4.7	1.6
Zn I 213.856	4.0	1.5
Zn II 206.191	4.4	1.4

Conventional solution nebulization with HF-FF was a suitable sample introduction method for Cd, Pb, Cu, and Zn determination by ICP-OES. The detection limits for these analyte elements were investigated. The results are summarized in Table 5.13.

Table 5.13 Limit of detection obtained for various elements by conventional solution nebulization with HF-FF.

Analytes	LOD ($\mu\text{g L}^{-1}$) in the presence of matrix elements	LOD ($\mu\text{g L}^{-1}$) in the absence of matrix elements
Cd I 214.438	1.26	3.29
Cd I 226.502	0.56	2.54
Pb I 217.000	181	31.3
Pb II 220.351	23.9	12.2
Cu I 324.754	60.5	127
Cu II 224.700	62.1	179
Zn I 213.856	39.3	42.8
Zn II 206.191	35.7	41.9

5.3.3.3 Vapor Generation Method

By using optimized vapor generation conditions in Table 5.7, the calibration and sensitivity improvement factor of vapor generation method were determined. NaBH_4 and acidified sample were introduced separately to the bottom and top of the LMSC, respectively. The acidified sample dropped down and mixed with the incoming NaBH_4 . Volatile products liberated in the reaction were transported into the plasma by argon carrier gas. Wastes were drained continuously from the chamber. The results are summarized in Table 5.14 and 5.15.

From calibration results, the analyte elements that can be determined by vapor generation method were As, Cd, Se, and Hg while Pb, Cu, and Zn were not observed. The relatively low yield of plumbane (PbH_4) is due to the very low redox potential of $\text{Pb}^{2+}/\text{PbH}_4$ pair and possible alternative pathways of reduction producing elemental lead (Pb^0) instead of volatile hydride. Lead (IV) species are very unstable and difficult to keep in solution, being spontaneously reduced to lower oxidation states within minutes [110]. In the case of Cu and Zn, these metals require rapid separation of the volatile species from the reaction medium, suggesting the product is very unstable in the liquid phase. This leads to relatively poor vapor generation efficiencies [87]. Therefore, only As, Cd, Se, and Hg were further examined. Moreover, relationship between emission intensities from conventional solution nebulization and those from vapor generation were plotted as summarized in Appendix A (Table A-3).

The As, Se, and Hg slopes in matrices were almost equal to those in the absence of matrices and percent difference of slopes (Table 5.16) was $< 5\%$, except Cd. The results indicated no effect from matrices in this method for As, Se, and Hg. However, the Hg slope slightly increased in the presence of matrices. The increase in signal was possibly due to greater transfer of the volatile Hg to the vapor phase. High concentration of electrolytes (matrix elements) in aqueous solution lower the solubility of dissolved gases in that solution. This effect is known as “salting-out”

[111]. The Cd slope was rather small and the coefficient of determination (r^2) was $< 0.9xxx$.

The sensitivity improvement factor of As, Se, and Hg was calculated from ratio of slope obtained from vapor generation compared with conventional solution nebulization without HF-FF. The sensitivity improvement factor of As, Se, and Hg with matrices was higher than without matrices due to effect of EIEs as described in Section 5.3.3.1. Conversely, the Cd sensitivity with vapor generation method was less than conventional solution nebulization without HF-FF. The compromised vapor generation condition was not suitable for generation of volatile Cd. Therefore, vapor generation method cannot improve Cd sensitivity under the conditions used herein.

Table 5.14 Calibration functions obtained for various elements by vapor generation method.

Analytes	Slope and r^2 in the presence of matrix elements		Slope and r^2 in the absence of matrix elements	
	Slope	r^2	Slope	r^2
As I 189.042	388	0.9987	388	0.9992
As I 193.759	278	0.9987	277	0.9994
Se I 196.090	429	0.9985	435	0.9993
Cd I 214.438	35	0.9494	27	0.8624
Cd I 226.502	27	0.8361	1	0.8930
Hg I 184.950	3307	1	3177	0.9996
Hg II 194.227	2134	1	2047	0.9995

Table 5.15 Sensitivity improvement factors obtained for various analyte elements by vapor generation method.

Analytes	Preconcentration factor in the presence of matrix elements	Preconcentration factor in the absence of matrix elements
As I 189.042	27.3	19.1
As I 193.759	33.2	18.2
Se I 196.09	69.0	36.0
Hg I 184.95	58.6	44.4
Hg II 194.227	63.3	42.9

Table 5.16 Percent difference of slope between with and without matrices obtained for various analyte elements by vapor generation method.

Analytes	Percent difference of slope by vapor generation method
As I 189.042	0.00
As I 193.759	0.36
Se I 196.09	1.38
Cd I 214.438	29.6
Cd I 226.502	2006
Hg I 184.95	4.09
Hg II 194.227	4.25

Vapor generation method was a suitable sample introduction for As, Se, and Hg determination. The detection limits are shown in Table 5.17.

Table 5.17 Limit of detection obtained for various elements by vapor generation method.

Analytes	LOD ($\mu\text{g L}^{-1}$) in the presence of matrix elements	LOD ($\mu\text{g L}^{-1}$) in the absence of matrix elements
As I 189.042	5.09	2.89
As I 193.759	6.78	5.10
Se I 196.09	3.96	2.71
Hg I 184.95	0.94	0.15
Hg II 194.227	1.28	0.47

5.3.4 Summary: Trace Element Analysis by ICP-OES Detection Using Conventional Solution Nebulization with or Without HF-FF, and Vapor Generation Sample Introduction

In conventional solution nebulization without HF-FF, the sensitivity of analyte with matrix elements was suppressed by the effect of easily ionized elements (EIEs) on the metal excitation in the plasma. However, conventional solution nebulization with HF-FF and vapor generation method was used as alternative sample introduction methods.

The analytes can be categorized into two groups. The first group is the analyte elements which are suitable for conventional solution nebulization with HF-FF sample introduction. There are Cd, Pb, Cu, and Zn. The preconcentration factors obtained for these elements were in the range ~ 3 -5 with matrix elements and ~ 0.7 -2 without matrix elements. The higher preconcentration factors for solution containing matrix elements might be affected by charge repulsion between uncomplexed analyte ions and matrix elements. The charge repulsion between uncomplexed analyte ions and matrix ions caused less amount of uncomplexed analyte ions penetrated through the membrane pore. Therefore, the amount of analyte retained in hollow fiber channel was higher in the presence of matrices.

The second group is the analyte elements which are suitable for vapor generation method. There are As, Se, and Hg. Percent difference of slopes between with and without matrix elements was < 5% suggesting no effect from matrix elements for determination of As, Se and Hg by this method. The sensitivity improvement factors were in the range of ~30-70 with matrix elements and ~20-45 without matrix elements. Since, sensitivity improvement factor was calculated from ratio of slope compared with conventional solution nebulization without HF-FF. In conventional solution nebulization without HF-FF, sensitivity of with matrix elements was smaller than without matrix elements resulting from signal suppression by EIEs. Therefore, sensitivity improvement factor in absence of matrix elements was higher than that in the presence of matrix elements.

Vapor generation method can be used for improvement of LOD compared to conventional solution nebulization without HF-FF. The LODs of As, Se, and Hg in vapor method were in the range of 0.15 to 6.78 $\mu\text{g L}^{-1}$ whereas without HF-FF the LODs were in the range of 3.12 to 128 $\mu\text{g L}^{-1}$. The results are illustrated in Table 5.18. However, conventional solution nebulization with HF-FF cannot improve LOD, as shown in Table 5.19. The LODs of Pb, Cu, and Zn with HF-FF were higher than those without HF-FF, except for Pb in absence of matrix elements.

Table 5.18 Limit of detection (LOD, $\mu\text{g L}^{-1}$) of vapor generation method compared to conventional solution nebulization without HF-FF.

Analytes	Presence of matrix elements		Absence of matrix elements	
	Vapor	Solution	Vapor	Solution
As I 189.042	5.09	38.0	2.89	19.4
As I 193.759	6.78	82.7	5.10	39.7
Se I 196.090	3.96	128	2.71	37.6
Hg I 184.950	0.94	3.12	0.15	6.85
Hg II 194.227	1.28	16.9	0.47	10.6

Table 5.19 Limit of detection ($\mu\text{g L}^{-1}$) of conventional solution nebulization with HF-FF compared to without HF-FF.

Analytes	Presence of matrix elements		Absence of matrix elements	
	With HF-FF	Without HF-FF	With HF-FF	Without HF-FF
Pb I 217.000	181	163	31.3	144
Pb II 220.351	23.9	14.4	12.2	9.38
Cu I 324.754	60.5	6.70	127	6.64
Cu II 224.700	62.1	9.12	179	8.32
Zn I 213.856	39.3	2.18	42.8	1.69
Zn II 206.191	35.7	1.80	41.9	2.09

CHAPTER VI

CONCLUSION

The performance of hollow fiber flow filtration (HF-FF) using an opposed flow method was examined for matrix removal and analyte preconcentration before detection by GFAAS, CVAAS, and ICP-OES. In case of mercury detection by GFAAS with HF-FF system, interference from sodium chloride was removed by filtering off the membrane during HF-FF matrix removal process. The HF-FF system can be used to prevent the introduction of high sodium chloride concentration into furnace, which could affect on signal and peak shape of mercury. For the determination of mercury by CVAAS, HF-FF matrix removal may not be necessary, as the separation of analyte from the matrix was possible by converting analyte elements into gaseous form. With HF-FF system, the preconcentration factors in range 1.0-1.3 and 1.2-1.5 times were obtained for GFAAS and CVAAS, respectively. Therefore, HF-FF system was not sufficient to improve the sensitivity. Nonetheless, a higher preconcentration factor can be obtained by introducing a larger sample volume into HF-FF. In trace element detection by ICP-OES, HF-FF system can be used to prevent the introduction of high salt concentration, which could cause matrix interference in ICP. HF-FF showed good performance for matrix removal and analyte preconcentration. The preconcentration factors in the range of ~ 0.7-5 were obtained for ICP-OES. From this study, it appeared that HF-FF system could be an interesting suitable method to be used with atomic spectrometric detection for the determination of trace element in high salt medium. However, HF-FF system is not totally matrix independent. Therefore, calibration by standard addition or matrix matching might be needed.

The vapor generation sample introduction was used to increase sample transport efficiency in ICP-OES detection. The parameters affecting matrix removal and sensitivity improvement in this process were concentrations of reductant and acid

carrier. Vapor generation sample introduction showed no effect from matrix elements for As, Se and Hg. Moreover, the sensitivity improvement factors in the range of ~ 20-70 times were obtained.

Suggestion for future work

Suggestions for the future work are given as follows:

1. In HF-FF system, the sample volume should be increased to obtain higher preconcentration factor.
2. A more suitable condition should be investigated for multi-element vapor generation to improve efficiency of this system.

REFERENCES

1. Otero-Romaní J, Moreda-Piñeiro A, Bermejo-Barrera A. Evaluation of commercial C18 cartridges for trace elements solid phase extraction from seawater followed by inductively coupled plasma-optical emission spectrometry determination. *Anal Chim Acta*. 2005;536(1-2):213-8.
2. Carasek E. A low-cost flame atomic absorption spectrometry method for determination of trace metals in aqueous samples. *Talanta*. 2000;51(1):173-8.
3. Kojuncu Ý, Bundalevska JM, Ay Ü, Čundeva K, Stafilov T, Akçin G. Atomic absorption spectrometry determination of Cd, Cu, Fe, Ni, Pb, Zn, and Tl traces in seawater following flotation separation. *Sep Sci Technol*. 2004;39(11):2751–65.
4. Abbasse G, Ouddane B, Fischer JC. Determination of total and labile fraction of metals in seawater using solid phase extraction and inductively coupled plasma atomic emission spectrometry (ICP-AES). *J Anal At Spectrom*. 2002;17(10):1354–8.
5. Rao GPC, Veni SS, Pratap K, Rao TK, Seshaiiah K. Solid phase extraction of trace metals in seawater using morpholine dithiocarbamate-loaded amberlite XAD-4 and determination by ICP-AES. *Anal Lett*. 2006;39:1009–21.
6. Meeravali NN, Reddy MA, Kumar SJ. Cloud point extraction of trace metals from seawater and determination by electrothermal atomic absorption spectrometry with iridium permanent modifier. *Anal Sci*. 2007;23:351-6.
7. Pretty JR, Blubaugh EA, Evans EH, Caruso JA, Davidson TM. Determination of copper and cadmium using an on-line anodic stripping voltammetry flow cell with detection by inductively coupled plasma mass spectrometry. *J Anal At Spectrom*. 1992;7(8):1131-7.
8. Pretty JR, Evans EH, Blubaugh EA, Shen W-L, Caruso JA, Davidson TM. Minimisation of sample matrix effects and signal enhancement for trace

- analytes using anodic stripping voltammetry with detection by inductively coupled plasma atomic emission spectrometry and inductively coupled plasma mass spectrometry. *J Anal At Spectrom.* 1990;5(6):437-43.
9. Vassileva E, Furuta N. Application of iminodiacetate chelating resin muromac A-1 in on-line preconcentration and inductively coupled plasma optical emission spectroscopy determination of trace elements in natural waters. *Spectrochim Acta B.* 2003;58(8): 1541-52.
 10. Sawatsuk T, Shiowatana J, Siripinyanond A. Matrix removal and analyte preconcentration before inductively coupled plasma spectrometric detection: use of a laboratory-made hollow fibre flow filtration unit. *J Anal At Spectrom.* 2006;21(11):1331-5.
 11. Sangsawong S, Shiowatana J, Siripinyanond A. Matrix removal before inductively coupled plasma spectrometric detection: another capability of flow field-flow fractionation. *J Anal At Spectrom.* 2006;21(11):1336-9.
 12. McLaughlin RLJ, Brindle ID. A new sample introduction system for atomic spectrometry combining vapour generation and nebulization capacities. *J Anal At Spectrom.* 2002;17(11):1540-8.
 13. Asfaw A, Wibetoe G. Dual mode sample introduction for multi-element determination by ICP-MS: the optimization and use of a method based on simultaneous introduction of vapor formed by NaBH₄ reaction and aerosol from the nebulizer. *J Anal At Spectrom.* 2006;21(10):1027-35.
 14. Simultaneous determination of As, Bi, Se, Sn and Te in high alloy steels – re-evaluation of hydride generation inductively coupled plasma atomic emission spectrometry. *J Anal At Spectrom.* 2007;22:1083-8.
 15. Rudner PC, Torres AG, Pavón JMC, Rojas FS. On-line preconcentration of mercury by sorption on an anion-exchange resin loaded with 1,5-bis[(2-pyridyl)-3-sulphophenyl methylene] thiocarbonohydrazide and determination by cold-vapour inductively coupled plasma atomic emission. *Talanta.* 1998;46(5):1095-1105.
 16. <http://www.jyemission.com/>. Jobin Yvon Ultra-Ace 2000. Chemistry lab cookbook ICP concepts v 210.0 instrument. 15 October 2008.

17. O'hanlon K, Ebdon L, Foulkes M. Effect of easily ionisable elements on the mass transport efficiency of solutions and slurries used in plasma emission spectrometry. *J Anal At Spectrom.* 1997;12(3):329-31.
18. Todolí JL, Gras L, Hernandis V, Mora J. Elemental matrix effects in ICP-AES. *J Anal At Spectrom.* 2002;17(2):142-69.
19. Romero X, Poussel E, Mermet JM.. The effect of sodium on analyte ionic line intensities in inductively coupled plasma atomic emission spectrometry: influence of the operating conditions. *Spectrochim Acta B.* 1997;52(4):495-502.
20. Ramsey MH, Thompson A. High-accuracy analysis by inductively coupled plasma atomic emission spectrometry using the parameter-related internal standard method. *J Anal At Spectrom.* 1987;2:497.
21. Thompson A. The capabilities of inductively coupled plasma atomic-emission spectrometry-some conjectures and refutations. *Analyst.* 1985;110(5):443.
22. Wu M, Hieftje GM. The effect of easily ionized elements on analyte emission efficiency in inductively coupled plasma spectrometry. *Spectrochim Acta B.* 1994;49(2):149-61.
23. Galley PJ, Glick M, Hieftje GM. Easily ionizable element interferences in inductively coupled plasma atomic emission spectroscopy-I effect on radial analyte emission patterns. *Spectrochim Acta B.* 1993;48(6-7):769-88.
24. Galley PJ, Hieftje GM. Easily ionizable element (EIE) interferences in inductively coupled plasma atomic emission spectrometry II. minimization of EIE effects by choice of observation volume. *Spectrochim Acta B.* 1994;49(7):703-24.
25. Ivaldi JC, Tyson JF. Performance evaluation of an axially viewed horizontal inductively coupled plasma for optical emission spectrometry. *Spectrochim Acta B.* 1995;50(10):1207-26.
26. Hobbs SE, Olesik JW. The influence of incompletely desolvated droplets and vaporizing particles on chemical matrix effects in inductively coupled plasma spectrometry: time-gated optical emission and laser-induced fluorescence measurements. *Spectrochim Acta B.* 1997;52(3):353-67.

27. Blades MW, Horlick G. Interference from easily ionizable element matrices in inductively coupled plasma emission spectrometry-a spatial study. *Spectrochim Acta B*. 1981;36(9):881-900.
28. Matousek JP, Orr BJ, Selby M. Interferences due to easily ionised elements in a microwave-induced plasma system with graphite-furnace sample introduction. *Spectrochim Acta B*. 1986;41(5):415-29.
29. Rayson GD, Hieftje GM. A steady-state approach to evaluation of proposed excitation mechanisms in the analytical ICP. *Spectrochim Acta B*. 1986;41(7):683-97.
30. Miller MH, Eastwood D, Hendrick MS. Excitation of analytes and enhancement of emission intensities in a d.c. plasma jet: a critical review leading to proposed mechanistic models. *Spectrochim Acta B*. 1984;39(1):13-56.
31. Jankowski K, Dreger M. Study of an effect of easily ionizable elements on the excitation of 35 elements in an Ar-MIP system coupled with solution nebulization. *J Anal At Spectrom*. 2000;15(3):269-76.
32. Turk GC, Axner O, Omenetto N. Optical detection of laser-induced ionization in the inductively coupled plasma for the study of ion-electron recombination and ionization equilibrium. *Spectrochim Acta B*. 1987;42(7):873-81.
33. Chan GC-Y, Hieftje GM. Investigation of plasma-related matrix effects in inductively coupled plasma-atomic emission spectrometry caused by matrices with low second ionization potentials-identification of the secondary factor. *Spectrochim Acta B*. 2006;61(6):642-59.
34. Carroll J, Miller-Ihli NJ, Harnly JM, O'Haver TC, Littlejohn D. Comparison of sodium chloride and magnesium chloride interferences in continuum source atomic absorption spectrometry with wall, platform and probe electrothermal atomization. *J Anal At Spectrom*. 1992;7(3):533-8.
35. Chaudhry MM, Mouillere D, Ottaway BJ, Littlejohn D, Whitley JE. Investigation of chloride salt decomposition and pre-atomization interferences in electrothermal atomic absorption spectrometry. *J Anal At Spectrom*. 1992;7(4):701-6.

36. Cabon JY, Bihan AL. Interference of salts on the determination of lead by electrothermal atomic absorption spectrometry. ion chromatographic study. *Spectrochim Acta B*. 1996;51(6):619-31.
37. Rió-Segade S, Bendicho C. On - line high-performance liquid-chromatographic separation and cold vapor atomic absorption spectrometric determination of methylmercury and inorganic mercury. *Talanta*. 1999;48(2):477-84.
38. Krata A, Pyrzyńska K, Bulska E. Use of solid - phase extraction to eliminate interferences in the determination of mercury by flow-injection CVAAS. *Anal Bioanal Chem*. 2003;377(4):735-9.
39. Szmyd E, Baranowska I. Elimination of interferences from Cu, Pb, Ag, Au, Pt, Pd and Se in the determination of mercury by CVAAS using sodium tetrahydroborate(III) reduction in copper concentrates. *Fresenius' Z Anal Chem*. 1994;350:178-80.
40. Zhanga D-q, Yanga L-l, Suna H-w. Determination of mercury by cold vapour atomic absorption spectrometry with derivative signal processing. *Anal Chim Acta*. 1999;395(1-2):173-8.
41. Kalāihne R, Henrion G, Hulanicki A, Garboś S, Walcerz M. Comparison of AAS with hydride concentration in a graphite furnace with other spectrometric techniques. *Spectrochim Acta B*. 1997;52(9-10):1509-16.
42. Haase O, Klare M, Krenzel-Rothensee K, Broekaert JAC. Evaluation of the determination of mercury at the trace and ultra-trace levels in the presence of high concentrations of NaCl by flow injection-cold vapour atomic absorption spectrometry using SnCl₂ and NaBH₄ as reductants. *Analyst*. 1998;123(6):1219-22.
43. Cabon JY. Determination of Cd and Pb in seawater by graphite furnace atomic absorption spectrometry with the use of hydrofluoric acid as a chemical modifier. *Spectrochim Acta B*. 2002;57(3):513-24.
44. Huang S-D, Shih K-Y. Direct determination of copper in sea-water with a graphite furnace atomic absorption spectrometer. *Spectrochim Acta B*. 1993;48(12):1451-60.

45. Cabon JY, Bihan AL. The determination of Cr, Cu and Mn in seawater with transversely heated graphite furnace atomic absorption spectrometry, *Spectrochim Acta B*. 1995;50(13):1703–16.
46. Xiao-Quan S, Radziuk B, Welz B, Vyskocilova O. Determination of manganese in river and seawater samples by electrothermal atomic absorption spectrometry with a tungsten atomizer, *J Anal At Spectrom*. 1993;8(3):409-13.
47. Huang S-D, Lai W-R, Shih K-Y. Direct determination of molybdenum, chromium and manganese in seawater by graphite furnace atomic absorption spectrometry, *Spectrochim Acta B*. 1995;50(10):1237-46.
48. Chen C-L, Danadurai S-K, Huang S-D. Direct and simultaneous determination of copper, manganese and molybdenum in seawater with a multi-element electrothermal atomic absorption spectrometer, *J Anal At Spectrom*. 2001;16(4):404–8.
49. Lan C-H, Alfassi ZB. Direct determination of manganese in seawater by electrothermal atomic absorption spectrometry with sodium hydroxide as chemical modifier for interference removal, *Analyst*. 1994;119(5):1033-35.
50. Cabon JY. Improvement of direct determination of Cu and Mn in seawater by GFAAS and total elimination of the saline matrix with the use of hydrofluoric acid. *Talanta*. 2005;65(2):402-7.
51. Carnrick GR, Slavin W, Manning DC. Direct determination of manganese in seawater with the L'vov platform and Zeeman background correction in the graphite furnace. *Anal. Chem*. 1981;53(12):1866–72.
52. Cabon JY. Determination of Cu and Mn in seawater by graphite furnace atomic absorption spectrometry with the use of hydrofluoric acid as a chemical modifier. *Spectrochim Acta B*. 2002;57(5):939-50.
53. Rohr U, Ortner HM, Schlemmer G, Weinbruch S, Welz B. Corrosion of transversely heated graphite tubes by mineral acids. *Spectrochim Acta B*. 1999;54(5):699–718.
54. Colbert D, Johnson KS, Coale KH. Determination of cadmium in seawater using automated on-line preconcentration and direct injection graphite furnace atomic absorption spectrometry. *Anal Chim Acta*. 1998;377(2-3):255-62.

55. Wang H-C, Hwang Y-C, Hsieh C-J, Kuo M-S. Determinations of total mercury in drinking water and of methylmercury in air by graphite-furnace atomic absorption spectrophotometry using 2,3-dimercaptopropane-1-sulfonate as a complexing agent. *Anal Sci.* 1998;14:983.
56. Zalups RK. Influence of 2, 3 - dimercaptopropane - 1 -sulfonate (DMPS) and meso-2,3-dimercaptosuccinic acid (DMSA) on the renal disposition of mercury in normal and uninephrectomized rats exposed to inorganic mercury. *J Pharmacol Exp Ther.* 1993;267:791-800.
57. Zhang D-Q, Yang L-L, Sun H-W. Determination of mercury by cold vapour atomic absorption spectrometry with derivative signal processing. *Anal Chim Acta.* 1999;395:173-78.
58. Welz B, Schubert-Jacobs M. Cold vapor atomic absorption spectrometric determination of mercury using sodium tetrahydroborate reduction and collection on gold. *Fresenius J Anal Chem.* 1988;331(3-4):324-9.
59. Baxter DC, Frech W. Determination of mercury by atomic absorption spectrometry using a platinum-lined graphite furnace for in situ preconcentration. *Anal Chim Acta.* 1989;225:175-83.
60. Kopýš E, Pyrzyńska K, Garboš S, Bulska E. Determination of mercury by cold-vapor atomic absorption spectrometry with preconcentration on a gold-trap. *Anal Sci.* 2000;16(14):1309-12.
61. Ombaba JM. Total mercury determination in biological and environmental standard samples by gold amalgamation followed by cold vapor atomic absorption spectrometry. *Microchem J.* 1996;53:195-200.
62. Costley CT, Mossop KF, Dean JR, Garden LM, Marshall J, Carroll J. Determination of mercury in environmental and biological samples using pyrolysis atomic absorption spectrometry with gold amalgamation. *Anal Chim Acta.* 2000;405(1-2):179-83.
63. Lazo P, Cullaj A. Determination of the different states of mercury in seawater near the Vlora and Durres Bays. *Anal Bioanal Chem.* 2002;374(6):1034-8.

64. Arbab-Zavar MH, Rounaghi GH, Chamsaz M, MASROURNIA Masrounia M. Determination of mercury(II) ion by electrochemical cold vapor generation atomic absorption spectrometry. *Anal Sci.* 2003;19(5):743-6.
65. Kagaya S, Kuroda Y, Serikawa Y, Hasegawa K. Rapid determination of total mercury in treated waste water by cold vapor atomic absorption spectrometry in alkaline medium with sodium hypochlorite solution. *Talanta.* 2004;64(2):554-7.
66. http://www.alibaba.com/product-gs/205799893/Hollow_fiber_UF_membrane_equipment.html. 1 October 2008.
67. <http://www.cheresources.com/hmembranes.shtml>. 2 September 2008.
68. Bishop EJ, Mitra S. Hollow fiber membrane concentrator for on - line preconcentration. *J Chromatogr A.* 2004;1046 (1-2).11-7.
69. Shaw TJ, Duncan T, Schnetger B. A preconcentration/matrix reduction method for the analysis of rare earth elements in seawater and groundwaters by isotope dilution ICP MS. *Anal Chem.* 2003;75(14):3396-403.
70. Chang XJ, Gong B-L, Yang Z-XSD, Luo X-Y. ICP-OES determination of traces of Ru, Au, V and Ti preconcentrated and separated by a new poly(epoxy-melamine) chelating resin from solutions. *Fresenius J Anal Chem.* 1998;360(6):736-9.
71. Farias GM, Cerutti S, Gasquez JA, Olsina RA, Martinez LD. ICP - OES determination of cobalt in natural water using a flow injection system after preconcentration on activated carbon. *Atom Spectrosc.* 2003;24(6):213-7.
72. Yu JC, Chan SM, Chen Z. Preconcentration using diethylenetriaminetetraacetic acid-functionalized polysiloxane (DETAP) for determination of molybdenum(VI) in seawater by ICP-OES. *Anal Bioanal Chem.* 2003;376(5):728-34.
73. Rao GPC, Veni SS, Pratap K, Rao YK, Seshaiiah K. Solid phase extraction of trace metals in seawater using morpholine dithiocarbamate-loaded amberlite XAD-4 and determination by ICP-AES. *Anal Lett.* 2006;39:1009-21.

74. Batterham GJ, Munksgaard NC, Parry DL. Determination of trace metals in sea-water by inductively coupled plasma mass spectrometry after off-line dithiocarbamate solvent extraction. *J Anal At Spectrom.* 1997;12(11):1277-80.
75. Lo JM, Yu JC, Hutchison FI, Wai CM. Solvent extraction of dithiocarbamate complexes and back-extraction with mercury(II) for determination of trace metals in seawater by atomic absorption spectrometry. *Anal Chem.* 1982;54(14):2536.
76. Rivasa BL, Pereiraa ED, Moreno-Villosladab I. Water-soluble polymer-metal ion interactions. *Prog Polym Sci.* 2003;28:173-208.
77. Geckeler KE, Volchek K. Removal of hazardous substances from water using ultrafiltration in conjunction with soluble polymers. *Environ Sci Technol.* 1996;30(3):725-34.
78. Al-Ammar A, Siripinyanond A, Barnes RM. Simultaneous sample preconcentration and matrix removal using field-flow fractionation coupled to inductively coupled plasma mass spectrometry. *Spectrochim Acta B.* 2001;56:1951-62.
79. Canizares P, Perez A, Camarillo R. Recovery of heavy metals by means of ultrafiltration with water-soluble polymers: calculation of design parameters. *Desalination.* 2002;144(1-3):279-85.
80. Uludag Y, Özbelge HÖ, Yilmaz L. Removal of mercury from aqueous solutions via polymer-enhanced ultrafiltration. *J Membrane Sci.* 1997;129:93-9.
81. Barron-Zambrano J, Laborie S, Viers P, Rakib M, Durand G. Mercury removal from aqueous solutions by complexation--ultrafiltration. *Desalination.* 2002;144(1-3):201-6.
82. Vujicic G, Steffan I. A new continuous hydride generator for ICP - AES. *Mikrochim Acta [Wien].* 1989;III, 267-72.
83. Pohl P. Hydride generation - recent advances in atomic emission spectrometry. *Trends in Analytical Chemistry.* 2004;23(2):87-101.
84. Thompson M, Pahlavanpour B, Walton SJ, Kirkbright GF. Simultaneous determination of trace concentrations of arsenic, antimony, bismuth,

- selenium and tellurium in aqueous solution by introduction of the gaseous hydrides into an inductively coupled plasma source for emission spectrometry. Part I. Preliminary studies. *Analyst*. 1978;103:568-579.
85. Goulden PD, Anthony DHJ, Austen KD. Determination of arsenic and selenium in water, fish, and sediments by inductively coupled argon plasma emission spectrometry. *Anal Chem*. 1981;53(13):2027-29
86. Feng Y-L, Lam JW, Sturgeon RE. Expanding the scope of chemical vapor generation for noble and transition metals. *Analyst*. 2001;126:1833-7.
87. Feng Y-L, Sturgeon RE, Lam JW. Chemical vapor generation characteristics of transition and noble metals reacting with tetrahydroborate(III). *J Anal A Spectrom*. 2003;18:1435-42.
88. Sharp BL. Pneumatic nebulisers and spray chambers for inductively coupled plasma spectrometry. a review. part 2. spray chambers. *J Anal A Spectrom*. 1988;3:939-63.
89. Dubuisson C, Poussel E, Todolí JL, Mermet JM. Effect of sodium during the aerosol transport and filtering in inductively coupled plasma atomic emission spectrometry. *Spectrochim Acta B*. 1998;53:593-600.
90. Feng Y-L, Sturgeon RE, Lama JW, D'Ulivo A. Insights into the mechanism of chemical vapor generation of transition and noble metals. *J Anal A Spectrom*. 2005;20:255-65.
91. Moor C, Lama JW, Sturgeon RE. A novel introduction system for hydride generation-inductively coupled plasma mass spectrometry: determination of selenium in biological materials. *J Anal A Spectrom*. 2000;15:143-149.
92. Pohl P, Zyrnicki W. Study of chemical vapour generation of Au, Pd and Pt by inductively coupled plasma atomic emission spectrometry. *J Anal A Spectrom*. 2001;16:1442-5.
93. Pohl P, Zyrnicki W. Study of the reaction of Ir, Os, Rh and Ru ions with NaBH₄ in the acid medium by the inductively coupled plasma atomic emission spectrometry. *J Anal A Spectrom*. 2002;17:746-9.
94. Pohl P, Zyrnicki W. Analytical features of Au, Pd and Pt chemical vapour generation inductively coupled plasma atomic emission spectrometry. *J Anal A Spectrom*. 2003;18:798-801.

95. Maestre S, Mora J, Todolí J-L, Canals A. Evaluation of several commercially available spray chambers for use in inductively coupled plasma atomic emission spectrometry. *J Anal A Spectrom.* 1999;14:61-7.
96. Application note 13, O. Hirsch, Comparison of classical hydride generator and concomitant metals analyzer (CMA), Jobin Yvon S.A.S. (www.jyhoriba.com). 13 September 2008.
97. Pohl P, Zyrnicki W. Simultaneous determination of As, Bi, Se and Sn and non-hydride forming elements by HG-ICP-AES without liquid phase separation. *Chem Anal (Warsaw)*. 2000;45(5):699-708.
98. McLaughlin RLJ, Brindle ID. A new sample introduction system for atomic spectrometry combining vapour generation and nebulization capacities. *J Anal A Spectrom.* 2002;17:1540-8.
99. Asfaw A, Wibetoe G. Simultaneous determination of hydride (Se) and non-hydride-forming (Ca, Mg, K, P, S and Zn) elements in various beverages (beer, coffee, and milk), with minimum sample preparation, by ICP-AES and use of a dual-mode sample-introduction system. *Anal Bioanal Chem.* 2005;382:173-9.
100. Asfaw A, Wibetoe G. Dual mode sample introduction for multi-element determination by ICP-MS: the optimization and use of a method based on simultaneous introduction of vapor formed by NaBH₄ reaction and aerosol from the nebulizer. *J Anal A Spectrom.* 2006;21:1027-35.
101. Matusiewicz H, Ślacheński M. Simultaneous determination of hydride forming (As, Bi, Ge, Sb, Se, Sn) and Hg and non-hydride forming (Ca, Fe, Mg, Mn, Zn) elements in sonicate slurries of analytical samples by microwave induced plasma optical emission spectrometry with dual-mode sample introduction system. *Microchem J.* 2007;86:102-11.
102. Olson LK, Vela NP, Caruso JA. Hydride generation, electrothermal vaporization and liquid chromatography as sample introduction techniques for inductively coupled plasma mass spectrometry. *Spectrochim Acta B.* 1995;50(4-7):355-68.

103. Evans EH, Giglio JJ. Interferences in inductively coupled plasma mass spectrometry. a review. *J Anal At Spectrom.* 1993;8:1-18.
104. Chan M-S, Huang S-D. Direct determination of cadmium and copper in seawater using a transversely heated graphite furnace atomic absorption spectrometer with Zeeman-effect background corrector. *Talanta.* 2000;51:372-80.
105. Thiptanasup K. Continuous-flow dialysis system with element-specific detection for estimation of selenium bioaccessibility and interelemental effect of calcium, iron and zinc on selenium food supplements. M.Sc. Thesis in Applied Analytical and Inorganic Chemistry, Faculty of Graduate Studies, Mahidol University, 2007.
106. Dadfarnia S, Salmanzadeh AM, Shabani AMH. Preconcentration and determination of mercury (II) and methylmercury in waters by immobilized 1,5-diphenylcarbazone and cold vapor atomic absorption spectrometry. *Korean Chem. Soc.* 2002;23(12):1719-23.
107. Rojas I, Murillo M, Carrión N, Chirinos J. Investigation of the direct hydride generation nebulizer for the determination of arsenic, antimony and selenium in inductively coupled plasma optical emission spectrometry. *Anal Bioanal Chem.* 2003;376:110-7.
108. Schaldach G, Berger L, Razilov I, Berndt H. Characterization of a cyclone spray chamber for ICP spectrometry by computer simulation. *J Anal At Spectrom.* 2002;17:334-44.
109. Machat J, Otruba V, Kanicky V. Spectral and non-spectral interferences in the determination of selenium by inductively coupled plasma atomic emission spectrometry. *J Anal At Spectrom.* 2002;17:1906-1102.
110. Dědina J, Tsalev D L. Hydride generation atomic absorption spectrometry. 1995;130.
111. Ellis RI, Sundin NG, Tyson JF, McIntosh SA, Hanna CP, Carnrick G. Effect of high salt concentrations on the determination of arsenic and selenium by flow injection hydride generation electrothermal atomic absorption spectrometry. *Analyst.* 1998;123.
112. Pohl P, Prusisz B. Chemical vapor generation of noble metals for analytical spectrometry. *Anal Bioanal Chem* 2007;388:753-62.

113. Liu Z-S, Huang S-D. Automatic on - line preconcentration system for graphite furnace atomic absorption spectrometry for the determination of trace metals in sea water. *Anal Chim Acta*. 1993;281(1):185-90.
114. Zolotov YA, Kuzmin NM. in: G. Svehla (Ed.), *Wilson and Wilson's Comprehensive analytical chemistry*, Elsevier, Amsterdam, 1990:372.
115. Dumarey R, Heindryck R, Dams R, Hoste J. Determination of volatile mercury compounds in air with the coleman mercury analyzer system. *Anal Chim Acta*. 1979;107:159-67.
116. Amara M, Kerdjoudj H. Modification of the cation exchange resin properties by impregnation in polyethyleneimine solutions: application to the separation of metallic ions. *Talanta*. 2003;60:991-1001.
117. Gao B, An F, Liu K. Studies on chelating adsorption properties of novel composite material polyethylene/silica gel for heavy-metal ions. *Appl Surf Sci*. 2006;253:1946-52

APPENDIX

APPENDIX A

**COMPARISON OF EMISSION INTENSITIES OBTAINED FROM
THE PROPOSED METHODS WITH THOSE FROM
CONVENTIONAL SOLUTION NEBULIZATION**

Table A-1 Calibration functions of correlation plots between emission intensities obtained from conventional solution nebulization (x-axis) and with HF-FF (y-axis). (good correlation coefficient, $r > 0.9xxx$)

Analytes	Slope and r in the presence of matrix elements		Slope and r in the absence of matrix elements	
	Slope	r	Slope	r
Cd I 214.438	4.6	0.9997	1.8	0.9997
Cd I 226.502	4.8	0.9999	1.8	0.9982
Pb I 217.000	3.1	0.9864	0.7	0.9508
Pb II 220.351	3.5	0.9970	0.8	0.9904
Cu I 324.754	4.1	0.9997	1.5	0.9997
Cu II 224.700	4.7	0.9999	1.6	0.9977
Zn I 213.856	4.0	0.9990	1.5	0.9987
Zn II 206.191	4.4	0.9992	1.4	0.9985

Table A-2 Calibration functions of correlation plots between emission intensities obtained from conventional solution nebulization (x-axis) and with HF-FF (y-axis). (poor correlation coefficient, $r < 0.9xxx$).

Analytes	Slope and r in the presence of matrix elements		Slope and r in the absence of matrix elements	
	Slope	r	Slope	r
Pb I 405.780	3.3	0.8926	0.9	0.8336
As I 189.042	0.1	0.3895	0.4	0.5991
As I 193.759	0	0.1918	0.3	0.6446
Se I 196.090	0	0.0055	0.2	0.6925
Hg I 184.950	3.0	0.7206	2.8	0.9844
Hg II 194.227	3.2	0.7215	2.6	0.9778

Table A-3 Calibration functions of correlation plots between emission intensities obtained from conventional solution nebulization (x-axis) and vapor generation (y-axis).

Analytes	Slope and r in the presence of matrix elements		Slope and r in the absence of matrix elements	
	Slope	r	Slope	r
As I 189.042	27	0.9975	19	0.9995
As I 193.759	33	0.9918	18	0.9999
Se I 196.090	66	0.9729	36	0.9977
Hg I 184.950	54	0.9630	44	0.9949
Hg II 194.227	59	0.9656	43	0.9960
Cd I 214.438	0.1	0.9755	0	0.9277
Cd I 226.502	0.1	0.9145	0.1	0.9472

BIOGRAPHY

NAME	Ms. Kamolchanok Kotakanok
DATE OF BIRTH	15 October 1982
PLACE OF BIRTH	Sakon Nakhon, Thailand
INSTITUTIONS ATTENDED	Kasetsart University, 2005: Bachelor of Science (Chemistry) Mahidol University, 2008: Master of Science (Applied Analytical and Inorganic Chemistry)
GRANTS	Recipient of a Teaching Assistance Scholarship from the Department of Chemistry, Faculty of Science, Mahidol University in the academic year of 2006-2007. Recipient of scholarship from the Higher Education Development Project: Center of Excellence for Innovation in Chemistry: Postgraduate Education and Research Program in Chemistry (PERCH-CIC), 2005-2007.
HOME ADDRESS	162, Moo 5, Hang Hong, Muang, Sakon Nakhon, 47000, Thailand. Tel. +66-042-162037 E-mail: kamolchanok_noon@hotmail.com